THESIS

VOLATILE ORGANIC COMPOUND CONCENTRATIONS AND THE IMPACTS OF FUTURE OIL AND NATURAL GAS DEVELOPMENT IN THE COLORADO NORTHERN FRONT RANGE

Submitted by

Derek T. Weber

Department of Atmospheric Science

In partial fulfillment of the requirements

For the Degree of Master of Science

Colorado State University

Fort Collins, Colorado

Spring 2018

Master's Committee:

Advisor: Jeffrey L. Collett Jr.

Emily V. Fischer
Shantanu H. Jathar
Arsineh Hecobian

ABSTRACT

VOLATILE ORGANIC COMPOUND CONCENTRATIONS AND THE IMPACTS OF FUTURE OIL AND NATURAL GAS DEVELOPMENT IN THE COLORADO NORTHERN FRONT RANGE

Recent advances in unconventional extraction of oil and natural gas (O&NG) have caused an increase in the number of wells in the Colorado Northern Front Range (CNFR) which has doubled Colorado's natural gas production over the last 15 years. Increased O&NG activity can lead to increased emissions of Volatile Organic Compounds (VOCs) which may negatively impact air quality and human health. This study looks at five sites (an elementary school, residential area, Fossil Creek Natural Area, Soapstone Natural Area, and a gas station) in Fort Collins and Timnath with the objectives of determining the gradient of VOC concentrations across a subsection of the CNFR, providing a baseline to compare potentially elevated VOC concentrations from future O&NG development, and a better understanding of the influence of O&NG emissions on air quality in the CNFR. Whole air samples were collected at all locations using an evacuated 6L stainless steel canister equipped with a calibrated flow controller that sampled at a constant flow rate for approximately 1 week. Sampling began at the elementary school and gas station in the summer of 2015 and concluded in November of 2016. Sampling at the two natural areas and the residential area took place in the fall of 2015. VOC concentrations were analyzed using an online gas chromatography flame ionization detector (GC-FID) system. An in-situ real-time GC was also deployed along with an All-In-One (AIO) weather station at the

residential area providing hourly VOC and meteorological measurements for approximately 3 weeks in the fall of 2015.

A suite of 48 VOCs were measured in this study. Ambient concentrations of BTEX compounds (Benzene, Toluene, Ethylbenzene, and Xylenes) are often of particular interest due to their carcinogenic effects and toxicity; therefore, they were studied in-depth as part of this thesis. Benzene was found to have median ambient concentration at the elementary school, residential area, Fossil Creek Natural Area, Soapstone Natural Area, and the gas station of 0.18, 0.14, 0.32, 0.09, and 0.55ppbv, respectively.

Through the use of VOC correlations with propane and acetylene and VOC ratios, it was determined that O&NG emissions have a large influence on ambient VOC concentrations in the CNFR. The mean ratio of i-pentane to n-pentane found at the elementary school, residential area, Fossil Creek Natural Area, Soapstone Natural Area, and the gas station was 1.07, 1.17, 1.16, 1.05, and 2.35, respectively. This indicates that the elementary school and Soapstone Natural Area are strongly influence by O&NG emissions while the residential area and Fossil Creek Natural Area have a mixed influence from O&NG activity as well as vehicular emissions. In contrast the gas station, displayed a clear combustion signature, as expected. Additional VOC ratios were utilized; however, i-pentane to n-pentane ratio was determined to be the most robust tool to assess source apportionment in the CNFR. In addition, through the use of meteorological data coupled with the real-time GC VOC measurements, there is strong evidence that local O&NG sources can have a large impact on air quality at the residential area.

The OH reactivity at each location was evaluated in order to compare the ozone production potential by the VOCs measured at each site. Fossil Creek NA showed the largest total OH reactivity in the fall while Soapstone NA displayed the lowest. At Soapstone NA,

66.7% of the total OH reactivity resulted from aromatics, which is the highest, and 11.4% resulted from alkenes, which is the lowest compared to each group's contribution at other sites. At the elementary school, 3.2% of the OH reactivity in the summer was attributed to isoprene, whereas in the fall, winter, and spring only 2.0%, 0.41%, and 0.76% of the OH reactivity resulted from isoprene, respectively.

Development of new unconventional O&NG wells is ongoing in the CNFR and there are plans to develop wells in close proximity to the elementary school. The American Meteorological Society (AMS)/Environmental Protection Agency (EPA) steady-state dispersion model AERMOD was utilized to project the potential increased concentration of benzene as a result of this development. The model was run utilizing the 5^{th}, 25^{th}, median, 75^{th}, and 95^{th} percentile emission rates of benzene found by a past study at production sites in the CNFR. The annual average concentration increases above background at the school (0.18 ± 0.08ppbv) for the 5^{th}, 25^{th}, median, 75^{th}, and 95^{th} percentile emission rates were found to be 0.0067, 0.11, 0.33, 0.89, and 6.7ppbv, respectively. The strongest benzene enhancement at the school occurred 0:00 (midnight) - 08:00 and 17:00 - 23:00 (0.46ppbv); however, during school attendance hours (08:35 - 15:13) the concentration increase was 0.024ppbv.

ACKNOWLEDGEMENTS

The City of Fort Collins and the Town of Timnath provided funding and motivation for this study. Access to sampling sites was crucial for the completion of this study. The Larimer County Natural Resources Department provided access to Fossil Creek and Soapstone Natural Areas. Bethke Elementary School and the Poudre School District provided access to the elementary school campus. The Costco Wholesale in Timnath provided access to the gas station sampling site. Darby Nabors provided access to her house and backyard for canister sampling and in-situ real-time GC setup.

Dr. Yong Zhou conducted the majority of the canister analysis and assisted extensively with the analytical methods. A very special acknowledgement goes to Dr. Arsineh Hecobian for her guidance over the last 2 and a half years. Finally, a special thank you to my advisor: Dr. Jeff Collett. The tremendous opportunity to join your research group and the guidance you have provided during my time at Colorado State University has been invaluable.

TABLE OF CONTENTS

LIST OF TABLES

LIST OF FIGURES

Chapter 1

Introduction

1.1 Motivation

The production of oil and natural gas (O&NG) in the United States (U.S.) has increased by about 75% over the past 30 years, and is projected to continue to grow annually by nearly 4% over the next several years (Figure 1.1) [EIA, 2017]. Much of the recent and projected future growth are the result of improved technologies, including horizontal drilling and hydraulic fracturing [Swarthout et al., 2013].

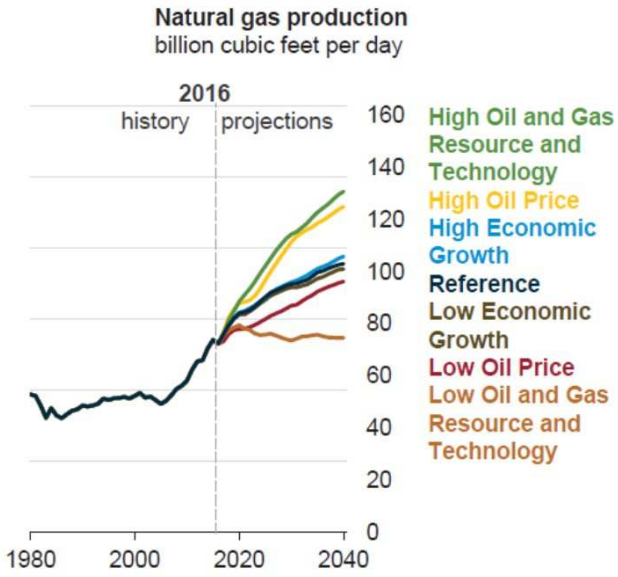

Figure 1.1: Historical and projected U.S. natural gas production rates under high and low scenarios of technological growth, oil price, and economic growth [EIA, 2017].

Conventional reservoirs of natural gas are created when the gas is trapped in a large pocket beneath an impermeable rock layer. Traditional wells are drilled vertically into a reservoir and the extraction process simply consists of collecting the natural gas that flows out [King et al., 2017] (Figure 1.2a). More recent well exploration and extraction activities have used horizontal drilling and artificial stimulation, commonly known as hydraulic fracturing or "fracking", in order to access shale natural gas reserves [API, 2017]. Shale natural gas is

contained within many tiny pores in underground rock formations that necessitates the use of artificial stimulation to be extracted and trapped [Baird et al., 2012].

In many unconventional wells, well bores are drilled vertically thousands of meters into the earth and then angled horizontally. Small explosive charges are detonated in the horizontal portion to initiate fissures, followed by large volumes of water, chemicals, and sand being pumped down the well and pressurized. This expands fractures in the shale rock to facilitate recovery of natural gas [Hoffman, 2015]. The pressure from the escaping gas causes some of the water and chemicals to flow up to the surface while the sand remains in the fissured rock to hold open the fractures [Harper, 2014]. The natural gas continues to flow to the surface for the production lifetime of the well (Figure 1.2b). Some wells must be "re-fracked' periodically to stimulate continued production.

These technological advances in unconventional extraction techniques, have provided access to previously impractical O&NG reserves contained in numerous shale rock formations in the U.S. [Swarthout et al., 2013]. Between 2005 and 2013, 82,898 hydraulic fracturing wells were drilled in the U.S., over 18,000 of which were located in Colorado [Ridlington et al., 2013]. Unconventional gas production is forecast to comprise 64% of the total U.S. gas production as soon as 2020 [API, 2017].

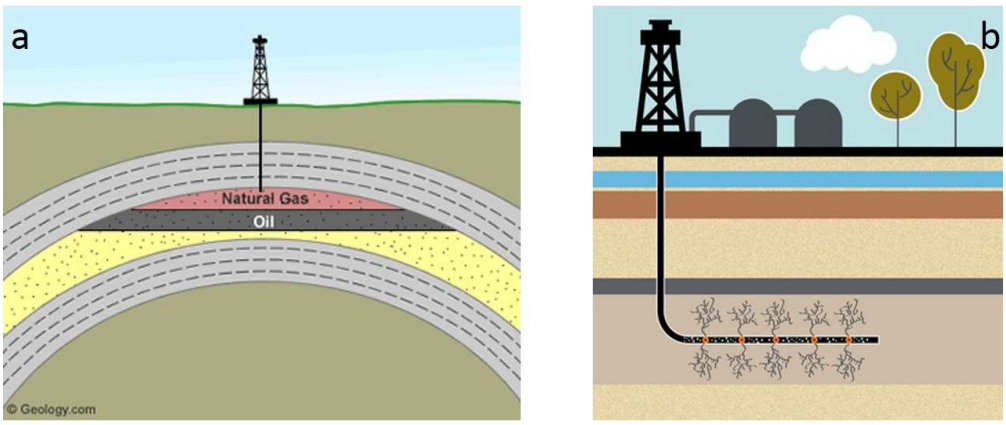

Figure 1.2: Diagram of a traditional, vertically drilled gas well (a) and a horizontally drilled, hydraulic fracturing well (b) [Netto, 2016; King et al., 2017].

Colorado is rich in energy resources due to its unique geology. There are several shale and sedimentary rock basins throughout the state and many deposits of coal in the northwest and southern regions of the state [Weiner, 2014]. Eleven of the 100 largest U.S. natural gas fields are located completely or partly in Colorado [EIA, 2016] and in 2015, 8.3% of all the producing O&NG wells in the U.S. were located in Colorado [EIA, 2016]. One of the largest shale formations in the U.S. is the Denver-Julesburg Basin (D-J Basin) which covers over 180,000km^2 in five different states and includes the majority of northeastern Colorado (Figure 1.3). Located in the Colorado Northern Front Range (CNFR) and within the D-J Basin is the Wattenberg field which is located predominantly under Weld County but extends into Larimer, Boulder, Broomfield, Denver, and Adams Counties.

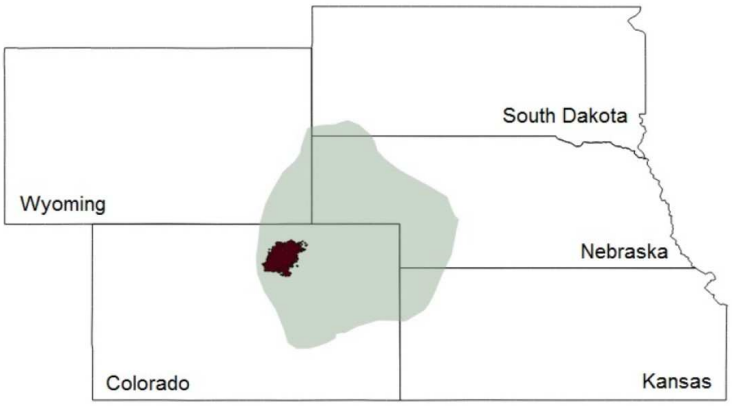

Figure 1.3: Map of Colorado, Wyoming, South Dakota, Nebraska, and Kansas with the Denver-Julesberg Basin (D-J Basin) shaded in light green. The Wattenberg gas field within the D-J Basin is highlighted in red [Collett et al., 2016].

Following the national trend, the production of O&NG in Colorado more than doubled between 2001 and 2016 [COGCC, 2016a]. As of 2014, over 90% of the new O&NG wells drilled in Colorado utilized hydraulic fracturing and between 1990 and 2012 the production of natural gas in Colorado increased by approximately 8 times, which was a direct result of the use of hydraulic fracturing technology [Weiner, 2014].

Growth in O&NG activity may be accompanied by an increase in the emissions of atmospheric pollutants such as volatile organic compounds (VOCs), which can be important due to their impacts on air quality and their effects on human health [Gilman et al., 2013]. While it was not quantified in this thesis, methane (CH_4) emissions from unconventional extraction of O&NG have been found to be significant [Collett et al., 2016; Gilman et al., 2013; Pétron et al., 2012; Swarthout, 2014]. Globally, CH_4 emissions are of interest because it acts as a greenhouse gas (GHG) that is 25 times more potent than carbon dioxide (CO_2) over a 100-year time scale [Jacob, 1999]. This thesis focuses on the regional impacts of non-methane hydrocarbon (NMHC) emissions from O&NG activity.

Many VOCs can react in the atmosphere to produce ozone (O_3) which is of particular interest in the CNFR since the region has been designated as a federal non-attainment area for O_3 by the U.S. Environmental Protection Agency (EPA) for several years [Thompson et al., 2014]. Most of the VOCs emitted from O&NG operations have been associated with elevated O_3 levels [Gilman, 2013; Swarthout et al., 2013; Thompson et al., 2014].

Figure 1.4 shows a typical sequence of reactions that yield O_3 starting with a VOC. The sequence is initiated when a VOC molecule reacts with a hydroxy radical (OH) in the presence of oxygen (O_2) producing an organic peroxy radical (RO_2) and water vapor (H_2O). RO_2 then reacts with nitric oxide (NO) in the presence of O_2 to form a secondary VOC, a hydroperoxyl radical (HO_2), and nitrogen dioxide (NO_2). HO_2 reacts with NO to form NO_2 which is then photolyzed by sunlight ($h\nu$) to form atomic oxygen (O). O is highly unstable and quickly reacts with O_2 forming O_3.

$$\mathrm{VOC + OH \rightarrow RO_2 + H_2O}$$
$$\mathrm{RO_2 + NO \rightarrow secondary\ VOC + HO_2 + NO_2}$$
$$\mathrm{HO_2 + NO \rightarrow OH + NO_2}$$
$$\mathrm{NO_2 + h\nu \rightarrow NO + O}$$
$$\mathrm{O + O_2 + M \rightarrow O_3 + M}$$

$$\mathbf{Overall:\ VOC + NO + h\nu + O_2 \rightarrow H_2O + secondary\ VOC + O_3}$$

Figure 1.4: A typical sequence of reactions that yield O_3 starting with a VOC. Adapted from Sillman [2003].

The direct impact of VOCs emitted from O&NG production on human health are of particular concern when O&NG operations are close to residential areas, schools, and businesses. Exposure to some aromatic VOCs has been associated with increased cancer risk, respiratory distress, and endocrine disruption [Bolden et al, 2015]. Benzene, toluene, ethylbenzene, and xylenes (BTEX) are a subset of aromatic VOCs that are classified by the EPA as Hazardous Air Pollutants (HAPs) [EPA, 2015]. In particular, exposure to benzene has been linked to leukemia, anemia and other blood disorders and cancers, immune system impairment, decreased respiratory function, and neural tube defects in newborns [Halliday et al., 2016]. While there is still a lot of uncertainty in specific source apportionment of benzene, the 2011 EPA National Air Toxic Assessment attributed 32% of all benzene emissions to a combination of the evaporation of fuels at gas stations, the use of solvents, and O&NG operations and processing plants [Bolden et al., 2015].

In addition to air toxics being emitted from O&NG wells, concern regarding site dangers due to infrastructure degradation and blowouts due to gas explosions have prompted state governments to enact minimum required setback distances for O&NG developments [Hoffman, 2015]. However, the distance that constitutes a safe setback between O&NG activities and populated areas is not well understood and research is currently lacking regarding distances that are adequate to protect the health and safety of the public [Haley et al., 2016]. As of 2016 when this study was completed, the Colorado Oil and Gas Conservation Commission (COGCC) minimum required setback distance for a drilling operation from a high occupancy building (i.e. schools) was 1,000ft (304.8m), and 500ft (152.4m) from all other building units [COGCC, 2016b].

The work detailed in this thesis took place in the City of Fort Collins and the Town of Timnath which are both located in Larimer County which partially overlaps the Wattenberg field. At any one time there are a few hundred wells in operation in Larimer County; however, the majority of the Wattenberg field lies within Weld County where there were over 24,000 wells in operation throughout 2016, which is approximately 41% of all the producing wells in

Colorado [COGCC, 2016a]. Figure 1.5 shows a map of the O&NG wells in the CNFR as of 2016.

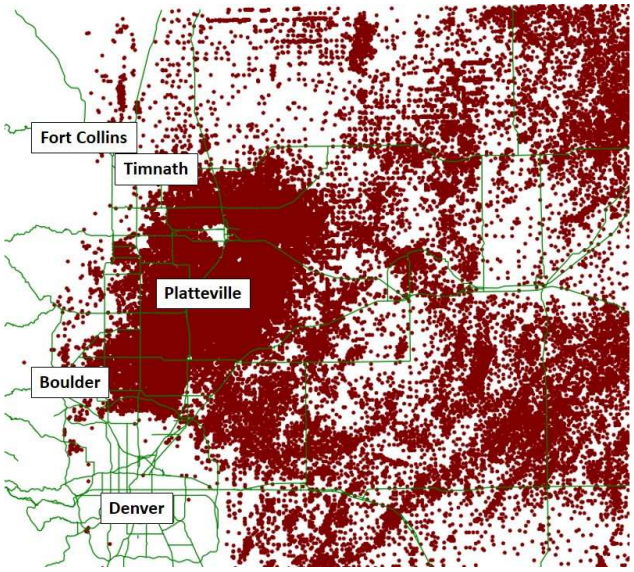

Figure 1.5: Map of the active O&NG wells in the CNFR. Individual wells are denoted by a red dot [COGCC, 2017].

1.2 Recent VOC Studies in the CNFR

Several recent VOC studies have been conducted in the CNFR utilizing whole air canister sampling and/or in-situ real-time gas chromatography (GC) techniques to estimate the impact of O&NG development on ambient VOC concentrations [ARS, 2014; Gilman et al., 2013; Halliday et al., 2016; Swarthout et al., 2013; Thompson et al., 2014]. In addition to reporting the raw concentrations of VOCs, these studies utilize the correlation and ratio between particular VOCs to help apportion contributing source types.

In the CNFR propane has been shown to be a strong tracer of O&NG activity while acetylene has been used as a vehicular emission marker [Gilman et al., 2013]. The primary source of i-pentane, n-pentane, n-butane and ethane in the CNFR is O&NG production [Halliday et al., 2014]; therefore, an air mass influenced strongly by O&NG activity would be expected to display a strong correlation between concentrations of these 4 light alkanes and propane and a poor correlation with acetylene. Table 1.1 summarizes the coefficients

of determination of i-pentane, n-pentane, n-butane, ethane, and benzene with propane and acetylene found in recent studies.

Another way to determine the influence of O&NG vs vehicular emissions on an air mass is by utilizing ratios of the pentane isomers (i-pentane and n-pentane) [Gilman et al., 2013], the butane isomers (i-butane and n-butane), and the ratio of toluene to benzene [Halliday et al., 2014]. Emissions from vehicle combustion are richer in i-pentane thus an elevated i-pentane to n-pentane ratio indicates a strong vehicle influence [Halliday et al., 2014]. Based on previous work comparing VOC data from the CNFR and major US cities, an i-pentane to n-pentane ratio of approximately 1.0 or less indicates a primarily O&NG influence while an i-pentane to n-pentane ratio of approximately 2.3 or greater indicates a primarily vehicular influence [Gilman et al., 2013]. Vehicular emissions show elevated n-butane concentrations and previous studies have reported pure vehicular exhaust to display an i-butane to n-butane ratio of 0.2 to 0.3 and O&NG emissions to have a ratio of 0.6 to more than 1 [Russo et al., 2010]. Fresh traffic emissions have displayed a toluene to benzene ratio of over 2 whereas emissions more influenced by O&NG generally exhibit toluene to benzene ratios less than 2 [Halliday et al., 2014]. The delineation in this ratio is not as clear for source apportionment; however, as the delineation for i-pentane to n-pentane and i-butane to n-butane ratios. The toluene to benzene ratio is also influenced by the differing oxidation rates of these two species in the atmosphere; toluene is more reactive than benzene [Seinfeld et al., 2016]. Table 1.2 summarizes the VOC ratios found in recent studies conducted in the CNFR.

Gilman et al. [2013] quantified a suite of VOCs using an in-situ 2-channel GC mass spectrometer (MS) at the Boulder Atmospheric Observatory (BAO) tower in Boulder, CO during the NACHTT (Nitrogen, Aerosol Composition, and Halogens on a Tall Tower) experiment. The BAO tower is located approximately 55km south of Fort Collins, approximately 30km north of the Denver metropolitan area, and is in the southwestern portion of Wattenberg Field. The measurements in this study took place from February 18, 2011 to March 7, 2011.

They observed i-pentane, n-pentane, n-butane, and ethane coefficients of determination (r^2) of 0.94, 0.94, 0.98, and 0.96 with propane and 0.30, 0.29, 0.29, and 0.37 with acetylene, respectively. They also calculated a coefficient of determination of 0.77 between benzene and propane concentrations and a coefficient of determination of 0.62 between benzene and acetylene. The average i-pentane to n-pentane ratio, i-butane to n-butane ratio, and toluene to benzene ratio measured was 0.89, 0.43, and 1.03, respectively. The high correlation of propane with compounds known to be associated with O&NG along with the reported VOC ratios led to the conclusion that O&NG production near BAO had a significant impact on the characteristics of the local air mass [Gilman et al., 2013]. Swarthout et al. [2013] also analyzed data from the NACHTT experiment and found similar results.

Thompson et al. [2014] collected a total of 30 24-hour time-integrated whole air canisters outside 7 different residences within and north of the town of Erie, CO. The measurements in this study were collected between March, 2013 and June, 2013.

They observed i-pentane, n-pentane, and n-butane coefficients of determination (r^2) of 0.91, 0.94, and 0.95 with propane and 0.08, 0.12, and 0.15 with acetylene, respectively. They also saw a coefficient of determination of 0.73 between benzene and propane and a coefficient of determination of 0.29 between benzene and acetylene. The average i-pentane to n-pentane ratio, i-butane to n-butane ratio, and toluene to benzene ratio measured was 1.01, 0.43, and 0.75, respectively. These results, reported by Thompson et al. [2014], led to a similar conclusion as Gilman et al. [2013]: O&NG emissions have a large-scale regional impact on ambient air quality.

Halliday et al. [2016] collected whole air canister grab samples at the Platteville Atmospheric Observatory (PAO) tower in Platteville, CO from mid-July to mid-August of 2014. The area around PAO is primarily rural, and there are areas of dense O&NG activity in the immediate vicinity. The tower is located approximately 45km southeast of Fort Collins and approximately 55km northeast of downtown Denver.

They observed i-pentane, n-pentane, n-butane and ethane coefficients of determination (r^2) of 0.99, 0.97, 0.99, and 0.94 with propane and 0.49, 0.43, 0.50, and 0.42 with acetylene, respectively. They also saw a coefficient of determination of 0.78 between benzene and propane and a coefficient of determination of 0.38 between benzene and acetylene. The average i-pentane to n-pentane ratio was 0.89 and the mean toluene to benzene ratio observed under calm conditions was 1.32. The results presented by Haliday et al. [2016] further agree with the conclusions made by Gilman et al. [2013] and Thompson et al. [2014] that there is a strong O&NG signature in NMHC detected in the CNFR.

Table 1.1: Summary of i-pentane, n-pentane, n-butane, ethane, and benzene coefficients of determination (r^2) with propane and acetylene found in recent studies conducted in the CNFR. NR indicates the coefficients of determination was not reported in the study.

	Propane					Acetylene				
Study	i-pentane	n-pentane	n-butane	ethane	benzene	i-pentane	n-pentane	n-butane	ethane	benzene
Gilman et al. [2013]	0.94	0.94	0.98	0.96	0.77	0.30	0.29	0.29	0.37	0.62
Thompson et al. [2014]	0.91	0.94	0.95	NR	0.73	0.08	0.12	0.15	NR	0.29
Halliday et al. [2016]	0.99	0.97	0.99	0.94	0.78	0.49	0.43	0.5	0.42	0.38

Table 1.2: Summary of VOC ratios found in recent studies conducted in the CNFR.

Study	i-pentane to n-pentane	i-butane to n-butane	toluene to benzene
Gilman et al. [2013]	0.89	0.43	1.03
Thompson et al. [2014]	1.01	0.43	0.75
Halliday et al. [2016]	0.89	0.41	1.32

Between November 15, 2013 and February 15, 2014, the City of Fort Collins and Memorial Resource Development, LLC (MRD) jointly funded a short term air quality monitoring assessment in order to quantify ambient air quality around O&NG development projects. Air Resource Specialists, Inc. (ARS) was contracted to conduct the study locally and the laboratory analysis was performed by the Eastern Research Group, Inc. (ERG). In part, the short term ARS [2014] study quantified 79 ambient VOC concentrations using 24-hour whole air time-integrated canister sampling in compliance with the EPA TO-12 methods. This study is the most comparable data to the work presented in this thesis since samples were

collected relatively close geographically, at a similar time of year, and analyzed using similar methods.

ARS [2014] measured VOC concentrations at 2 sites in northeast Fort Collins and 2 sites near Downtown Fort Collins. The 2 northwest Fort Collins sites were co-located with active O&NG projects. The "Well Pad" site was located near a producing well pad in an open field and the "Tank Battery" site was located near O&NG infrastructure that included storage tanks. The "City Park" site was located near a public pool in a park maintained by the City of Fort Collins and the "Mason Street" site was located on the roof of a Colorado State University (CSU) maintenance building on the school's main campus. A total of five canister samples were collected at each site every 12^{th} day following a recommended schedule from the EPA.

The mean i-butane to n-butane ratio observed at the "Well Pad" and "Tank Battery" sites were 0.55 and 0.38, respectively. The mean i-butane to n-butane ratio at the "City Park" and "Mason Street" sites were both 0.42. The mean toluene to benzene ratio at the "Well Pad" and "Tank Battery" sites were 1.82 and 1.37, respectively. The mean toluene to benzene ratio at the "City Park" and "Mason Street" sites were 1.75 and 1.82, respectively.

Although source apportionment conclusions are not explicitly stated in this report, the VOC ratios indicate that all 4 sites are influenced by a combination of O&NG operation and vehicular emissions. However, it is difficult to draw substantial conclusions on the influence of different VOC sources on ambient air quality in Fort Collins, having only sampled for 5 days over a 3 month period. In part, this thesis works to expand the available ambient VOC concentration data in Fort Collins and Larimer County.

In addition to quantifying VOC concentrations and determining source apportionment, recent studies in the CNFR have seen a connection between VOC emissions from O&NG and elevated ground level O_3 concentrations [Abeleira et al., 2017; Gilman et al., 2013]. Since May of 2012 the CNFR has been designated as a marginal non-attainment area for the 2008 8 Hour Ozone National Ambient Air Quality Standard (NAAQS) of 75ppbv [CDPHE

AQCC, 2016]. The propensity of a VOC to initiate the O_3 production cycle (R_{OH}), can be estimated as simply the product of the VOC mixing ratio in molecules cm^{-3} and the VOC rate constant with OH (k_{OH}), which has units of s^{-1}. The sum of the R_{OH} for each VOC is the total measured OH reactivity [Albeleira et al., 2017]. This calculation only accounts for the initial step in the O_3 production cycle; therefore, it is a very rough estimate of the total O_3 formation resulting from the measured suite of VOCs. Although it is difficult to compare OH reactivity observed across different studies, as the suite of VOCs measured through different methods varies, the total observed reactivity, as well as the fraction attributed to different VOC categories (i.e. alkanes, alkenes, aromatics, etc.), can still provide insight into the sources of O_3 formation in a region [Swarthout et al., 2013].

Abeleira et al. [2017] collected hourly measurements of 46 VOCs at the BAO tower over 16 weeks in the spring and summer of 2015. Their VOC suite included C_2-C_8 NMHCs, C_1-C_2 halocarbons, C_1-C_5 alkyl nitrates, and several oxygenated VOCs (OVOCs). They observed an average total VOC reactivity of $2.7s^{-1}$ in the spring and $4.0s^{-1}$ in the summer. In the summer, VOCs accounted for 50 - 64% of the total OH reactivity whereas in the spring VOCs accounted for only 35 - 48%. The remaining OH reactivity was attributed to a combination of NO_X, CH_4, and carbon monoxide (CO). Among the VOCs, the majority of the OH reactivity was attributed to a combination of alkanes, alkenes, and aromatics in the spring; however, these compounds only dominated in the morning during the summer with biogenic emissions (primarily isoprene) dominating in the afternoon. Although measurements were not recorded in the fall and winter, it was noted that VOCs would contribute more OH reactivity in the spring and summer due to the increase of biogenic sources along with increased evaporative emissions of anthropogenic hydrocarbons [Abeleira et al., 2017].

Gilman et al. [2013] observed a median total VOC reactivity of $2s^{-1}$ in wintertime. Their measured VOC suite contained additional OVOCs and biogenics compared to Abeleira et al. [2017] and the measurements were collected in a different season. These VOCs are highly reactive, and many display a strong seasonal variation, making direct comparisons between

the magnitude of the measured OH reactivity in these studies difficult. Gilman et al. [2013] estimated that C_2-C_6 alkanes accounted for 55 $\pm$ 18% of the OH reactivity in the winter and that on average 72 - 96% of these light alkanes were attributed to O&NG operations. This led the conclusion that O&NG production in northeastern Colorado is a significant source of O_3 precursors.

1.3 Thesis Overview

The work done in this thesis was initiated, in separate efforts, by the City of Fort Collins and the Town of Timnath because of concerns over the potential effects of O&NG operations on ambient air quality. The main goals of the combined studies, as analyzed here, were to determine the gradient of VOC concentrations across Fort Collins and Timanth, and provide a baseline to compare with future VOC measurements as O&NG development continues to increase in the CNFR. This work utilized one week time-integrated whole air canister sampling and gas chromatography flame ionization detection (GC-FID) to quantify a suite of VOCs collected at five sampling locations in Fort Collins and Timnath. In addition, a real-time in-situ GC was utilized at one of the sampling locations to provide higher time resolution (approximately hourly) VOC measurements.

In-depth analysis using the VOC concentration data was performed in order to compare the measured concentrations to those found in previous works, estimate source apportionment using various VOC ratios and meteorological data, and determine O_3 production potential through OH reactivity calculations.

Further motivation for the Timnath measurements was the possibility of the development of six new unconventional wells near an elementary school in Timnath. While the O&NG activity will take place outside the legal setback distance, the potential emissions and their effects concerned the parents of students as well as the staff of the school [Kyle, 2015]. Most community members who express concern regarding O&NG development near residential areas, schools, and businesses note that the uncertainty as to what the effects of further development will be is their biggest worry. Therefore, with the potential of new O&NG

development in close proximity to the school, a secondary objective of this thesis was to assess the localized impact of a future O&NG development using the American Meteorological Society (AMS)/EPA air dispersion model AERMOD.

The following chapter details the methods of field measurements and sample analysis as well as describing the utilization of AERMOD. Chapter 3 presents the results and analysis of the VOC data and AERMOD simulations. Chapter 4 provides conclusions and recommendations for future work.

Chapter 2

Methods

2.1 Experimental Design

2.1.1 Sampling Locations

Time-integrated whole air canister samples were collected at a constant flow rate over the course of approximately one week at five locations in Larimer County, CO. The objectives of this aspect of the thesis were to determine the gradient of VOC concentrations across a subsection of the CNFR, provide a baseline to compare potentially elevated VOC concentrations from future O&NG development, as well as provide a better understanding of the current influence of O&NG emissions in the CNFR. Whole air samples were collected at an elementary school, residential area, two natural areas, and a gas station (Figure 2.1) in Fort Collins and Timnath. The number of samples collected and the range of dates varied among the five locations. More details regarding the canister sampling and analysis methods are provided in Section 2.2. In addition, an in-situ gas chromatography (GC) system measured real-time ambient VOC measurements at the residential area. More details regarding the in-situ GC sampling method are provided in Section 2.3.

Figure 2.1: Map of the five sampling locations in the CNFR.

The first site was an elementary school (40.515^o, -104.950^o) located in the Town of Timnath, CO in Larimer County. The school campus is within 0.5km of the border of Weld County, CO where there is extensive O&NG activity. It is surrounded by actively developing residential neighborhoods and is approximately 3.5km east of the interstate highway (I-25). The canister was affixed to the roof line of a mobile classroom approximately 3m above the ground (Figure 2.2). The classroom was located on the northeast side of the campus and was the closest structure to the location of a potential future O&NG development site.

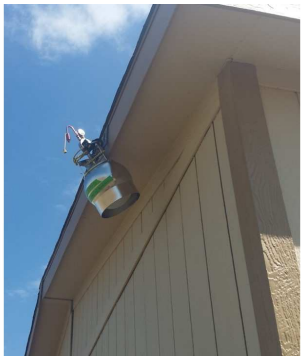

Figure 2.2: Canister affixed to the roof line of a mobile classroom on the elementary school campus.

The second site was a residential area (40.619^o, -105.033^o) located in north Fort Collins, CO in Larimer County. It is positioned approximately 2.5km west of the interstate highway (I-25) and 5.5km northeast of downtown Fort Collins. While there is not nearly as much O&NG development in Larimer County compared to Weld County, there is an area approximately 1.5km northwest of the residential area that contains several producing O&NG wells. The sampling canister was affixed to a tripod at about 2m above ground in a grassy area in the backyard of a house. The only building structure near the sampling setup was a one story residence about 5m to the west. There were undeveloped land parcels and fallow fields directly east of the site and the Anheuser-Busch Brewery was located further east (about 2km). Although it is not modeled in this thesis, it should be noted that there is a proposed O&NG development in the fields to the east of this site. Concern regarding the effect of

O&NG emissions on the nearby residential area was an important factor in motivating the City of Fort Collins to fund this portion of the study.

The third site was Fossil Creek Natural Area (40.484^o, -105.016^o) located in southeast Fort Collins, CO in Larimer County and positioned approximately 2.0km west of the interstate highway (I-25) and less than 0.5km north of a busy roadway (County Rd. 32). Unlike the residential area, there is no dense O&NG development in the immediate vicinity and there are no actively producing wells within a 3km radius. The sampling canister was affixed to a building adjacent to the parking lot of the Natural Area at about 2m above ground. The parking lot is only used by the Natural Area staff and visitors and has a maximum capacity of about 40 vehicles. Visitation to this location peaks in Apr.-Jun. (43%) and is lowest in Oct.-Dec. (16%) [City of Fort Collins, 2003].

The fourth site was Soapstone Natural Area (40.986^o, -105.009^o) located in northern Larimer County, CO about 40km north of Fort Collins and only about 1.5km south of the Wyoming border. It is positioned approximately 8km west of the interstate highway (I-25) and there is little traffic or O&NG development in the immediate vicinity. The area surrounding the sampling location is mostly open and undeveloped prairie lands. The canister was affixed to a wooden pole outside of a shed at approximately 1m above ground (Figure 2.3). The building was seldom utilized and vehicular traffic was sparse on the surrounding dirt roads. This location is used as the park ranger headquarters throughout the year.

Figure 2.3: Canister affixed to post at the Soapstone NA ranger headquarters.

Sampling was also conducted at a gas station (40.523^o, -104.989^o) in order to provide data that was directly influenced by vehicular combustion and gasoline vaporization to compare to the other four sampling sites where it was anticipated that O&NG emissions would be the predominant influence. The gas station is located in the Town of Timnath, CO and is adjacent to a major roadway (Harmony Rd.). It is located 0.25km east of an interstate highway (I-25). The canister was affixed to the back of a sign approximately 20m north of the gasoline pumps (Figure 2.4). In addition to the heavy vehicle traffic on the roadways and in the gas station parking lot, there is a major shopping center and another gas station located across the street (approximately 100m north).

Figure 2.4: Canister affixed to an exit sign north of the gas station pumps.

2.1.2 Sampling Duration

Due to logistical and funding restrictions, sampling at the residential area and the two Natural Areas was limited to the Fall of 2015. A real-time in-situ GC sampled for a period of approximately 3 weeks in the Fall of 2015; however, it sampled at approximately an hourly interval, providing a comparatively higher resolution data set. Whole air sampling at the elementary school and the gas station began in the summer of 2015 and spanned 32 weeks spaced over more than 1 year, providing a much more complete data set than was obtained at the other canister sampling locations. Figure 2.5 lists the study sampling periods as well as the total number of whole air week-long time-integrated canisters collected at each site.

Sample Site	Number of Weekly Canister Samples
Elementary School	32
Residential Area	4
Fossil Creek NA	9
Soapstone NA	11
Gas Station	32

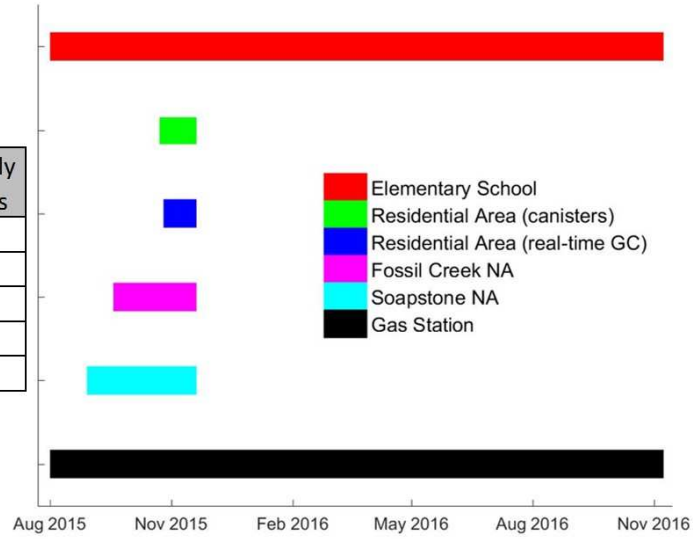

Figure 2.5: Canister and real-time in-situ GC sampling timeline and the number of weekly integrated canisters collected at each of the five sampling locations.

2.1.3 Meteorological Data

A Climatronics Corporation All-In-One (AIO) Weather Sensor was set up to collect data for wind speed, wind direction, and temperature at the residential area for the duration of sample collection. This AIO weather station was attached to the same tripod as the sampling canister. For the elementary school, wind speed and direction data were obtained from the Timnath Ranch Weather Station (KCOTIMNA3: 40.505^o -104.958^o) [The Weather Company] located approximately 1.2km southwest of the elementary school. For the two Natural Areas, meteorological data were downloaded from two Colorado Agricultural Meteorological network (CoAgMet) surface stations. The Fort Collins AERC (FTC01: 40.595^o, -105.137^o) station was used to represent conditions at Fossil Creek NA and the Cherokee Park (CKP01: 40.826^o, -105.267^o) station was used for Soapstone NA [CoAgMet].

2.2 Whole Air Time-Integrated Canister Sampling

2.2.1 Whole Air Sampler Description

Entech Instruments 6L Stainless Steel Canisters with an internal Silonite® coating were used to collect weekly integrated whole air samples (Figure 2.6). The Silonite® coating of the canisters provides an inert internal surface that allows for long term storage of collected VOCs. These types of canisters have been shown to hold VOC concentrations stable for more than a month [LeBouf et al., 2012] and samples were stored for shorter durations (no longer than 30 days) prior to analysis in this work. The canister along with the base, valve, and handle is approximately 31.5cm in height and the spheroid body of the canister has a central diameter of approximately 23cm. The canister is equipped with an Entech Toxic Organics Valve (TOV-2) which ensures a leak resistant seal. All of the components and specifications of the Entech 6L canisters are certified to meet or exceed the requirements of the EPA TO-14a and TO-15 methods.

Figure 2.6: Photo of the Entech Instruments 6L Silonite®-coated canister used for time-integrated collection of whole air samples.

2.2.2 Flow Controller Calibration

An Entech Instruments CS1200ES Flow Controller (Figure 2.7) was affixed to a 6L canister in order to perform time-integrated whole air sampling. The CS1200E Flow Controller consists of three main parts: the vacuum controller body, the flow restrictor, and the inlet. Proper

calibration prior to field deployment of the flow controller was important to ensure that ambient sampling flow rates were consistent throughout the study. The flow rates were checked and corrected as needed prior to each field deployment.

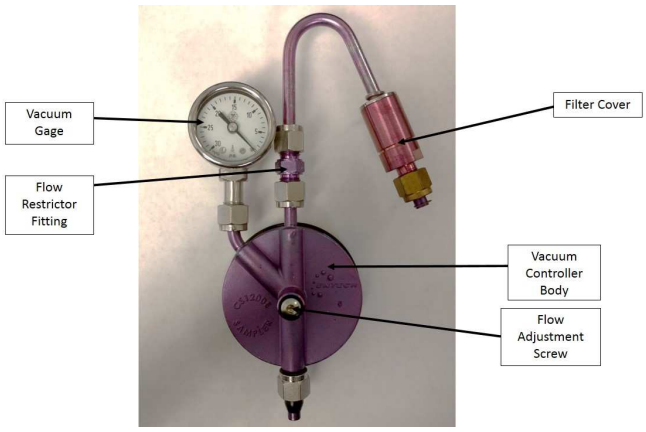

Figure 2.7: Entech Instruments CS1200ES Flow Controller.

The vacuum controller maintains a -0.4 to -1.5 psi pressure differential relative to atmospheric pressure, no matter what the vacuum is on the outlet [Entech, 2015]. Prior to calibration, the correct flow restrictor fitting must be attached. Several sizes are provided with the flow controller in order to accommodate a wide range of desired flow rates. The flow restrictor fitting utilized in this thesis can provide between 2 and 7 days of constant flow. For any given restrictor, the flow rate can be adjusted by a factor of 3 to 4 in order to finely tune the exact desired flow rate [Entech, 2015] using the flow adjustment screw to control the pressure on the vacuum controller. The vacuum gage reports a range of 0" Hg to 30" Hg of vacuum. The flow controller contains a filter at the sample inlet and a brass cap is attached at the filter cover to prevent contaminants from entering the sample inlet when the flow controller is not in use.

To calibrate the CS1200ES Flow Controller, it was attached to a cleaned and evacuated 6L Silonite®-coated stainless steel canister (Figure 2.8). The brass cap was removed from the flow controller and the canister was opened and then immediately closed. If the canister had been properly cleaned and evacuated and there were no leaks in the setup, the vacuum gage

showed a value over 20" Hg of vacuum. The time it took for the vacuum pressure to drop from 20" Hg to 10" Hg was recorded. According to the Entech CS1200ES Flow Controller Operation and Care Guide [Entech, 2015] a time of 65.5 seconds equates to a constant flow rate of $0.52\frac{mL}{min}$, which would fill a 6L canister in approximately 1 week. If the time recorded was more or less than 65.5 seconds the flow controller was adjusted by turning the flow adjustment screw and retested.

Figure 2.8: Photo of the Flow Controller attached to the 6L Silonite®-coated canister, prepared for field deployment.

2.2.3 Sampling Canister Cleaning and Evacuation

Proper cleaning and testing of the Silonite®-coated 6L canisters prior to field deployment is important to ensure that ambient sampling results are not biased by contamination or off-gassing occurring in the canister. Prior to each deployment, the canisters were cleaned and evacuated using an Entech Instruments 3100D Canister Cleaning System (Figure 2.9) controlled by Entech Instruments 3000/3100 Canister Cleaner v3.6 Software. The procedure used was based on the recommendations of Entech Instruments and the cleanliness certification required by EPA Compendium Methods TO-12, TO-14A, and TO-15.

Figure 2.9: Photo of the Entech Instruments 3100D Canister Cleaning System used to clean and evacuate the 6L Silonite®-coated canisters.

The canister cleaning system has the capacity to clean four 6L canisters simultaneously. Canisters were cleaned by evacuating to approximately 1torr and refilling to ambient pressure with Ultra High Purity (UHP) Nitrogen. This sequence was repeated 8 times inside an oven heated to 80^{o}C in order to remove VOCs introduced during the previous sampling. After cleaning, the canisters were pumped down to 0.01torr using a molecular drag pump to prepare them for the next sampling deployment. In each cleaning batch, one of the canisters was selected as a batch blank and filled with UHP Nitrogen. This canister was analyzed along with the canisters that were utilized in field sampling in order to ensure the performance of the cleaning system and that no contamination occurred as a result of the cleaning procedure.

2.2.4 Canister Analysis using the 5-channel GC

The concentrations of 48 VOCs in the canister samples were analyzed using a 5 channel GC coupled with three Flame Ionization Detectors (FID), an Electron Capture Detector (ECD) and a quadrupole mass spectrometer (MS). The VOC concentrations reported in this thesis were obtained using the 3 FIDs; however, the GC system has the capability to report hundreds of VOC concentrations if all 5 channels are utilized. The 5-channel GC

system was comprised of a 30cm long stainless steel cryogenic pre-concentration loop with an internal diameter of 0.3175cm packed with 1mm diameter glass beads, a splitter box, an excess volume canister, and three GC systems (Figure 2.10).

The first GC was a Shimadzu Corporation GC-17A that contained 2 analytical columns: (1) a 50m long Varian-Chromopack $Al_2O_3/NaSO_4$ PLOT column with an internal diameter of 0.53mm and a film thickness of 10μm; (2) a 25m long Varian-Chromopack CP-PoraBond Q column with an internal diameter of 0.25mm and a film thickness of 3μm coupled with a 30m long Restek XTI-5 column with an internal diameter of 0.25mm and a film thickness of 0.25μm. These columns were connected to a FID and were used to measure C_2-C_7 NMHCs and C_6-C_{10} NMHCs, respectively. The second GC was a Shimadzu Corporation GC-17A that also contained 2 analytical columns: (1) a 60m long Varian-Chromopack VF-1ms column with an internal diameter of 0.32mm and a film thickness of 1μm; (2) a 60m long Ohio Valley Specialty Chemical OV-1701 column with an internal diameter of 0.25mm and a film thickness of 1μm. These columns were connected to a FID used to measure C_4-C_{10} NMHCs and an ECD used to measure C_1-C_2 halocarbons, and C_1-C_5 alkyl nitrates, respectively. The third GC was a Shimadzu Corporation GCMS-QP5050A and contained one analytical column: a 60m long Ohio Valley Specialty Chemical OV-624 column with an internal diameter of 0.25mm and a film thickness of 1.4μm. This column was connected to a quadrupole MS used to measure C_6-C_{10} NMHCs and C_1-C_2 halocarbons. Additional details regarding the 5 channel GC system are available in Appendix A. The EPA TO-15 method for sample analysis was followed and this method is further detailed in Sive [1999], Zhou et al. [2010], Russo et al. [2010], and Swarthout [2014]. The detector data were collected using the Agilent MSD ChemStation Data Analysis Software. The details of chromatogram data analysis are discussed in Section 2.2.6.

Prior to entering the analytical columns, the air sample aliquot was cryogenically pre-concentrated in order to facilitate the trapping of the light VOC molecules. The pre-concentration procedure was as follows. First, the system, except for the excess volume can,

was purged with UHP helium for 4 minutes. After the helium flow was shut off, the system was pumped down to below 0.5torr. The pre-concentration loop was submerged in a small dewar of liquid nitrogen for 2 minutes. The canister containing the air sample was then attached and 300torr of air from the canister was allowed to flow into the pre-concentration loop trapping a 540cm^3 (STP) aliquot of the sample. After allowing 1 minute for the pressure to stabilize, the loop was isolated, the canister was removed, and the system was pumped down. The pre-concentration loop was submerged in water at approximately 95^{o}C in order to re-volatilize the trapped analytes. At this point the sample was ready to be injected into the GC columns.

When the sample was injected, the helium carrier gas directed the contents of the pre-concentration loop to a 1/16" stainless steel transfer line leading to the splitter box which evenly divided the homogeneous sample and directed it to each of the 5 analytical columns. The carrier gas was allowed to flow through the loop for 5 minutes to ensure all trapped analytes flowed to the columns. Following the sample analysis, the GCs were cooled using liquid nitrogen using a pre-programmed sequence to ensure reproducibility. A complete cycle of pre-concentrating a sample, injection, and analysis took approximately 33 minutes.

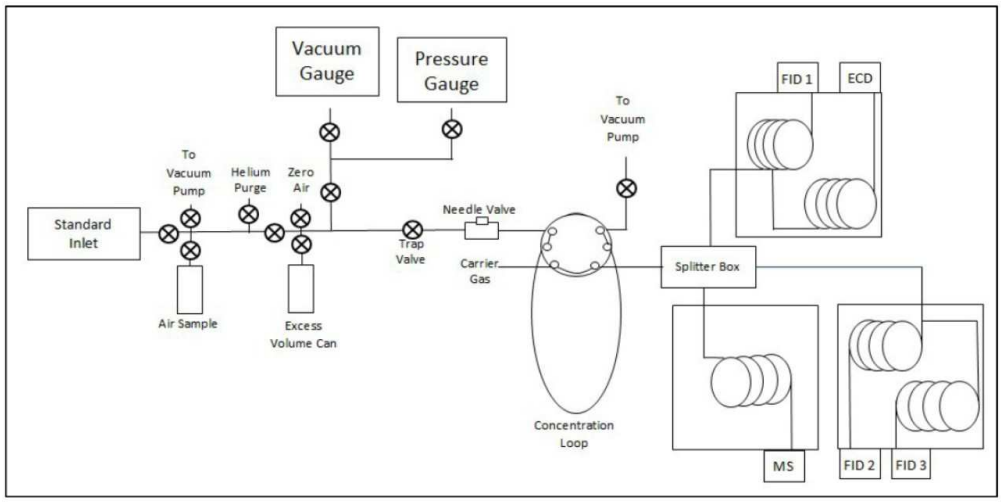

Figure 2.10: Schematic of the 5-channel GC pre-concentration system and GC instruments used for canister sample analysis [Hilliard, 2016].

2.2.5 5-channel GC Quality Control

System baseline and any carryover from previous samples were addressed by trapping and analyzing 200torr of VOC-free air (zero air). All steps for analysis of the zero air were identical to those of the ambient samples. Zero air was produced by removing VOCs from ambient air by pumping it through a 0.5% pb, Al_2O_3 catalytic converter heated to 425^{o}C.

At the end of each analysis day a Linde Gas North America LLC high-pressure standard was used in order to track instrumental drift over time. The procedure for running a standard was also the same as the samples, except the standard was used to fill the excess volume can which was then used to trap 200torr of the standard gas in the pre-concentration loop. Through multiple standard analysis, the relative standard deviation (RSD) of the 5 channel GC system was found to be 1 - 8% for NMHCs, 3 - 15% for halocarbons, and 3 - 8% for alkyl nitrates [Zhou et al., 2017].

Prior to the analysis of the canister samples presented in this thesis, a nine point calibration was performed in order to obtain the calibration curve slope for each of the 48 VOCs. Each of the nine points was analyzed twice to ensure precision. The same Linde Gas North America LLC high-pressure standard run at the end of each day was used and in order to obtain the desired concentration, the standard was diluted using the zero air generator.

Zero air blank runs were used to determine the limit of detection (LOD) of the system. The LOD was calculated using the following equation [Swarthout, 2014]:

$$\text{LOD} = \frac{\bar{x}+3\sigma}{slope} \tag{2.1}$$

where $\bar{x}$ is the mean area of the integrated analyte peak for each VOC in the blank samples, σ is the standard deviation of the integrated analyte peak area for each VOC in the blank samples, and *slope* is the slope of the calibration curve for each VOC. For measurements where the values of VOCs were below the LOD, a value of $\frac{LOD}{2}$ was used for the corresponding VOC. Appendix B shows the LOD and calibration statistics for the 5 channel GC.

2.2.6 Chromatogram Post-Processing

Shimadzu CLASS-VP software was used to analyze the chromatogram output from the 5-channel GC. The method used to identify each peak was constructed based on the retention time of VOCs in previous standard runs. The peak corresponding to each VOC in the sample chromatograms was analyzed manually to obtain the integrated peak area. Using the calibration curve slopes for each VOC (Appendix B) and correcting for the difference in pressure between the sample and the calibration standard run, the concentration of each VOC was obtained. The system background was very low; therefore, it was not necessary to correct the VOC concentrations based on blank sample runs. Swarthout [2014] noted that small but consistent peaks in the blank samples were seen on a very similar GC-FID system for only four compounds: methanol, ethanol, acetone, and methyl ethyl ketone (MEK), none of which were quantified in this thesis. The following equation was used to calculate the concentration of each VOC in a sample:

$$\text{Sample Conc.} = \frac{(Cal.CurveSlope)*(PeakArea)}{(Samp.Pressure/Std.Pressure)} \tag{2.2}$$

where $Cal.CurveSlope$ is the slope of the established calibration curve for a particular VOC, $PeakArea$ is the area of the sample peak obtained through chromatogram post-processing, $Samp.Pressure$ is the pressures of the canister sample and $Std.Pressure$ is the pressure of the standard run on the 5-channel GC system.

2.3 Real-Time In-Situ GC Sampling

2.3.1 Real-Time GC Analysis System

In addition to canister sampling at the residential area, an in-situ 4 channel GC was used for the near real-time collection and analysis of air samples for 23 VOCs. The in-situ GC had a total sampling cycle of 1 hour (15 min for ambient sample collection and 45 min for the cryogen-free pre-concentration process and sample analysis). The in-situ GC system is comprised of a Chart Inc. Qdrive 2s102K cryocooler, a 4" long stainless steel tube with an

internal diameter of 3/16" packed with Ohio Valley 1mm diameter glass beads, a splitter box, and two GC systems.

The first GC was a Shimadzu Corporation GC-17A that contained 2 analytical columns: (1) a 50m long Varian-Chromopack $Al_2O_3/NaSO_4$ PLOT column with an internal diameter of 0.53mm and a film thickness of 10μm; (2) a 60m long Varian-Chromopack VF-1ms column with an internal diameter of 0.32mm and a film thickness of 1μm. Both of these columns were connected to a FID and were used to measure C_2-C_7 NMHCs and C_6-C_{10} NMHCs, respectively. The second GC was a Shimadzu Corporation GC-17A that contained 2 analytical columns: (1) a 60m long Varian-Chromopack CP-PoraBond Q column with an internal diameter of 0.25mm and a film thickness of 3μm (2) a 60m long Varian-Chromopack VF-1701 column with an internal diameter of 0.25mm and a film thickness of 1μm. These columns were connected to a FID used to measure select OVOCs and an ECD used to measure C_1-C_2 halocarbons and C_1-C_5 alkyl nitrates. Additional details of the real-time in-situ GC used can be found in Appendix A. The in-situ GC system used in this thesis was similar to that detailed in Sive et al. [2005], Abeleira et al. [2017], and Zhou et al. [2017].

An internal program initiated the process of trapping ambient air in the loop when it was cooled by the cryocooler to a set point temperature of -180^{o}C by pulling 1000cm^3 of ambient air through the loop at a rate of 200$\frac{cm^3}{min}$. After trapping of the sample was complete, 100cm^3 of helium at a rate of 100$\frac{cm^3}{min}$ was passed through the loop. When the ambient sample is reheated, O_3 and alkenes will react [Koppman et al., 1995]; therefore, helium was passed through the sample loop in order to quench O_3-alkene reactions. Since the loop temperature is maintained at -180^{o}C, passing helium through does not impact the trapped VOCs; however, it does remove the bulk N_2, O_2, and O_3 from the loop [B. Sive, personal communication, October 3, 2017]. Many studies have shown this to be a superior method for alleviating O_3-alkene reactions to passing the sample through an O_3 scrubber, because the components of the scrubber can cause artifacts and it requires regular maintenance [Sive et al., 2005]. The loop was then isolated from the system and heated rapidly to 100^{o}C in order to volatilize

the trapped VOCs. The sample was then carried by a flow of helium to the splitter box via a Silonite®-coated transfer line. The splitter evenly divided the homogeneous sample and directed it to each of the 4 analytical columns.

After 10 ambient air samples had been analyzed, two whole air standards were analyzed in order to track any instrumental drift over the duration of the system deployment and determine the measurement precision. The relative standard deviation (RSD) of the in-situ GC system was found to be 1 - 8% for NMHCs, 3 - 15% for halocarbons, and 3 - 8% for alkyl nitrates [Zhou et al., 2017].

The in-situ GC system was operated at the residential area for approximately 3 weeks in the fall of 2015. It was located in the basement of a single family residence and the inlet of the system (1/8" stainless steel tubing) was positioned outside the building at a height of approximately 2m above ground. The total length of the inlet was approximately 3m.

2.4 AERMOD Dispersion Modeling

2.4.1 Model Overview

The American Meteorological Society/Environmental Protection Agency air dispersion and regulatory modeling program (AERMOD) is a steady-state plume model that assumes Gaussian pollutant distribution in the vertical and horizontal directions in a stable boundary layer (SBL). In a convective boundary layer (CBL) AERMOD assumes a Gaussian horizontal pollutant distribution and a bi-Gaussian vertical pollutant distribution. In a CBL, AERMOD accounts for portions of the plume mass being lofted to the top of the boundary layer before mixing and plume mass that penetrates beyond the boundary layer and later returns. Other dispersion models utilize a variety of additional variables which complicate the process and introduce additional uncertainties whereas the AERMOD approach does not, allowing it to be physically realistic while also being simpler to implement [Cimorelli et al., 2004]. AERMOD's performance has been shown to be superior or equivalent to other commonly applied regulatory air dispersion models [Perry et al., 2005].

The AERMOD modeling system consists of 3 major components: a terrain data pre-processor (AERMAP), a meteorological data pre-processor (AERMET), and the main dispersion model program (AERMOD). AERMET is used to generate the boundary layer parameters for input into AERMOD, while AERMAP generates the terrain data for the modeled region for input into AERMOD (Figure 2.11). AERMOD then calculates the average pollutant concentration increase for a specified time period based on a series of input parameters (described in Section 2.4.2).

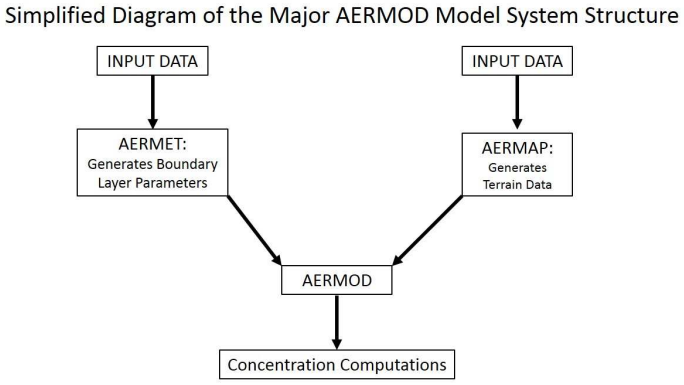

Figure 2.11: Simplified diagram of the major AERMOD model system structure. Adapted from Cimorelli et al. [2004].

2.4.2 Model Input Parameters

AERMOD simulations for benzene were performed at the potential location of six new directional wells near the elementary school in order to estimate increased ambient levels when the wells go into production. Model simulations were conducted using meteorological data for the year 2009 collected near the western shore of Hamilton Reservoir in Fort Collins, CO (40.854^o, -105.038^o) [Malone, 2009]. This meteorological station is approximately 40km north of the elementary school; however, it was the closest station that could provide the standard hourly surface and upper air sounding meteorological data and the 1-minute automated surface observing system (ASOS) wind data needed for an entire year to run the model. This meteorological data was obtained pre-processed in accordance with USEPA Guideline on Air

Quality Models directly from the CDPHE. A ground level square receptor grid consisting of 961 points separated horizontally by 100m was centered on the proposed new well site providing a 3.0km x 3.0km grid that covered the elementary school and the surrounding neighborhoods (Figure 2.12). This fine resolution receptor grid exceeds the CDPHE recommendation of 250m grid spacing for 1km - 3km grids for permitting purposes [CDPHE, 2011].

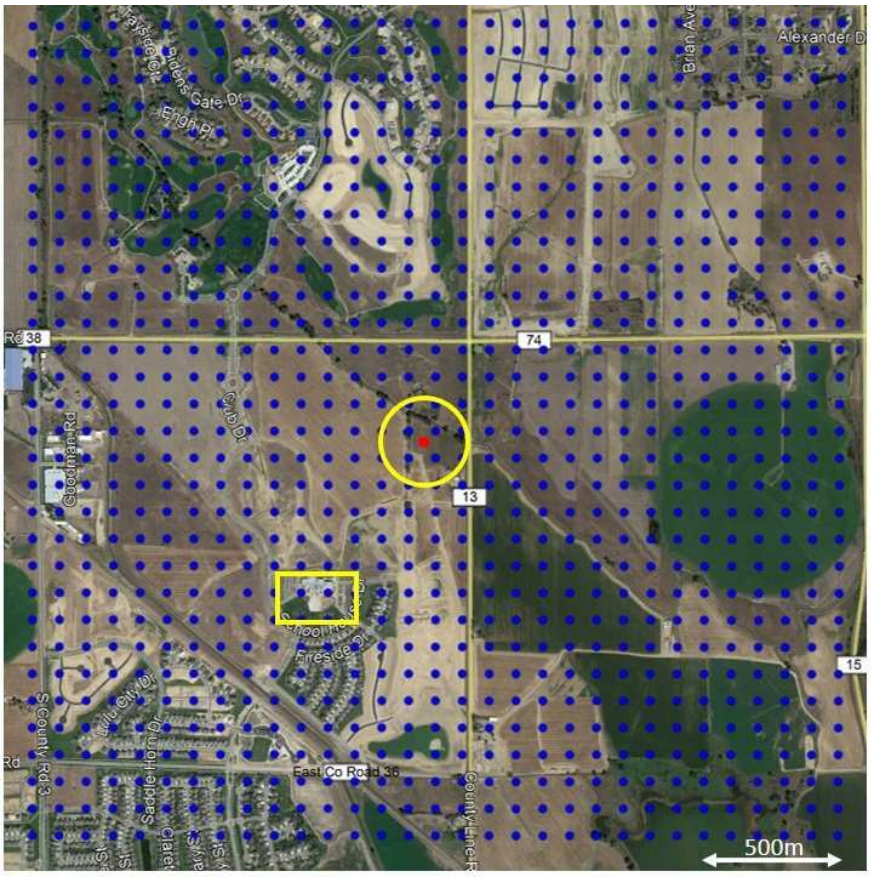

Figure 2.12: Map of the 3.0km x 3.0km receptor grid consisting of 961 points separated by 100m (blue dots). The proposed well site is marked by a red dot inside the yellow circle and the school campus is denoted by a yellow rectangle.

Regional land cover data was obtained from the United States Geological Service (USGS) National Land Cover Data 1992 archive (NLCD92). The regional terrain data were obtained from the USGS in the National Elevation Dataset (NED) format. Both of these data sets are publicly available from the USGS using the Multi-Resolution Land Characteristics Consortium (MRLC) viewer [USGS, 2017].

The future well pad was modeled as a 40.0m^2 (8.0m x 5.0m) area source (in accordance with the CDPHE regulatory guidelines) centered in the middle of the drilling area of the six proposed directional wells emitting at 3m above the ground. Five separate model runs were conducted using the 5^{th}, 25^{th}, median, 75^{th}, and 95^{th} percentile emission rates found at ten production well sites in the CNFR as reported by Collett et al., [2016].

AERMOD can model sites as line, volume, or point sources as well; however, it is believed that proposed well development sites are best modeled as area sources since a relatively large emitting area, such as a well pad, can be approximated as a source emitting from a flat plane with no temperature or velocity associated with the emissions [USEPA, 2004]. This introduces fewer variables than using multiple point sources for which these variables must be specified. Previous studies have modeled O&NG well pads as area sources [Collett et al., 2016; Friesema, 2012]. The average benzene concentration increases for every hour of the simulated year 2009 were obtained at each of the 961 receptor points. The main objective for utilizing AERMOD in this work was to estimate the increased benzene concentrations students and staff could be exposed to if the proposed directional wells were drilled near the school.

Chapter 3

Results

3.1 Whole Air Time-Integrated Canister Sampling

The concentrations of 48 VOCs were measured using week-long time-integrated whole air canister sampling at Fossil Creek NA, Soapstone NA, and a residential area in the City of Fort Collins and at an elementary school and gas station in the Town of Timnath. The whole air samples were processed using the methods described in Section 2.2. The chemical formulae and relevant sources of the VOCs analyzed are listed in Appendix C. The sampling duration and range of dates varied among the five locations. Sample collection took place from August, 2015 to November, 2016, with the highest number of samples collected at the elementary school (32) and the Gas Station (32). Sampling was limited to the fall of 2015 (September, 2015 - November, 2015) and thus fewer samples were collected at the residential area (4), Fossil Creek NA (9), and Soapstone NA (11). It is important to note potential limitations due to the smaller sample sizes at some locations, especially the residential area, while discussing the canister VOC data. Data obtained from the in-situ real-time GC at the residential area are analyzed in Section 3.2.2 to allow for a more robust statistical analysis of VOC concentration trends at this site.

3.1.1 VOC Concentrations in Fort Collins and Timanth

Figures 3.1 - 3.5 show plots of select VOC concentrations from weekly time-integrated whole air canister samples at the elementary school (3.1), residential area (3.2), Fossil Creek NA (3.3), Soapstone NA (3.4), and the gas station (3.5). While sampling time periods were different among the sites, all canister samples are shown in these plots since the concentrations of the presented VOC subset do not vary greatly on a seasonal basis (Appendix Figure D.1) . In the box and whiskers plots (Figures 3.1 and 3.3 - 3.5) the edges of the box represent the 25^{th} and 75^{th} percentiles while the line inside the box represents the median. The edges of the whiskers represent the 5^{th} and 95^{th} percentiles. Summary tables of all VOC concentrations at the five sampling locations can be found in Appendix Tables D.2 - D.6. Light alkanes

(ethane, propane, i-butane, n-butane, i-pentane, and n-pentane) are shown here because these compounds are commonly associated with O&NG emissions [Gilman et al., 2013; Halliday et al., 2014]. BTEX compounds are shown because they are known to be emitted from O&NG [Bolden et al., 2015] as well as combustion sources [Zhang et al., 2012] and can be harmful to human health [Bolden et al., 2015; Halliday et al., 2016]. Finally, acetylene data are shown because its emissions are associated primarily with combustion sources [Gilman et al., 2013], providing a comparison to the O&NG sources.

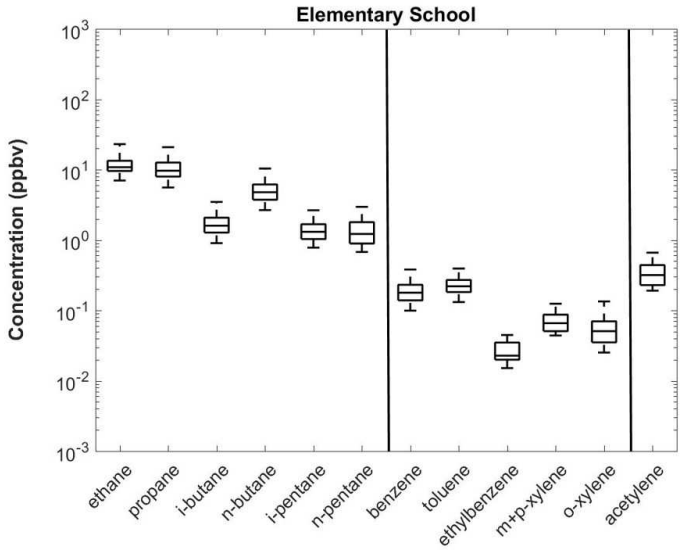

Figure 3.1: Select VOC concentrations from weekly time-integrated whole air canister samples at the elementary school (n=32).

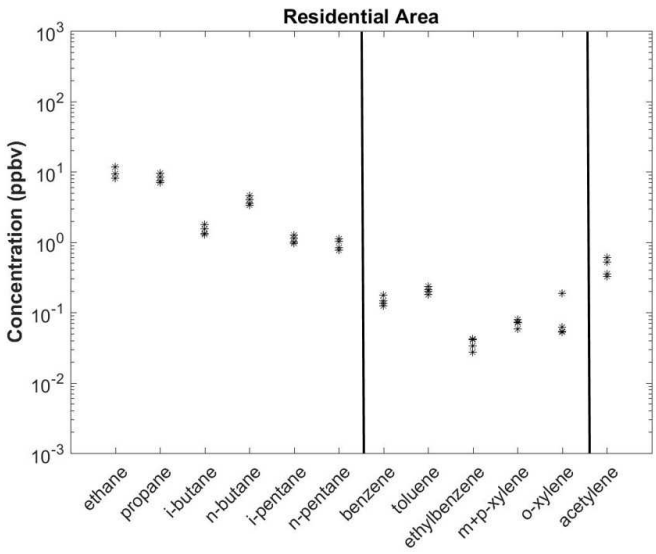

Figure 3.2: Select VOC concentrations from weekly time-integrated whole air canister samples at the residential area (n=4). All concentration values are shown.

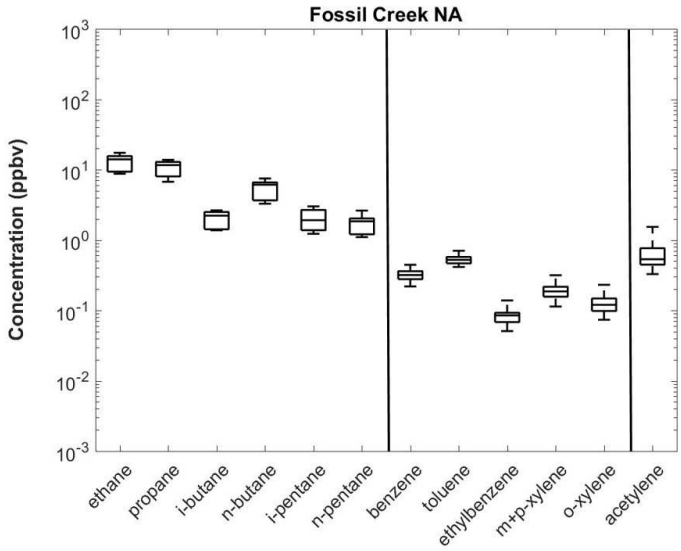

Figure 3.3: Select VOC concentrations from weekly time-integrated whole air canister samples at Fossil Creek NA (n=9).

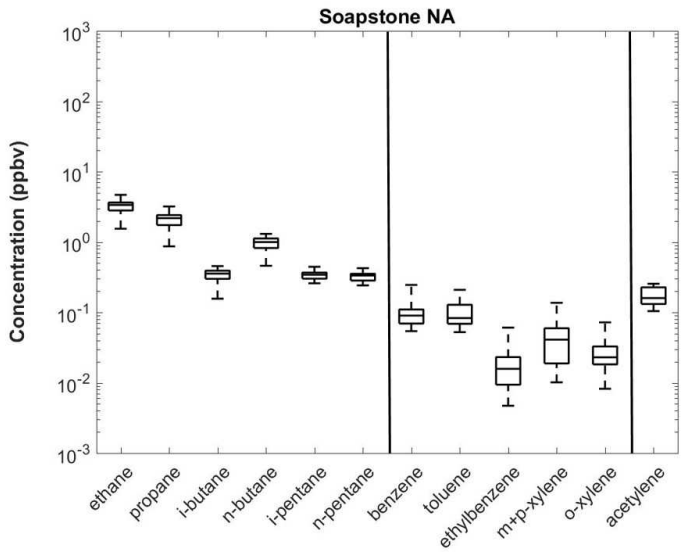

Figure 3.4: Select VOC concentrations from weekly time-integrated whole air canister samples at the Soapstone NA (n=11).

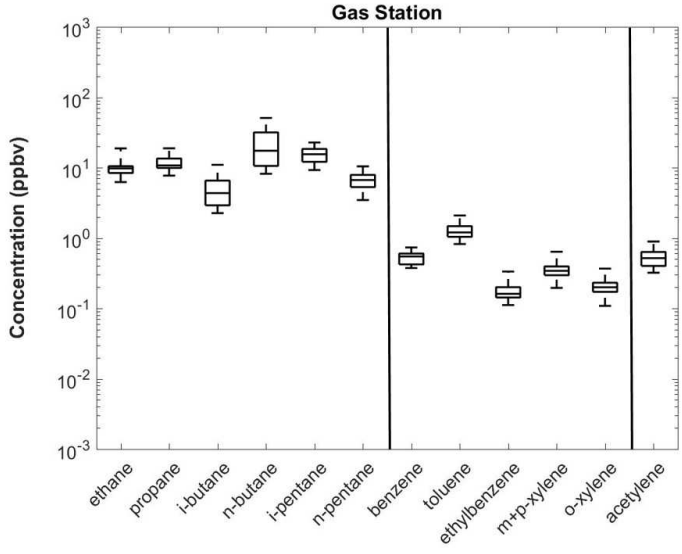

Figure 3.5: Select VOC concentrations from weekly time-integrated whole air canister samples at the gas station (n=32).

The highest median concentrations of all VOCs shown in Figures 3.1 - 3.5 were seen at the gas station, with the exception of ethane and propane where the highest median concentrations were seen at Fossil Creek NA. The gas station samples were expected to show

the highest concentrations of most VOCs due to the proximity of the sampling location to sources of gasoline vaporization and heavy vehicle traffic emissions. The objective in sampling near the gas station was to obtain a strong combustion/urban influenced sample to compare to the other four sampling locations. The main purpose of this study was to look at the influence of current O&NG emissions on ambient VOC concentrations; therefore, the analysis in Section 3.1 will focus mainly on the O&NG influence at the elementary school, residential area, Fossil Creek NA, and Soapstone NA.

Excluding the gas station site, the highest median concentrations of light alkanes, acetylene, and BTEX compounds were observed at Fossil Creek NA. The highest median acetylene being observed at Fossil Creek NA could be attributed to the increased emissions from vehicles in the natural area parking lot, which was a few meters away from the canister sampling location, and/or from the close proximity to the interstate highway (approximately 2.0km to the east). The lowest median concentration and lowest 25^{th} percentile concentration of light alkanes, acetylene, and BTEX compounds were observed at Soapstone NA, likely due to its remote location farther than the other sites from O&NG activity and vehicle traffic. The highest 95^{th} percentile concentration of light alkanes and toluene were found at the elementary school, the site closest to major O&NG regions to the east, while Fossil Creek NA showed the highest 95^{th} percentile concentration of the other BTEX compounds and acetylene.

3.1.2 Comparison with Long-term Regional Data

Between December 2011 and December 2016 the CDPHE collected 3-hour time-integrated canister samples at a site in Welby, CO (39.838^o, -104.950^o) and downtown Denver, CO (39.751^o, -104.988^o) [CDPHE, 2016]. The Denver site was located in the Five Points neighborhood of downtown Denver while the Welby site was located approximately 10km northeast of the Denver site. The Welby site was in a suburban setting and was close to a few industrial businesses with no O&NG developments within a 5km radius. The CDPHE collected canister samples approximately every 6^{th} day between 06:00 and 09:00. Although this dataset should

not be considered a direct comparison to the data collected in this study due to a different sampling length, interval, and time of day; it can still provide some context for the VOC concentrations in the CNFR. Figure 3.6 shows the same set of select VOCs as Figures 3.1 - 3.5 measured by the CDPHE in Welby and Denver.

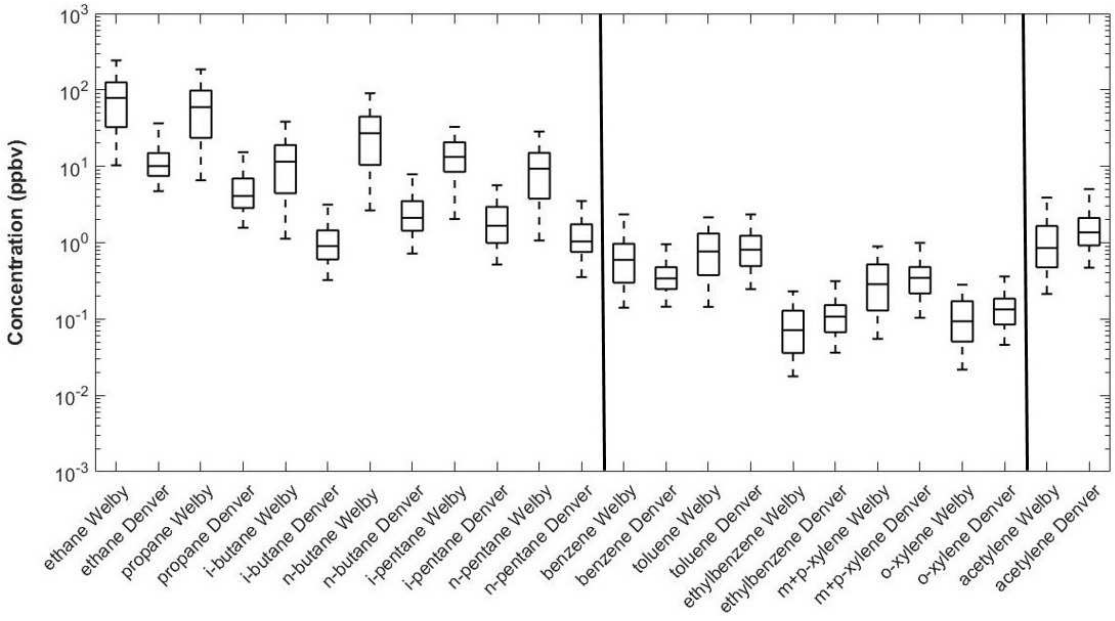

Figure 3.6: Select VOC concentrations measured by the CDPHE in Welby, CO (n = 340) and downtown Denver, CO (n = 392) [CDPHE, 2016].

The CDPHE 3-hour time-integrated canister samples were collected to show data representing the unreacted morning VOCs. The sampling interval (06:00 - 09:00) spanned hours in which traffic emissions would be expected to be elevated due to morning commuters, and the shallow mixed layer in the early morning traps surface emissions and limits their dilution. For these reasons, the concentrations measured by the CDPHE in Welby and Denver would be expected to be biased high compared with average VOC conditions at these locations and furthermore, higher than the data collected in this thesis where samples were averaged over a week. The CDPHE also collected hundreds of samples (Welby = 340, Denver = 392) over a much longer sampling time (approximately 5 years) compared with the much smaller sample sizes and sampling time periods in this study.

The median light alkane concentrations observed over 5 years of sampling in Welby, CO were several times higher than those measured in downtown Denver. The median ethane and propane concentrations measured in Welby were 78.5ppbv and 59.5ppbv, respectively, which is greater than the 95^{th} percentiles observed in this study at the elementary school of 42.1ppbv and 33.5ppbv. In addition, the median benzene concentration in Welby of 0.60ppbv was nearly double the median concentration measured in downtown Denver and greater than the 95^{th} percentile at Fossil Creek NA of 0.45ppbv. The toluene, ethylbenzene, and xylenes concentrations were comparable between Welby and Denver. The median ethylbenzene and xylenes concentrations at Welby and Denver were similar to the 95^{th} percentile concentrations observed at all sites in this study, while the median toluene concentrations in Welby and Denver were slightly less than the gas station median, but higher than the 95^{th} percentile concentrations observed at the other locations in this study. Finally, the median acetylene concentration in downtown Denver was over 60% greater than the median concentration measured in Welby and exceeded the 95^{th} percentile concentration measured at the gas station.

Higher BTEX and acetylene concentrations would be expected in the CDPHE samples compared to the samples in this study due to the sample location, time, and duration. The samples collected in Welby and Denver were collected from 06:00 to 09:00 which coincides with elevated combustion emissions and a shallow mixed layer during the morning commute hours whereas the samples in this study were collected for a longer duration and represent an average concentration for 7 days. Furthermore, the CDPHE data, particularly the downtown Denver samples, were collected closer to busy roadways with higher vehicular traffic than the weekly samples in this study.

Higher ethane and propane concentrations in the Welby samples than those seen at the elementary school were somewhat surprising since Welby was removed from areas of dense O&NG development. There are no O&NG developments within a 5km radius of the Welby sampling location whereas the elementary school is located with 1km of dense O&NG

development. It is likely that sampling for a shorter duration in the morning resulted in higher O&NG VOC compound concentrations due to a buildup during stable nighttime conditions.

3.1.3 Source Apportionment Using VOC Ratios and Correlations

Based on previous VOC studies conducted in the CNFR [Gilman et al., 2013; Halliday et al., 2014; Thompson et al., 2014; Swarthout et al., 2013] it was anticipated that O&NG emissions would have the most influence on many ambient VOC concentrations and a smaller influence would be observed from combustion sources. Natural gas in the CNFR has been shown to be 62% - 92% methane, 4% - 16% ethane, and 1% - 15% propane [COGCC, 2007] with heavier VOCs and non-energy components (ie. N_2, CO_2, H_2S, He) making up the rest [CCEI, 2013]. In the CNFR, propane has been shown to be a strong tracer of O&NG activity while acetylene has been used previously as a vehicular exhaust marker [Gilman et al., 2013]. The primary source of light alkanes in the CNFR is O&NG production with a lesser influence from combustion [Gilman et al., 2013; Halliday et al., 2014]. An air mass influenced strongly by O&NG activity would be expected to display a strong correlation between light alkanes and BTEX with propane and a poor correlation with acetylene. Conversely, an air mass influenced strongly by combustion emissions would be expected to display a strong correlation of VOCs emitted from vehicular exhaust with acetylene and a poor correlation with propane. This analysis, however, can be influenced by meteorological effects which can dilute or concentrate all VOC concentrations simultaneously. Table 3.1 shows the coefficient of determination (r^2) of concentrations of ethane, i-butane, n-butane, i-pentane, and n-pentane to propane and acetylene at the sampling locations. Significance testing utilizing a 95% confidence interval comparing the correlation coefficients for propane and acetylene at each location was conducted and the method and results are detailed in Appendix E. Table 3.2 shows if a significant difference was seen at the 95% confidence level between the propane and acetylene coefficients of determination at each sampling location.

Table 3.1: Coefficient of determination (r^2) for ethane, i-butane, n-butane, i-pentane, and n-pentane with propane and acetylene at the five sampling locations.

	Propane					Acetylene				
	Elementary School	Residential Area	Fossil Creek NA	Soapstone NA	Gas Station	Elementary School	Residential Area	Fossil Creek NA	Soapstone NA	Gas Station
ethane	0.92	0.89	0.80	0.94	0.87	0.27	0.67	0.21	0.38	0.40
i-butane	0.99	0.99	0.71	0.93	0.26	0.72	0.58	0.19	0.00	0.32
n-butane	0.99	0.99	0.76	0.89	0.17	0.23	0.86	0.09	0.33	0.55
i-pentane	0.97	0.99	0.32	0.26	0.00	0.25	0.87	0.30	0.32	0.00
n-pentane	0.95	0.96	0.61	0.21	0.03	0.20	0.79	0.04	0.34	0.01

Table 3.2 Determination of a significant difference between the propane and acetylene coefficients of determination at a 95% confidence interval at the five sampling locations.

	Elementary School	Residential Area	Fossil Creek NA	Soapstone NA	Gas Station
ethane	Yes	No	No	Yes	Yes
i-butane	Yes	No	No	Yes	No
n-butane	Yes	No	No	Yes	Yes
i-pentane	Yes	No	No	No	No
n-pentane	Yes	No	No	No	No

At the elementary school, the correlation with propane is high for ethane ($r^2 = 0.92$), i-butane ($r^2 = 0.99$), n-butane ($r^2 = 0.99$), i-pentane ($r^2 = 0.97$), and n-pentane ($r^2 = 0.95$), while the correlation with acetylene is low for ethane ($r^2 = 0.27$), n-butane ($r^2 = 0.23$), i-pentane ($r^2 = 0.25$), and n-pentane ($r^2 = 0.20$). The correlation with acetylene was relatively high for i-butane ($r^2 = 0.72$) which has been shown to be present in vehicular emissions [Broderick et al., 2002], but when compared with a near perfect correlation with propane, it is clear that these emissions are better correlated with propane. For all compounds the coefficients of determination were significantly different at a 95% confidence interval between propane and acetylene which implies that the air mass measured at the elementary school was primarily influenced by O&NG activity.

At the residential area it is difficult to draw strong statistical source apportionment conclusions from coefficients of determination due to the small sample size (4 weekly samples). The correlation with propane is high for ethane ($r^2 = 0.89$), i-butane ($r^2 = 0.99$), n-butane ($r^2 = 0.99$), i-pentane ($r^2 = 0.99$), and n-pentane ($r^2 = 0.96$). Unlike the elementary school, the residential area also displays stronger correlation with acetylene for ethane ($r^2 = 0.67$),

i-butane ($r^2 = 0.58$), n-butane ($r^2 = 0.86$), i-pentane ($r^2 = 0.87$), and n-pentane ($r^2 = 0.79$). None of these correlations were found to be significantly different and the presence of correlations with both propane and acetylene suggests the residential area is influenced by an air mass that includes a varying mix of O&NG and vehicular emissions.

At Fossil Creek NA, the correlation with propane is relatively high for ethane ($r^2 = 0.80$), i-butane ($r^2 = 0.71$), n-butane ($r^2 = 0.76$), and n-pentane ($r^2 = 0.61$), but lower for i-pentane ($r^2 = 0.32$). The correlation with acetylene is low for ethane ($r^2 = 0.21$), i-butane ($r^2 = 0.19$), n-butane ($r^2 = 0.09$), i-pentane ($r^2 = 0.30$), and n-pentane ($r^2 = 0.04$). Four of the 5 compounds displaying a relatively strong correlation with propane and all compounds showing a low correlation with acetylene suggests that O&NG is a dominant source of these VOCs at Fossil Creek NA; however, none of the compounds were found to have significantly different coefficients of determination at a 95% confidence interval, which could also be a function of a smaller sample size.

At Soapstone NA, the correlation with propane is high for i-butane ($r^2 = 0.93$), n-butane ($r^2 = 0.89$), and ethane ($r^2 = 0.94$), but lower for i-pentane ($r^2 = 0.26$) and n-pentane ($r^2 = 0.21$). The correlation with acetylene is low for ethane ($r^2 = 0.38$), i-butane ($r^2 = 0.00$), n-butane ($r^2 = 0.33$), i-pentane ($r^2 = 0.32$), and n-pentane ($r^2 = 0.34$). Ethane, i-butane, and n-butane display significantly different coefficients of determination at a 95% confidence interval while i-pentane and n-pentane do not. Three of the 5 compounds displaying very strong correlations with propane and all compounds showing low correlations with acetylene would suggest that the influence of O&NG is dominant at Soapstone NA; however, the O&NG signal is not as significant as the elementary school.

At the gas station, a very low correlation with propane for i-butane, n-butane, i-pentane, and n-pentane was observed and a low correlation with acetylene for i-pentane and n-pentane was observed. The coefficient of determination between n-butane and acetylene ($r^2 = 0.55$) was higher than expected and was significantly different at a 95% confidence interval than the coefficient of determination with propane; this could be explained by n-butane being a

common additive to gasoline [Doskey et al., 1992] and vaporization from the pumps influencing these correlations.

VOC correlations with propane and acetylene can be a guide when determining source apportionment, but it is qualitative as strong vs weak correlations can be a relative term. Another way to estimate the influence of O&NG vs vehicular emission on an air mass at a particular location are the ratios of the two pentane isomers (i-pentane and n-pentane) [Gilman et al., 2013], the two butane isomers (i-butane and n-butane), and toluene to benzene [Halliday et al., 2014]. An i-pentane to n-pentane ratio of approximately 1.0 or less indicates a primarily O&NG influence while an i-pentane to n-pentane ratio of approximately 2.3 or greater indicates a primarily vehicular influence [Gilman et al., 2013; Swarthout et al., 2015]. Direct vehicular exhaust has been shown to have an i-butane to n-butane ratio of 0.2 to 0.3 while O&NG emissions have a ratio of 0.6 to more than 1 [Russo et al., 2010]. Fresh traffic emissions have displayed a toluene to benzene ratio of over 2 whereas emissions more influenced by O&NG are generally less than 2 [Halliday et al., 2014]. Toluene to benzene ratio changes based on the age of an air mass, making this ratio less reliable for source apportionment. This is discussed in greater detail later in this section.

In Figures 3.7 - 3.9, the solid lines indicate the VOC ratios measured at the sampling locations in this study while the dashed lines indicate ratios measured in other relevant studies in the CNFR. Figure 3.7 shows the i-pentane to n-pentane ratios, Figure 3.8 shows the i-butane to n-butane ratios and Figure 3.9 shows the toluene to benzene ratios.

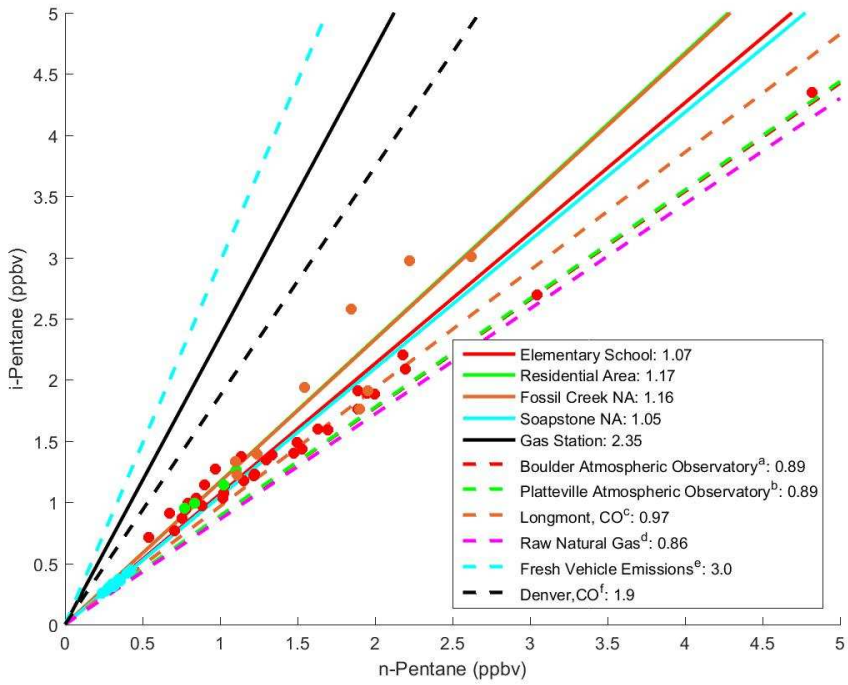

Figure 3.7: i-pentane to n-pentane ratio at each of the five sampling sites compared to ratios seen in other studies in the CNFR [[a]Gilman et al., 2013; [b]Halliday et al., 2016; [c]Thompson et al., 2014; [d]COGCC, 2007; [e]Broderick et al., 2002; [f]Baker et al., 2008].

The mean i-pentane to n-pentane ratio at the elementary school (1.07 $\pm$ 12.4%) and Soapstone NA (1.05 $\pm$ 3.0%) are just above 1.0, indicating that these two locations are strongly influenced by O&NG activity. These ratios are slightly above what was observed at the Boulder Atmospheric Observatory (0.89) by Gilman et al. [2013], the Platteville Atmospheric Observatory (0.89) by Halliday et al. [2016], in Longmont, CO (0.97) by Thompson et al. [2014], and for raw natural gas in the Wattenberg Gas Field (0.86) by COGCC [2007]. The sampling locations in these other studies were deemed to be almost entirely O&NG influenced. At the elementary school, the low i-pentane to n-pentane ratio further verifies the results discussed using correlations, that the air mass is heavily influenced by O&NG activity. The influence of the developing residential neighborhood with new construction surrounding the elementary school and traffic on the interstate highway approximately 3.5km to the west, could explain the slightly elevated i-pentane to n-pentane ratio.

The mean i-pentane to n-pentane ratio at the gas station (2.35 ± 10.0%) is above the ratio measured in downtown Denver, CO (1.9) [Baker et al., 2008] and below the ratio of fresh vehicular emissions (3.0) [Broderick et al., 2002]. A ratio in this range was expected at the gas station, since it is primarily influenced by emissions from vehicles in the gas station and shopping center parking lots as well as traffic on the busy roads and highway adjacent to the station. There is also an influece from gasoline vaporization which has been shown to display an i-pentane to n-pentane ratio of about 4.0 [Broderick et al., 2002].

The mean i-pentane to n-pentane ratios at the residential area (1.17 ± 4.5%) and Fossil Creek NA (1.16 ± 13.2%) were more elevated than what would be expected from a primarily O&NG signature, but still far below a strong vehicular signature. This indicates that there is a mixed influence from O&NG activity as well as vehicular emissions at these locations; with a stronger O&NG influence.

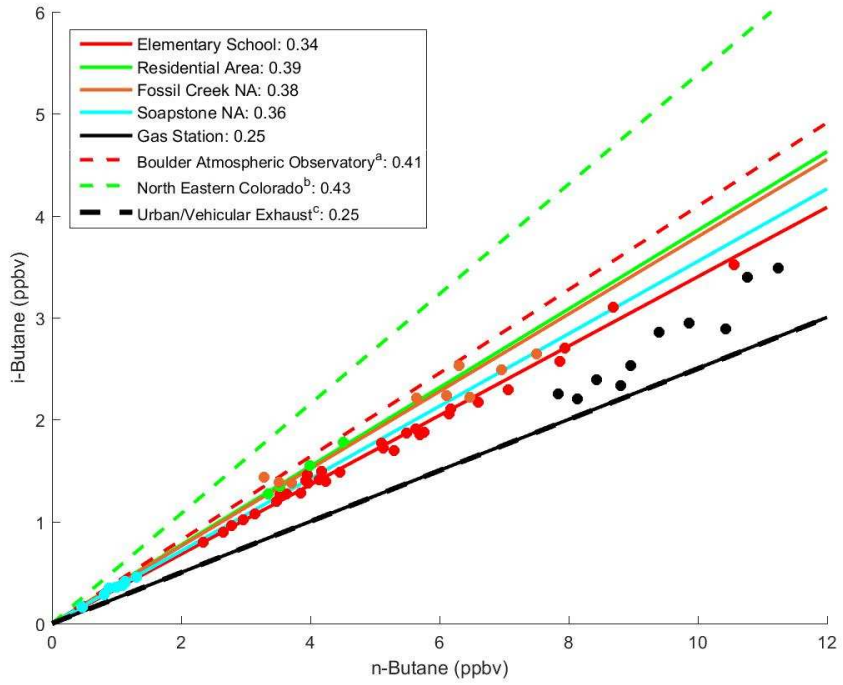

Figure 3.8: i-butane to n-butane ratio at each of the five sampling sites compared to ratios seen in other studies in the CNFR [[a]Swarthout et al., 2013; [b]Thompson et al., 2014; [c]Russo et al., 2010].

The mean i-butane to n-butane ratios at the elementary school (0.34 ± 3.4%), residential area (0.39 ± 1.8%), Fossil Creek NA (0.38 ± 7.8%), and Soapstone NA (0.36 ± 4.8%) are all similar and are in between the ranges of 0.2 - 0.3 that indicates vehicular emissions and 0.6 to more than 1 that indicates O&NG. Since these four ratios are higher than the proposed range for vehicular emissions and below the proposed minimum for O&NG, the i-butane to n-butane ratio indicates there is a mixture of source influences at these sites. Samples collected at BAO (0.41) [Swarthout et al., 2013] and in areas of Northeastern Colorado (0.43) [Thompson et al., 2014] are slightly higher, although still below the O&NG threshold of 0.6 suggested by Russo et al. [2010]. This further indicates that these samples are influenced by a mixture of vehicular and O&NG emissions. In contrast, the mean gas station ratio (0.25 ± 17.3%) is within the vehicular emission range and is the same as the ratio observed in fresh vehicular exhaust by Russo et al. [2010].

The i-butane to n-butane ratios found in this study, along with those previously reported, suggests that this ratio may not provide as clear of a delineation between O&NG and vehicular influences. Swarthout et al. [2013] and Thompson et al. [2014] both observed VOC correlations and other VOC ratios that indicated their samples were highly influenced by O&NG; however, their reported i-butane to n-butane ratios were below the proposed O&NG influence threshold of 0.6. The results of this study along with previous works seem to imply that i-pentane to n-pentane ratio is a much stronger and more reliable indicator of source apportionment in the CNFR than i-butane to n-butane ratio.

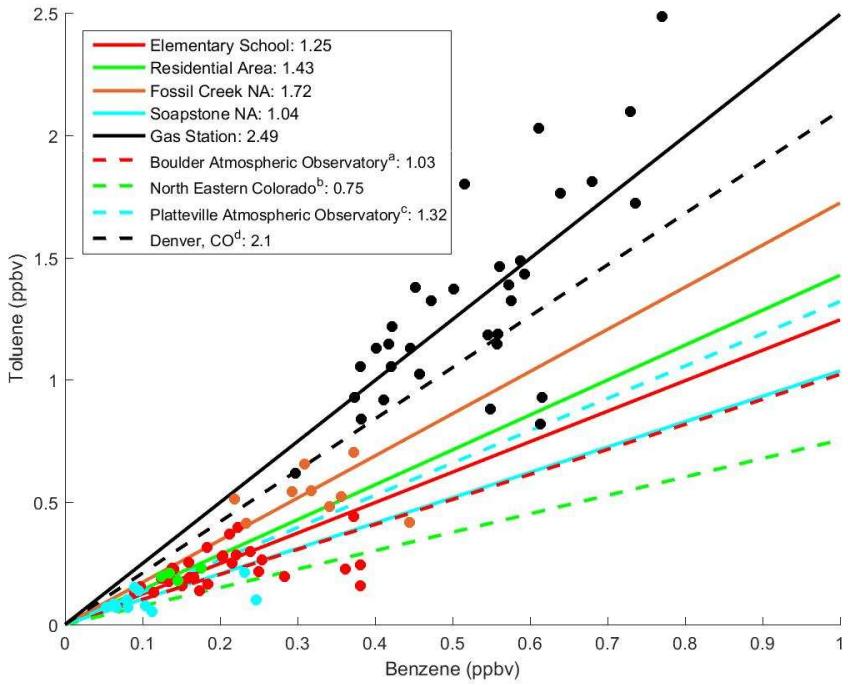

Figure 3.9: Toluene to benzene ratio at each of the five sampling sites compared to ratios seen in other studies in the CNFR [[a]Swarthout et al., 2013; [b]Thompson et al., 2014; [c]Halliday et al., 2016; [d]Baker et al., 2008].

The toluene to benzene ratio can be used to assess source apportionment if emissions are fresh; however, it is not as reliable as the i-pentane to n-pentane ratio because toluene reacts more quickly than benzene in the atmosphere. Toluene has an atmospheric lifetime of about 2.5 days compared to that of benzene which is about 12 days [Blake et al., 2002; Seinfeld et al., 2016]. Comparatively, both i-pentane and n-pentane have an atmospheric lifetime of about 4 days [Blake et al., 2002; Gilman et al., 2013], so the ratio of the isomers does not change over time. Therefore traffic emissions, which display a toluene to benzene ratio above 2, can decrease to ratios similar to O&NG emissions if the air mass has been aged and photochemically processed. This characteristic can be utilized, if the ratio of a source is known, to assess the photochemical age of an air mass [Halliday et al., 2016, Warneke et al., 2013], but this can alter source apportionment conclusions. Also, toluene to benzene ratio can vary diurnally as a result of its atmospheric reactivity. Measurements taken using a real-time

GC by Halliday et al., [2016] found lower toluene to benzene ratios during day versus night at the same location with the same meteorological conditions. The weekly sampling interval in this study averages out these variations and does not provide as accurate of a depiction of this ratio. As a result of these limitations, toluene to benzene ratio had a larger uncertainty in this study and was used as more of a guide for distinguishing O&NG and traffic emissions, not as definitive evidence of source apportionment.

The elementary school (1.25 ± 29.1%), residential area (1.43 ± 12.4%), Fossil Creek NA (1.72 ± 24.0%), and Soapstone NA (1.04 ± 38.7%) all display toluene to benzene ratios below 2 which is indicative of the rural and primarily O&NG influenced CNFR. Samples collected at BAO (1.03) [Swarthout et al., 2013] and in areas of Northeastern Colorado (0.75) [Thompson et al., 2014] display a lower ratio and were noted, through analysis of other source apportionment techniques, to be primarily influenced by O&NG emissions. This follows the conclusion drawn from the i-pentane to n-pentane ratio observations, that the air masses at the residential area and Fossil Creek NA are influenced by a mixture of O&NG and vehicular emission sources, whereas the air masses at the elementary school and Soapstone NA are influenced mainly by O&NG with a smaller contribution from vehicular emissions. In contrast, the Gas Station ratio (2.49 ± 19.5%) is much higher and was even above the ratio of 2.1 observed in downtown Denver by Baker et al. [2008].

During the summer of 2014 The Front Range Air Pollution and Photochemistry Experiment (FRAPPÉ) was conducted with the goal of better understanding the summertime air quality in the CNFR. As part of the study, ground level canister grab samples were collected by a research team from the University of California, Irvine (UCI) [Blake, 2014] and a research team from CSU [Zhou, 2014] and were analyzed using GC-FID. Figures 3.10 - 3.12 show a map of the CNFR with data collected during FRAPPÉ and during this study. Samples in Figure 3.10 are color coded by i-pentane to n-pentane ratio, samples in Figure 3.11 are color coded by i-butane to n-butane ratio, and samples in Figure 3.12 are color coded by toluene to benzene ratio. These ratios did not vary much seasonally, therefore, the average ratios

of all samples collected at four of the sampling locations (excluding the gas station) in this study were used.

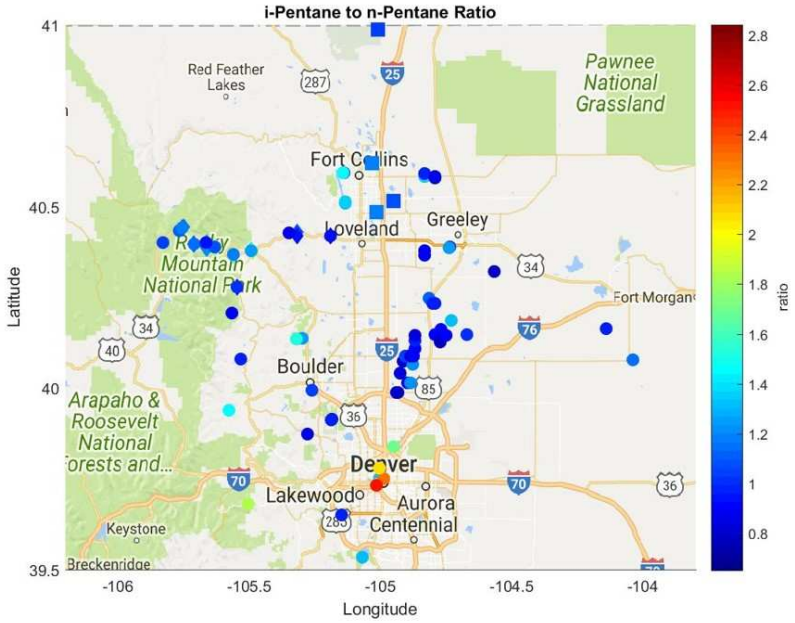

Figure 3.10: Map of the i-pentane to n-pentane ratios measured from ground level canister grab samples in the summer of 2014 as part of FRAPPÉ along with the average ratios seen in this study. Samples collected and analyzed by UCI [Blake, 2014] are denoted as circles, samples collected and analyzed by CSU [Zhou, 2014] are denoted by diamonds and samples collected and analyzed in this study are denoted by squares.

The majority of samples collected east of interstate highway 25 and north of the Denver metro area display i-pentane to n-pentane ratios of approximately 1.2 or less while samples collected in downtown Denver show higher ratios. This is expected, since the area northeast of Denver is rural and contains many O&NG developments whereas a populated urban environment, such as downtown Denver, has many more combustion sources.

The samples collected in this study in the Fort Collins area along with a few samples collected during FRAPPÉ, illustrate an interesting east to west gradient in i-pentane to n-pentane ratio. FRAPPÉ samples collected east of Fort Collins display i-pentane to n-pentane ratios of approximately 1 or less. At the elementary school, located west of these FRAPPÉ samples, the ratio increases slightly to an average of 1.07 $\pm$ 12.4%. Moving a few

kilometers farther west, the average ratios at the residential area and Fossil Creek NA were 1.16 ± 4.5% and 1.17 ± 13.2%, respectively. Finally, another group of FRAPPÉ samples were collected just west of Fort Collins and they displayed a ratio of approximately 1.3 and above. This gradient would be expected moving west from Weld County, an area with higher reported O&NG sources, to a more populated environment and therefore, an area with more combustion sources.

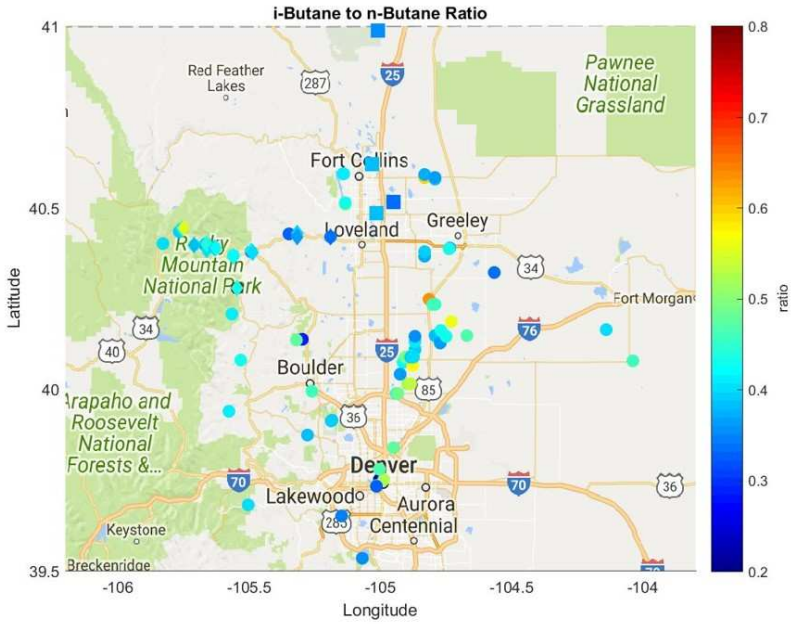

Figure 3.11: Map of the i-butane to n-butane ratios measured from ground level canister grab samples in the summer of 2014 as part of FRAPPÉ along with the average ratios seen in this study. Samples collected and analyzed by UCI [Blake, 2014] are denoted as circles, samples collected and analyzed by CSU [Zhou, 2014] are denoted by diamonds and samples collected and analyzed in this study are denoted by squares.

There is not a discernible pattern in the i-butane to n-butane ratios measured in the CNFR during FRAPPÉ. Over 85% of the samples display a ratio between 0.3 and 0.6, which is in between the range of 0.2 - 0.3 indicating O&NG and the range of 0.6 - >1 indicating vehicular emissions. This follows what was shown previously in Figure 3.8, that i-butane to n-butane ratio may not be a particularly useful tool for source apportionment in the CNFR.

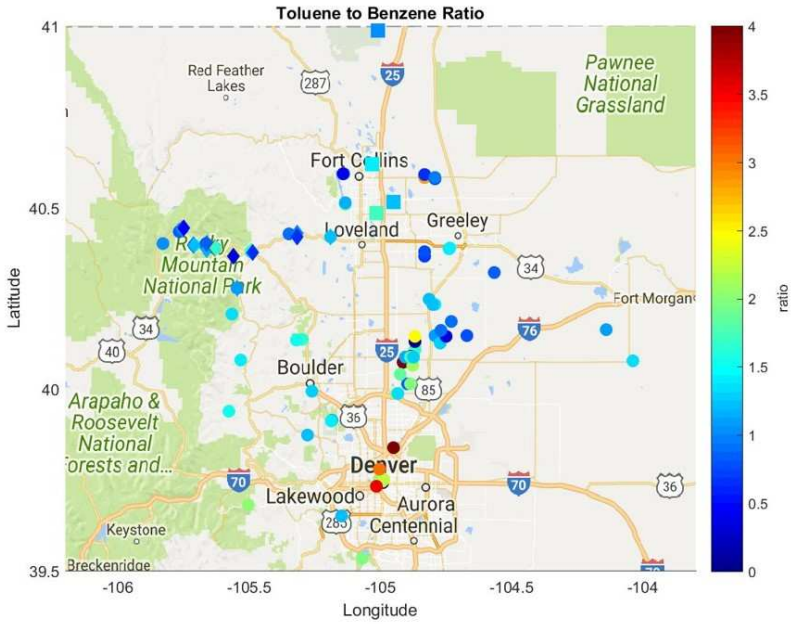

Figure 3.12: Map of the toluene to benzene ratios measured from ground level canister grab samples in the summer of 2014 as part of FRAPPÉ along with the average ratios seen in this study. Samples collected and analyzed by UCI [Blake, 2014] are denoted as circles, samples collected and analyzed by CSU [Zhou, 2014] are denoted by diamonds and samples collected and analyzed in this study are denoted by squares.

Most of the samples collected east of interstate highway 25 and north of the Denver metro area display a toluene to benzene ratio of less than 2 while samples collected in Downtown Denver show ratios greater than 2. It is important to note once again that toluene to benzene ratio is influenced by differences in atmospheric reactivity of the 2 compounds and is thus most useful for relatively fresh emissions.

When comparing the i-pentane to n-pentane ratios found during FRAPPÉ and this study (Figure 3.10) with the i-butane to n-butane (Figure 3.11) and toluene to benzene (Figure 3.12) ratios measured during FRAPPÉ and this study, it appears that i-pentane to n-pentane ratio is the most robust tool for estimating source apportionment in the CNFR. i-pentane to n-pentane ratio is not influenced by atmospheric reactivity, as toluene to benzene ratio is, and it shows a much clearer delineation between O&NG and combustion influences, than the i-butane to n-butane ratio.

While using VOC ratios is an improvement over simply looking at correlations with propane and acetylene and estimating source apportionment, Gilman et al. [2013] utilized a multivariate regression analysis technique to attempt to quantify the percent contribution of O&NG sources to ambient VOC concentrations. They calculated propane and acetylene multivariate regression coefficients utilizing the equation below [Gilman et al., 2013]:

$$[VOC] = Bkgd_{VOC} + ER'_{propane} \times [propane_o] + ER'_{acetylene} \times [acetylene_o] \qquad (3.1)$$

where $[VOC]$ is the measured VOC concentration, $Bkgd_{VOC}$ is the assumed background VOC concentration, $ER'_{propane}$ and $ER'_{acetylene}$ are the multivariate regression coefficients that are calculated, and $[propane_o]$ and $[acetylene_o]$ are the background subtracted observed propane and acetylene concentrations. In this analysis, the $Bkgd_{VOC}$ concentration represents an air mass that is unaffected by O&NG, combustion, or other local sources at the site of the measurements. To determine the $Bkgd_{VOC}$ concentration, Gilman et al. [2013] utilized the minimum VOC concentration measured at BAO in their 554 in-situ real-time GC samples. Since the sample numbers were less and the sample collection length was much longer in this study, implying that minimum local concentrations were never measured at the populated sites, the minimum VOC concentration observed in the 11 canister samples collected at Soapstone NA was used to represent the CNFR background VOC concentration. The remote Soapstone NA was the farthest sampling location from CNFR traffic and O&NG development; therefore, for the purposes of this thesis, it was assumed to represent the regional background VOC concentrations.

Once the ER' values had been obtained, the O&NG fractions for each VOC were calculated using the equation below [Gilman et al., 2013]:

$$[O\&NG_{fraction}] = \frac{ER'_{propane} \times [propane_o]}{Bkgd_{VOC} + ER'_{propane} \times [propane_o] + ER'_{acetylene} \times [acetylene_o]} \qquad (3.2)$$

While this method provides a more quantitative result than simply evaluating VOC ratios and estimating the contribution of O&NG, it has a few limitations. First, there is no term included for photochemical production and/or loss. This assumption may be appropriate in the wintertime; however, photochemistry could be a strong influence on the ambient VOC concentrations during other times of year [Gilman et al., 2013]. Also, if the air mass being measured is aged, mixing of other VOC sources as well as removal of more reactive VOCs, due to shorter lifetimes would lead to variability in the propane and acetylene correlations [Gilman et al., 2013]. Another limitation of this method is that $[propane_o]$ and $[acetylene_o]$ are not completely independent of one another. Natural gas contains only propane and no acetylene; however, some combustion emissions contain propane [Gilman et al., 2013]. Fossil fuel combustion emissions have a propane to acetylene ratio of less than 0.10 [Fraser et al., 1998] which is far less than the mean propane to acetylene ratios measured at the elementary school, residential area, and Fossil Creek NA of 32.0, 18.8, and 20.2, respectively. These relatively large ratios indicate that combustion sources have a small propane contribution and thus the calculation will not be heavily influenced by $[propane_o]$ and $[acetylene_o]$ being co-emitted from some combustion sources. Table 3.3 shows the O&NG contribution percentage of select VOCs at the elementary school, residential area, and Fossil Creek NA compared with the percentages found by Gilman et al. [2013] at BAO. The mean O&NG contribution percentage for propane was approximately 90% and the O&NG contribution percentage for acetylene was 0% in this study and in Gilman et al. [2013].

Table 3.3: O&NG contribution percentage of select VOCs at the elementary school, residential area, and Fossil Creek NA compared with the percentages found by Gilman et al. [2013] at BAO.

VOC	Mean Elementary School O&NG contribution (%)	Mean Residential Area O&NG contribution (%)	Mean Fossil Creek NA O&NG contribution (%)	Mean Gilman et al. [2013] O&NG contribution (%)
Ethane	78	86	74	72
Propane	91	89	91	90
i-Butane	90	86	79	93
n-Butane	90	88	85	95
i-Pentane	89	71	66	95
n-Pentane	81	57	83	96
n-Hexane	85	83	81	78
n-Heptane	84	82	89	73
Benzene	70	62	65	32
Toluene	76	81	69	31
Ethylbenzene	84	93	82	15
m+p-Xylenes	85	91	87	23
o-Xylene	72	97	93	20
Acetylene	0	0	0	0

The elementary school shows an O&NG contribution percentage over 78% for all listed alkanes and an O&NG contribution percentage greater than 70% for all BTEX compounds. The residential area shows an O&NG contribution percentage over 71% for all listed alkanes, with the exception of n-pentane (57%), and an O&NG contribution percentage greater than 81% for all BTEX compounds, with the exception of benzene (62%). Fossil Creek NA shows an O&NG contribution percentage over 66% for all listed alkanes and an O&NG contribution percentage greater than 65% for all BTEX compounds. Gilman et al. [2013] observed an O&NG contribution percentage over 72% for all listed alkanes, but an O&NG contribution percentage less than 32% for all BTEX compounds at BAO.

Based on the VOC ratios detailed previously in this section, it was anticipated that the highest O&NG contribution percentage of compounds mainly associated with O&NG would be seen by Gilman et al. [2013] in samples collected at BAO. The next highest percentage was predicted to be the elementary school, followed by the residential area and Fossil Creek NA having comparable percentages. This pattern is seen in the O&NG contribution percentage for i-butane, n-butane, and i-pentane; however, it is not seen as clearly in ethane or n-pentane.

BTEX compounds at BAO were found to have a much lower O&NG contribution percentage than this study. It was noted by Gilman et al [2013] that benzene has significant contributions at BAO from other sources. This agrees with the finding of a previous study conducted at BAO by Pétron et al. [2012]. Halliday et al. [2016] conducted a study at the PAO, approximately 55km northeast of Denver, and noted that with westerly and southwesterly winds higher benzene concentrations were measured. This was attributed to advection of the Denver pollution plume which could also be affecting measurements made at BAO. Farther north in the CNFR, O&NG would be expected to have a higher percent contribution to the ambient benzene concentration since the area has less combustion and more O&NG sources than locations closer to the Denver metro area. To put the differences in mobile combustion emission sources in perspective, there are 1,787,476 daily vehicle miles traveled (DVMT) in Larimer County (6,822km^2), compared to 5,694,188 DVMT in Denver County (401km^2) [CDOT, 2015]. The samples in this study were collected about 40km farther north than PAO, which would lessen the impact of the Denver pollution plume resulting from the higher amount of vehicle traffic.

3.1.4 VOC-OH Reactivity

O_3 production occurs when VOCs react with OH and other oxidants in the presence of NO_X ($NO + NO_2$), O_2, and $h\nu$ (reaction detailed in Section 1.1). Although it is only the first step of the cycle, the propensity of a particular VOC to initiate the O_3 production cycle by reacting with OH can be estimated using the following equation [Abeleira et al., 2017]:

$$R_{OH,VOC} = k_{OH+VOC} \times [VOC] \tag{3.3}$$

where $R_{OH,VOC}$ is the OH reactivity of the VOC, k_{OH+VOC} is the VOC rate constant for the reaction with OH, and $[VOC]$ is the mixing ratio of the VOC in molecules cm^{-3}. The k_{OH+VOC} values were obtained from previously published studies and a complete list of the values used can be found in Appendix F. It should be noted that this method does not

account for chain propagation or termination steps in the O_3 production cycle [Abeleira et al., 2017]. This approach is also limited in that it only looks at a subset of compounds that react to form O_3 and thus does not provide a comprehensive evaluation of O_3 formation. Differences in the suites of VOCs quantified also makes inter-comparison among studies difficult. However, despite its limitations this method can provide insight into the relative contributions of VOCs to O_3 formation [Abeleira et al., 2017; Swarthout et al., 2013].

The OH reactivity at each location was evaluated in order to compare the O_3 production potential by the VOCs measured at each site. It is important to note that this data set does not include secondary VOC species; therefore, a large portion of the overall OH reactivity is not included. Samples collected at the residential area, Fossil Creek NA, and Soapstone NA were only obtained during the fall of 2015 whereas samples collected at the elementary school spanned 1 year. Ambient OH concentration is a function of temperature and sunlight and thus total OH reactivity varies by season [Abeleira et al., 2017]; therefore, the average total OH reactivity shown in Figure 3.13 only utilizes samples collected in the fall of 2015 at the elementary school. The seasonal variability in average total OH reactivity was evaluated at the elementary school only and is shown later in Figure 3.14. A complete list of the VOCs in each category can be found in Appendix Table G.1.

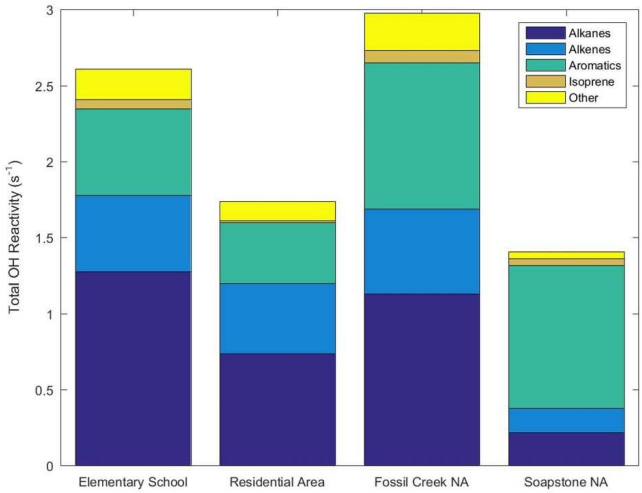

Figure 3.13: Average total OH reactivity measured at the elementary school, residential area, Fossil Creek NA, and Soapstone NA during the fall of 2015.

Fossil Creek NA had the highest total OH reactivity due to the highest ambient VOC concentration. The elementary school had a higher total OH reactivity than the residential area; however, the percent contribution from each VOC category is similar at both locations. Soapstone NA displays the lowest average total OH reactivity; however, 66.7% of the total results from aromatics, which is the highest, and 11.4% results from alkenes, which is the lowest compared to each group's contribution at other sites. Alkenes have much shorter tropospheric lifetimes with OH [Blake et al., 2002; Seinfeld et al., 2016]; therefore, this is likely a result of Soapstone NA being located far from emission sources compared to the other sampling sites, allowing time for the chemical processing of these more reactive hydrocarbons. The total VOC concentration, and as a result the total OH reactivity, is lowest at Soapstone NA due to the absence of local emissions.

Vegetation is a significant source of the highly reactive VOC isoprene which accounts for over half of the biogenic VOC emissions in North America [Di Carlo et al., 2004]. Fossil Creek NA and Soapstone NA had the highest percent contribution to the total OH reactivity from isoprene (2.7% and 3.0%, respectively) due to both areas being in closer proximity to foliage and grasslands than the others.

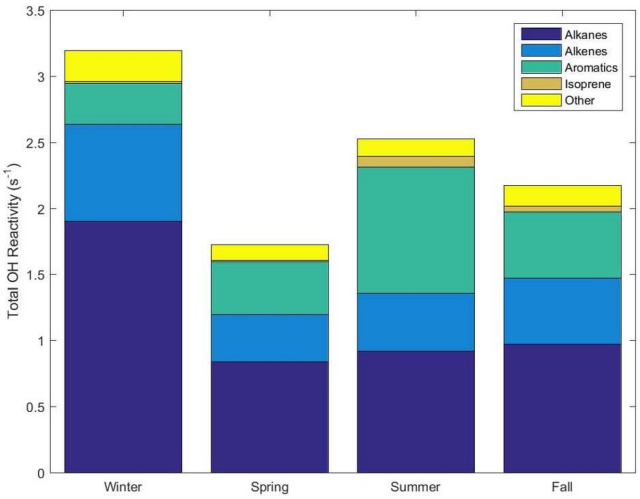

Figure 3.14: Average seasonal total OH reactivity measured at the elementary school.

Since alkenes are highly reactive with OH in the atmosphere, and OH concentration is positively correlated with sunlight, the ambient alkene concentration would be expected to decrease with increasing sunlight [Seinfeld et al., 2016]. In Figure 3.14 this trend is clearly seen at the elementary school as the largest percentage of the measured total reactivity resulting from alkenes is observed in the winter (22.9%) while the smallest amount is observed in the summer (17.3%). Alkanes also react with OH, but they are generally less reactive when compared to alkenes [Seinfeld et al., 2016]. The same trend is present in that the highest percentage of the total OH reactivity from alkanes is observed in the winter (59.9%) and the lowest is observed in the summer (36.4%). The opposite trend is present for aromatic compounds, in that the highest percentage is observed in the summer (37.9%), and the lowest percentage is observed in the winter (9.7%), which is likely a result of the increased reactivity of alkanes and alkenes in the summer.

Isoprene emissions are highly correlated with temperature and sunlight [Nolscher et al., 2012]; therefore, it would be expected that the OH reactivity of isoprene and percent contribution to the total OH reactivity from isoprene is largest in the summer. This pattern can be seen in Figure 3.14 where 3.2% of the average total OH reactivity in the summer at the elementary school results from isoprene, whereas in the fall, winter, and spring only 2.0%, 0.41%, and 0.76% of the average total OH reactivity results from isoprene, respectively. Figure 3.15 shows a timeline of the OH reactivity resulting from isoprene for each canister sample at the elementary school. The spikes in ambient isoprene concentration are clear in the summer months as a result of higher temperatures and increased sunlight. For most samples collected in the fall, winter, and spring, the isoprene concentration was below the limit of detection, and thus a concentration of $\frac{LOD}{2}$ was used (see Section 2.2.5) to calculate OH reactivity.

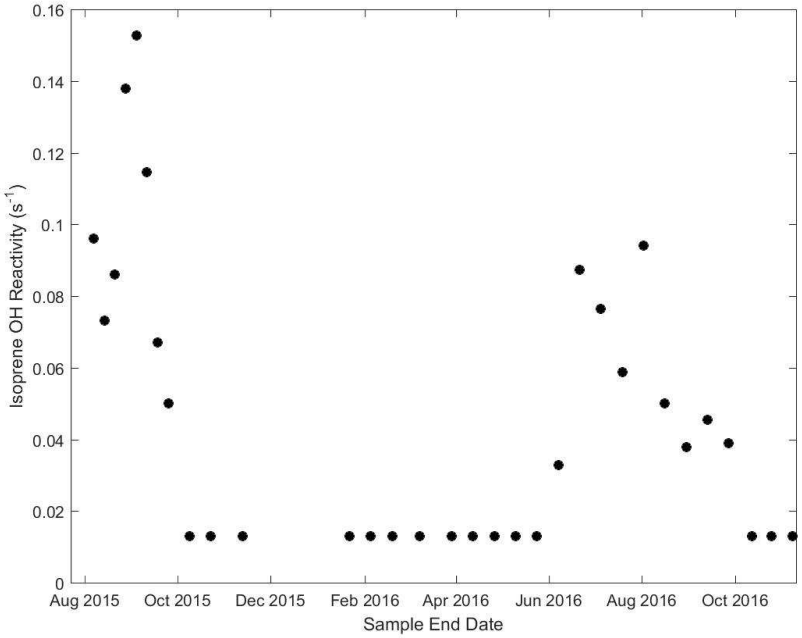

Figure 3.15: Timeline of the OH reactivity resulting from isoprene for the 32 samples collected at the elementary school.

3.2 Real-Time In-Situ GC Sampling

3.2.1 Comparison of Canister and In-situ Real-Time GC Measurements

Canisters and the in-situ real-time GC were deployed at the same location for approximately 3 weeks in the fall of 2015 at the residential area. This allows for some inter-comparison between the data collected in order to assess agreement between the sampling methods. Unfortunately, only 3 of the 4 canister samples collected at the residential area completely overlap in time with the real-time GC, further restricting the already limited sample availability to analyze the agreement between the methods. A summary table of all VOC concentrations found at the residential area using the in-situ real-time GC can be found in Appendix Table D.7. Figure 3.16 shows linear comparison plots of concentrations determined from canister sampling vs. the average concentration measured by the GC during the week the respective canister was deployed and Table 3.4 shows the slope and coefficient of determination (r^2) of the measurements.

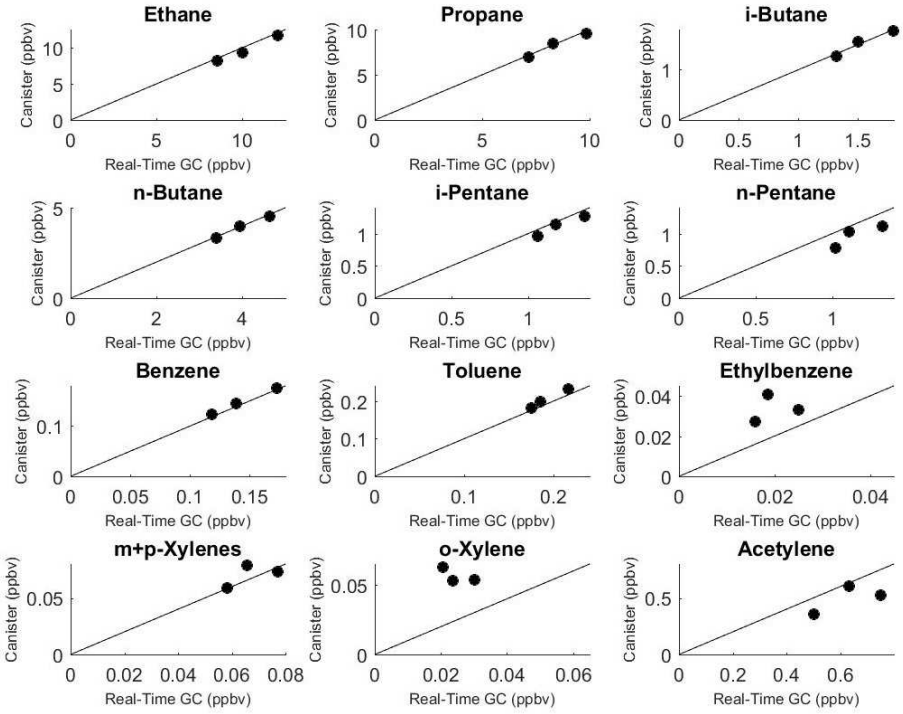

Figure 3.16: Linear comparison plots of concentrations determined from canister sampling vs. the average concentration measured by the GC during the week the respective canister was deployed. The solid black line indicates the 1:1 line.

Table 3.4: Slope and coefficient of determination (r^2) of concentrations determined from canister sampling vs. the average concentration measured by the GC during the week the respective canister was deployed.

	Slope (ppbv/ppbv)	r^2
Ethane	0.96	0.99
Propane	0.98	0.98
i-Butane	1.00	0.96
n-Butane	0.99	0.98
i-Pentane	0.93	0.94
n-Pentane	0.84	0.74
Benzene	1.03	1.00
Toluene	1.06	0.99
Ethylbenzene	1.65	0.04
m+p-Xylenes	1.04	0.36
o-Xylene	2.19	0.45
Acetylene	0.78	0.47

It should be reiterated that the use of only 3 data points limits the ability to draw strong conclusions from this inter-comparison. With this being noted, the light alkanes exhibit good

agreement between canister samples and the in-situ GC for all compounds except n-pentane, demonstrated by high correlations ($r^2 > 0.94$) and slopes between $0.93\frac{ppbv}{ppbv}$ and $1.00\frac{ppbv}{ppbv}$. While the agreement for n-pentane was not as strong as the other light alkanes, there is still a high correlation ($r^2 = 0.74$) and a slightly biased slope of $0.84\frac{ppbv}{ppbv}$. Benzene and toluene also exhibit a good agreement between the sampling methods exhibiting near perfect linear correlations and slopes of 1.03 and 1.06, respectively. Ethylbenzene, m+p-xylenes, o-xylene, and acetylene show relatively poor correlations ($r^2 < 0.47$) and biased slopes ranging from $0.78\frac{ppbv}{ppbv}$ to $2.19\frac{ppbv}{ppbv}$.

A few of factors could have contributed to the poor agreement of some compounds in this simple inter-comparison. The most significant is likely the small number of canister samples collected. Swarthout [2014] did a similar analysis with hundreds of samples and found strong agreement for a variety of compounds among whole air canister grab samples and in-situ GC samples. Having only 3 data points makes it difficult to accurately determine linear regression statistics and it is anticipated that if more week-long time-integrated canister samples were collected collocated with the real-time GC, the correlations could improve. Another factor that could contribute to deviation in slopes suggested by Swarthout [2014] was differences in the accuracy of standards used for calibration. The standard used in this study for the in-situ GC was different than the standard used on the 5-channel GC; therefore, some degree of error may have been introduced in this way.

3.2.2 Local O&NG Sources and Photochemical Age

An AIO weather station was deployed at the residential area to collect meteorological data at the same time as the real-time GC data were collected. It was anticipated that wind direction and wind speed could strongly influence the VOC concentrations and ratios observed at the residential area. In order to assess this impact, wind roses of the 10^{th} and 90^{th} percentile of propane concentration (Figure 3.17) are shown along with a map of O&NG wells around the residential area (Figure 3.18).

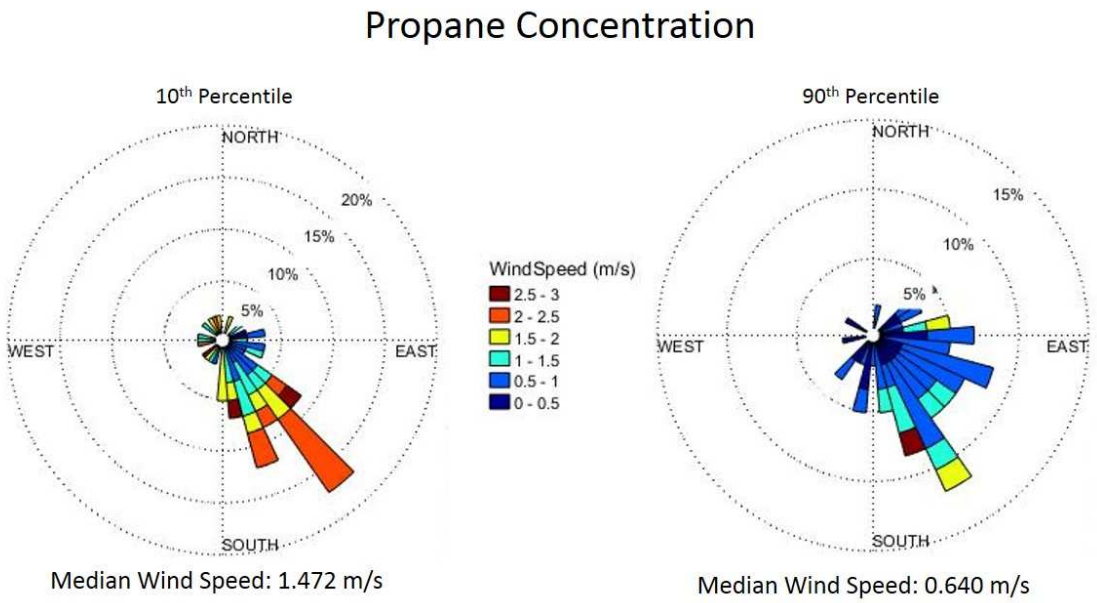

Figure 3.17: Wind roses of the 10^{th} and 90^{th} percentile of propane concentration.

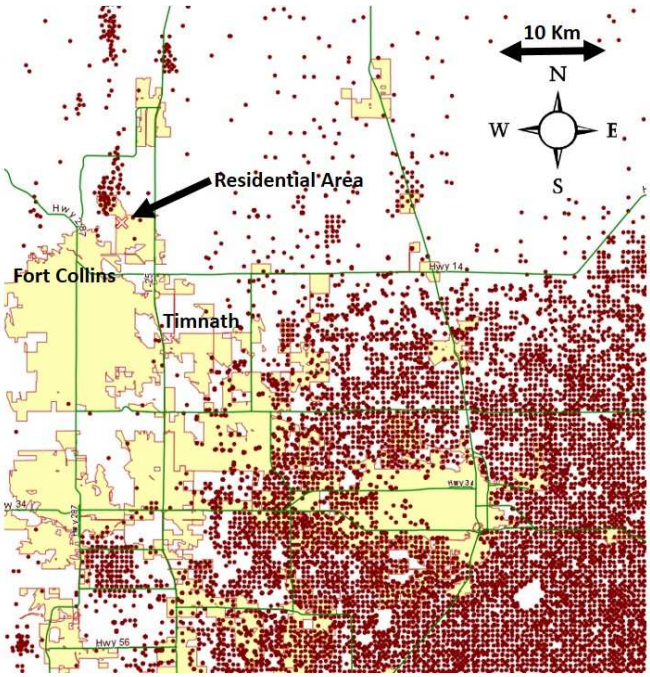

Figure 3.18: Map of O&NG wells around the residential area.

In Figures 3.17, the propane concentration is in the 10^{th} percentile for the higher median wind speed and the propane concentration is in the 90^{th} percentile for the lower median wind speed. There is a small concentrated development of approximately 50 wells about 1.5km northwest of the residential area whereas the much larger development consisting of thousands of wells is to the southeast and begins about 20km away (Figure 3.18).

58.9% of the overall wind direction measurements displayed southeasterly winds (90^o - 180^o) while 13.7% displayed southwesterly winds (180^o - 270^o), 9.5% displayed northwesterly winds (270^o - 360^o), and 17.9% displayed northeasterly winds (0^o - 90^o). The median propane concentration with southeasterly winds was 6.15ppbv and the median propane concentration with northwesterly winds was 1.52ppbv while the median propane concentration with southwesterly and northeasterly winds were 0.16pbv and 0.13ppbv, respectively. The enhanced propane concentrations correspond with regions of more O&NG development while the much lower propane concentrations, correspond with areas of less O&NG development. Considering both wind speed and direction, slower northwesterly and southeasterly winds corresponding with higher propane concentrations may imply that local O&NG sources have a strong impact on ambient air quality at the residential area.

While wind conditions may indicate VOC contributions from local O&NG sources near the residential area are important, in order to better understand this, a "photochemical clock" was used. This method utilizes the ratios of 2-pentyl nitrate, 2-butyl nitrate and their parent alkanes to estimate the age of the air mass [Evanoski-Cole et al., 2017]. The atmospheric reaction rates of n-pentane and n-butane to their respective alkyl nitrates are well known, thus allowing the ratio of the parent alkane to its alkyl nitrate to be used to estimate the age of the air mass [Evanoski-Cole et al., 2017].

Bertman et al. [1995] detailed this equation to model the evolution of alkyl nitrates in an air mass:

$$\frac{RONO_2}{RH} = \frac{\beta k_a}{k_b - k_a}(1 - e^{(k_a - k_b)t}) \tag{3.4}$$

where β is a unitless constant that accounts for the branching ratio leading to nitrate formation including the fraction of hydrogen (H) atom abstraction at the particular carbon, and the fraction of peroxy radicals that react with NO as opposed to other peroxy radicals. k_a and k_b are well established reaction rate constants, and t is the air mass age in seconds. The values of β, k_a, and k_b presented by Bertman et al. [1995] and used in the following calculations are listed in Table 3.5.

Table 3.5: Constants used to calculate and model the evolution of alkyl nitrates in an air mass. Ambient OH concentration is assumed to be 10^6 molecules cm^{-3} [Bertman et al., 1995].

	2-BuONO_2	2-PenONO_2
β	0.077	0.072
k_a (s^{-1})	2.54E-06	3.94E-06
k_b (s^{-1})	2.02E-06	3.05E-06

Ambient OH concentration is difficult to quantify and in most cases must be assumed in order to use this method. The values for β, k_a, and k_b presented by Bertman et al. [1995] were determined assuming an ambient OH concentration of 10^6 molecules cm^{-3}, at 40^oN in July. Spivakovsky et al. [2000] modeled monthly global OH concentrations and at 36^oN found a zonal mean in October at 800hPa of 1.1×10^6 molecules cm^{-3}. The samples in this study were collected in the fall at a latitude of 40.6^0N. In addition, Ebben et al. [2017] and Kim et al. [2014] derived comparable OH concentrations from measurements conducted in the CNFR. Therefore the assumptions made by Bertman et al. [1995] to calculate β, k_a, and k_b were applicable to the measurements and calculations in this thesis.

The solution to the Bertman et al. [1995] equation can be compared to the in-situ GC measurements to estimate the air mass age. Figure 3.19 shows the 2-pentyl nitrate to n-pentane ratio vs the 2-butyl nitrate to n-butane ratio indicating the photochemical age of VOC emissions measured using the in-situ real-time GC at the residential area. The points

are colored by i-pentane to n-pentane ratio. Figure 3.20 shows the same measurements with points colored by propane concentration.

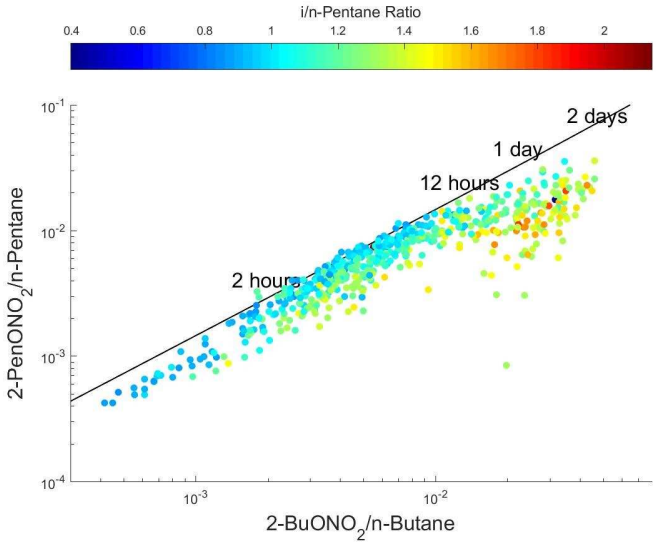

Figure 3.19: Photochemical age of measurements made using the in-situ real-time GC at the residential area. Points are color coded by the i-pentane to n-pentane ratio.

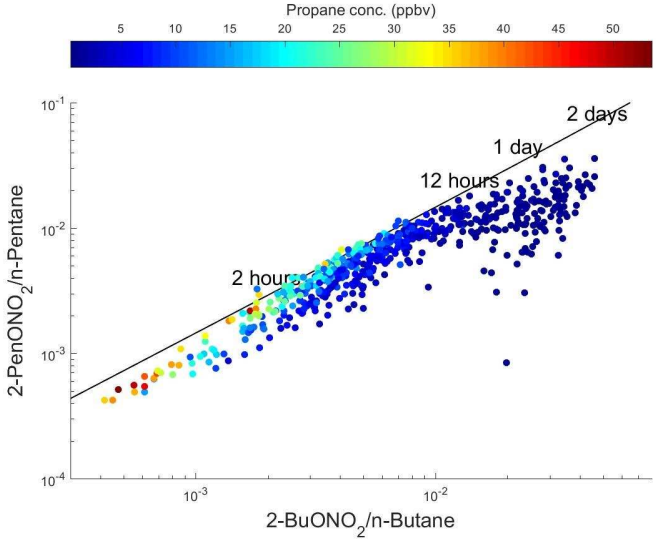

Figure 3.20: Photochemical age of measurements made using the in-situ real-time GC. Points are color coded by propane concentration.

Figures 3.19 and 3.20 show that in a more aged air mass, the i-pentane to n-pentane ratio is greater and the propane concentration is lower, whereas in a less aged air mass, the i-pentane to n-pentane ratio is lower and the propane concentration is greater. Evanoski-Cole et al. [2017] performed a similar analysis on data collected in the Bakken region of North Dakota and found a similar relationship that lower i-pentane to n-pentane ratios correspond with a younger air mass. Even though the locations of the studies were different, following the conclusions of Evanoski-Cole et al. [2017] and by relating both local wind data and photochemical age to O&NG markers, there is strong evidence that local O&NG operations have a significant impact on ambient VOC concentrations at the residential area.

3.2.3 VOC-OH Reactivity

OH reactivity calculations for the in-situ GC data were conducted similar to the canister samples, detailed in Section 3.1.4. The hourly measurements provided by the real-time GC allow the assessment of the diurnal pattern of total OH reactivity and the percent contribution from VOC categories. The in-situ GC data included some different VOCs than measured from the canister samples; therefore, the VOC categories are slightly different. Appendix Table G.2 lists the VOC categories specific to the in-situ GC. The data was grouped into four 6-hour time blocks, 00:00 (midnight) - 05:59, 06:00 - 11:59, 12:00 - 17:59, and 18:00 - 23:59. Figure 3.21 shows the average diurnal cycle of OH reactivity at the residential area for 3 weeks in the fall of 2015.

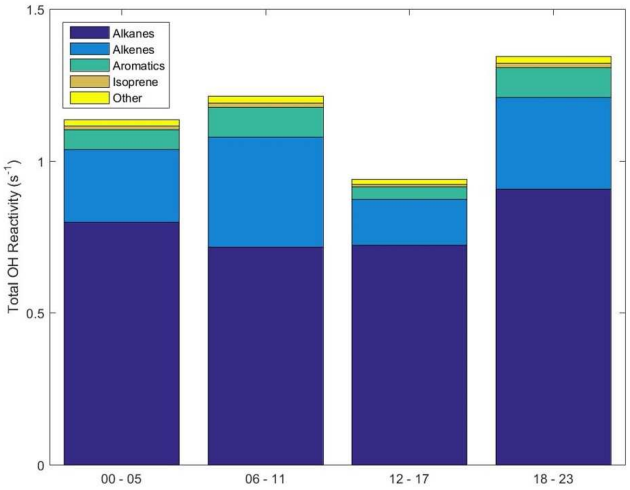

Figure 3.21: Average diurnal total OH reactivity measured at the residential area using the in-situ real-time GC (Oct. 26, 2015 - Nov. 20, 2015).

The diurnal pattern of total OH reactivity increasing in the morning, decreasing in the early afternoon and increasing again in the evening was observed by Abeleira et al. [2017] and Gilman et al. [2013] at the BAO. Abeleira et al. [2017] collected VOC data using the same real-time GC in the spring and summer of 2015 and measured a comparable size and type of VOC suite as this study. The approximate magnitude of the OH reactivity they measured in the spring was similar to this study; however, they observed a total reactivity maximum in the mid-morning of about $1.5s^{-1}$ whereas this study saw a maximum in the evening of about $1.35s^{-1}$. They observed a greater morning OH reactivity peak in the summer of approximately $3.0s^{-1}$. Gilman et al. [2013] collected VOC data using a real-time GC in the spring of 2011 and measured a suite that contained additional OVOCs and biogenics, which are more reactive, leading to a measured total OH reactivity peak in the mid-morning of about $5s^{-1}$. There was not much diurnal variation in the fractional contribution of each VOC category, consistent with the results of this study.

3.3 AERMOD Dispersion Modeling

3.3.1 Model Results

AERMOD dispersion modeling was utilized to evaluate the potential increase in ambient benzene concentrations at the elementary school, assuming the proposed well pad were constructed approximately 2000ft (609.6m) northeast of the campus. Figure 3.22 shows the proposed well site marked by a red rectangle and the school campus denoted by a yellow rectangle.

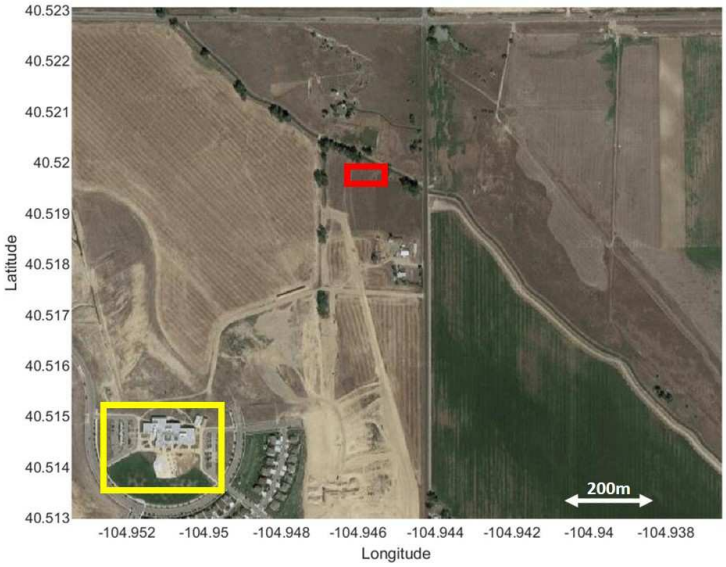

Figure 3.22: Map of the proposed well site marked by a red rectangle (not to scale) and the school campus denoted by a yellow rectangle.

Collett et al. [2016] quantified VOC emission rates from O&NG developments in the NCFR using the tracer ratio method (TRM) in which a tracer gas is released from a well pad at a known rate and canister samples are collected upwind and downwind. By multiplying the tracer release rate by the ratio of the background-corrected VOC and tracer concentrations the VOC emission rate can be determined. Model runs utilizing the 5^{th}, 25^{th}, median, 75^{th}, and 95^{th} percentile emission rates of benzene found at production well sites in the CNFR by Collett et al. [2016] were used and the hourly average concentration increases for 1 year were simulated. Further details on the model input parameters can be found in Section 2.4.2.

Figure 3.23 shows the median emission rate concentration field at the elementary school (the 5^{th}, 25^{th}, 75^{th}, and 95^{th} percentile emission rate contour plots are shown in Appendix H) and Figure 3.24 shows the distribution of benzene concentration increase at the elementary school along with the corresponding emission rates, annual average concentration increases, 99^{th} percentile concentration increases, and percentage of hourly outputs showing no concentration increases.

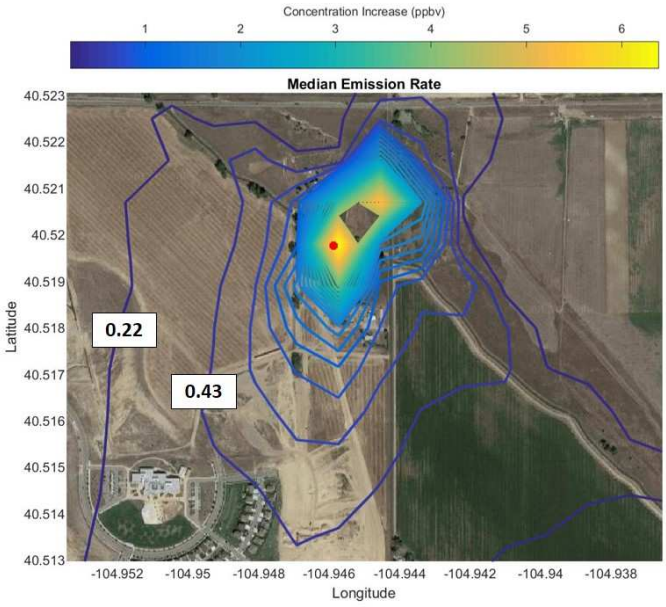

Figure 3.23: Contour plot of benzene concentration increase around the well pad under the median emission rate scenario ($1.5 \times 10^{-3} \frac{g}{s}$). The center of the well pad is denoted by a red dot. The elementary school campus can be seen in the lower left corner and the contours around the school are labeled with the concentration increase in ppbv.

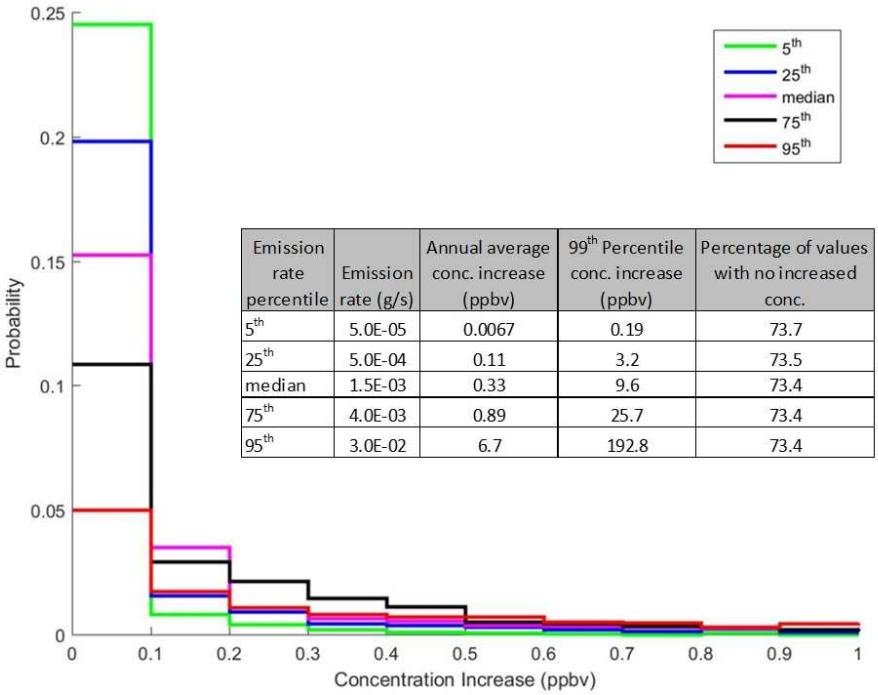

Emission rate percentile	Emission rate (g/s)	Annual average conc. increase (ppbv)	99th Percentile conc. increase (ppbv)	Percentage of values with no increased conc.
5th	5.0E-05	0.0067	0.19	73.7
25th	5.0E-04	0.11	3.2	73.5
median	1.5E-03	0.33	9.6	73.4
75th	4.0E-03	0.89	25.7	73.4
95th	3.0E-02	6.7	192.8	73.4

Figure 3.24: Distribution of benzene concentration increase at the elementary school along with the corresponding well pad emission rates, annual average concentration increases, 99^{th} percentile concentration increases, and percentage of hourly outputs showing no concentration increase.

The median concentration measured through week-long time-integrated canister sampling at the elementary school was 0.18 ± 0.08ppbv. Local meteorology, specifically wind conditions, is the main driver for the increase in benzene concentrations near the school due to emissions from a new well pad. Under all five emission rate scenarios, 73.4 - 73.7% of the year there is no benzene enhancement seen from the well site. Therefore, the benzene concentration at the school would be expected to be approximately 0.18 ± 0.08ppbv at those times, assuming similar source contributions as seen in sample collection in this study. This would be expected to be the case under southerly or westerly wind conditions (i.e. winds toward the well and away from the school campus). Expectedly, with an increase in emission rate, the distribution shown in Figure 3.24 widens, with fewer hours displaying a concentration increase of less than 0.1ppbv and the median and 99^{th} percentile increasing.

Under the 5^{th} percentile emission rate scenario ($5.0 \times 10^{-5} \frac{g}{s}$) the average benzene concentration at the school increases by about 4% (0.0067ppbv) and displays an increase of 0.19ppbv over the ambient concentration at the 99^{th} percentile. Under the 25^{th} percentile emission rate scenario ($5.0 \times 10^{-4} \frac{g}{s}$) the average benzene concentration at the school increases by about 61% (0.11ppbv) and displays an increase of 3.2ppbv over the ambient concentration at the 99^{th} percentile. Under the median emission rate scenario ($1.5 \times 10^{-3} \frac{g}{s}$) the average benzene concentration at the school increases by about 180% (0.33ppbv) and displays an increase of 9.6ppbv over the ambient concentration at the 99^{th} percentile. Under the 75^{th} percentile emission rate scenario ($4.0 \times 10^{-3} \frac{g}{s}$) the average benzene concentration at the school increases by nearly 5 times (0.89ppbv) and displays an increase of 25.7ppbv over the ambient concentration at the 99^{th} percentile. Under the 95^{th} percentile emission rate scenario ($3.0 \times 10^{-2} \frac{g}{s}$) the average benzene concentration at the school increases by over 37 times (6.7ppbv) and displays an increase of 192.8ppbv over the ambient concentration at the 99^{th} percentile.

These model simulations assume a constant benzene emission rate throughout the year. It is unlikely that a well site would exhibit regular emission in this manner; however, for the purposes of modeling a well that has not yet been constructed, this assumption was made. Also, these model simulations were done using benzene emission rates from only production well sites. In the fracking and flowback stages of well development, the benzene emission rates found by Collett et al. [2016] were significantly higher. However, these emissions would occur on a much shorter time scale (typically several days) than the production lifetime of the well (typically decades).

To further investigate the potential hourly benzene enhancement at the elementary school, the diurnal pattern of its concentration increase was evaluated. Figure 3.25 shows the hourly benzene concentration increases at the elementary school under the median emissions rate scenario for each hour of the day from the annual AERMOD simulation results.

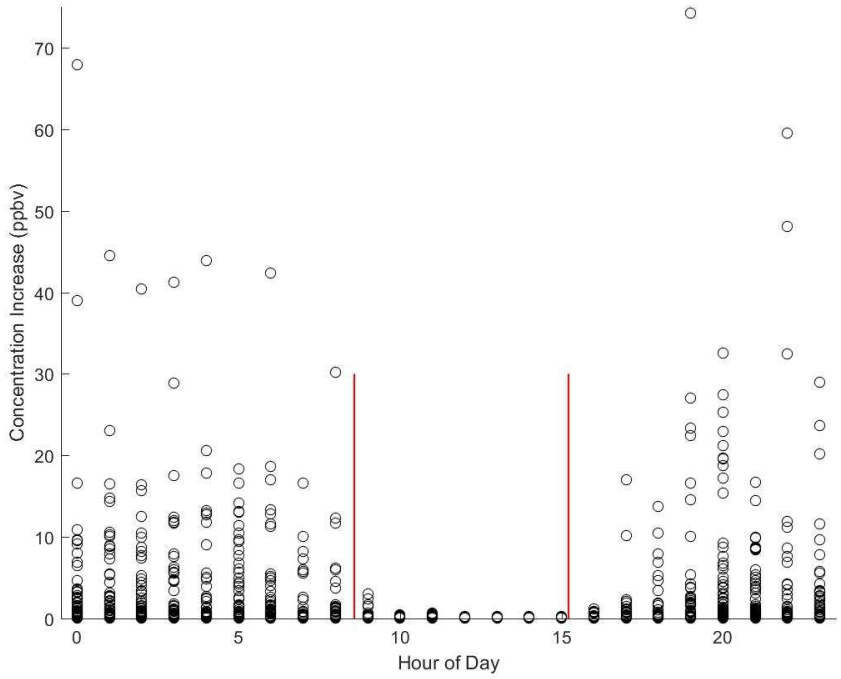

Figure 3.25: Benzene concentration increases at the elementary school under the median emissions rate scenario ($1.5 \times 10^{-3} \frac{g}{s}$) for each hour of the day. The vertical red lines indicate the start and end of school hours for student attendance.

Based on AERMOD simulations, the emissions from the potential well site do not result in any enhancements at the school for 73.4% of the year. Figure 3.25 only shows the instances in which there was a positive concentration increase. The strongest benzene enhancement occurs 00:00 (midnight) - 08:00 and 17:00 - 23:00. Interestingly, the elementary school hours for student attendance are 08:35 - 15:13 [PSD, 2017], which falls in the period of the day with the least benzene enhancement resulting from the development of a new well. During that time frame, the annual average benzene concentration increase is only 0.024ppbv, much less when compared to the overall annual average increase of 0.33ppbv. Outside of school hours, the annual average benzene concentration increase is 0.46ppbv. The elementary school and the Timnath community offer several extracurricular activities that take place on the school campus, so it is likely that many students would be at the school outside of standard attendance hours. To reiterate, these concentration increases assume that the potential well

site is emitting at the median production emission rate constantly throughout the year, and the benzene enhancements in Figure 3.25 would be expected to increase during the initial fracking and flowback stages of well development; however, these processes occur over several days whereas the production lifetime of wells is typically decades.

The lower modeled benzene concentration during school hours can be explained by more turbulent conditions and wind directions that do not result in influence from the well site. Figure 3.26 clearly shows that wind speeds are elevated during school hours and the wind directions are mainly southerly and northwesterly. In contrast, outside of school hours winds are generally calmer and have more of a northerly component, which result in the greater benzene enhancement that was modeled. It is also possible that deeper boundary layer conditions during the day lead to increased mixing and dilution of the well site emissions.

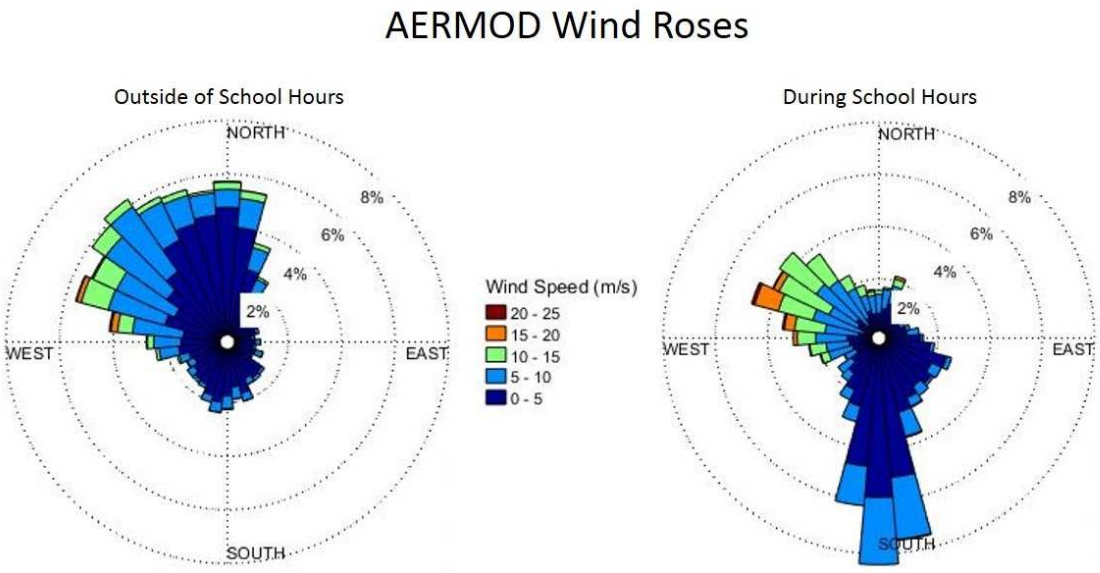

Figure 3.26: Wind roses showing the AERMOD input data outside and during the elementary school attendance hours.

3.3.2 Comparison With Air Quality Standards

Benzene in a known HAP that has been linked to leukemia, anemia and other blood disorders and cancers, immune system impairment, decreased respiratory function, and neural tube defects in newborns [Halliday et al., 2016]. Agencies such as the U.S. Occupational

Safety and Health Administration (OSHA) and the U.S. National Institute for Occupational Safety and Health (NIOSH) have set benzene exposure limits for short and long term exposure. Typically, these standards are applied in an indoor workplace so they are not directly applicable to the ambient outdoor concentrations measured and modeled at the elementary school; however, they do provide some context and comparison as to the potential health effects of the proposed well development. Furthermore, young children attending elementary school can be considered as part of a "sensitive population" which could lower the acceptable exposure limit. OSHA has established a permissible exposure value for benzene of 1ppmv (1000ppbv) averaged over 8 hours and a shorter term standard of 5ppmv (5000ppbv) averaged over 15 minutes [OSHA, 2017]. Under all five emission rate scenarios, the annual average concentration and the 99^{th} percentile concentration at the school are multiple orders of magnitude below the standards.

NIOSH recommends an exposure limit for benzene is 0.1ppmv (100ppbv) averaged over 8 hours and a shorter term standard of 1ppmv (1000ppbv) averaged over 15 minutes [NIOSH, 2014]. Under all five emission rate scenarios, the annual average concentration at the school does not exceed the recommended 8 hour exposure limit. The 99^{th} percentile concentration under the 95^{th} percentile emission rate scenario exceeds the 8 hour exposure limit, but once again, these concentrations would likely not be sustained over an 8 hour period and furthermore the 99^{th} percentile concentration under the 95^{th} percentile emission rate does not exceed the recommended 15 minute exposure limit.

The Agency for Toxic Substances and Disease Registry (ATSDR) has developed Minimal Risk Levels (MRLs) for air toxins through discussions with scientists within the Department of Health and Human Services (HHS) and the EPA. The published MRLs are defined as "an estimate of the daily human exposure to a hazardous substance that is likely to be without appreciable risk of adverse non-cancer health effects over a specified duration of exposure" [ATSDR, 2017]. The ATSDR lists MRLs for acute (1 - 14 days), intermediate (>14 - 364 days), and chronic (365 days and longer) exposure to air toxins. For benzene, the acute

MRL is 0.009ppm (9ppbv), the intermediate MRL is 0.006ppm (6ppbv), and the chronic MRL is 0.003ppm (3ppbv). There is a wide range of acute (1 - 9ppbv), intermediate (6 - 25ppbv), and chronic (8 - 52,000ppbv) exposure threshold levels that vary in range depending on the regulatory agency [TCEQ, 2015]. The ATSDR MRL's are presented here because they have been extensively reviewed by a panel of external reviewers and were derived with participation from several federal agencies [ATSDR, 2017]. The annual average concentration increase at the school exceeds the intermediate and chronic ATSDR MRLs only under the 95^{th} percentile emission rate scenario. The annual average concentration increase resulting from the lower emission rates does not exceed any of the 3 listed ATSDR MRLs. The 5^{th}, 25^{th}, and median percentile emission rates never exceed the acute ATSDR MRL for a 24 hour period. The 75^{th} percentile emission rate exceeds the acute ATSDR MRL for one 24 hour period while the 95^{th} percentile emission rate exceeds the acute ATSDR MRL for several 24 hour periods. The 99^{th} percentile concentration increases exceed at least one of the ATSDR MRLs for the 25^{th}, median, 75^{th}, and 95^{th} percentile emission rates. However, this percentile increase represents a one hour average concentration and would not be seen on the longer time scales established for the ATSDR MRLs.

Chapter 4

Conclusions and Future Work

The CNFR is located in the Wattenberg gas field within the Denver-Julesburg Basin which is one of the largest shale formations in the U.S. Advances in unconventional extraction of O&NG have allowed a large increase in the number of wells in the CNFR over the past few decades as this has provided access to natural gas reservoirs that were previously deemed economically infeasible. This growth in O&NG development may lead to increased emissions of VOCs which may negatively impact air quality and human health. In order to help assess this impact, this study utilized time-integrated whole air canister sampling at five locations in Fort Collins and Timnath and real-time in-situ GC measurements at a residential area in Fort Collins.

Fossil Creek NA in southeast Fort Collins close to I-25 was found to have the highest median concentration of ethane and propane while a gas station site at a busy intersection displayed the highest median concentration of butanes, pentanes, acetylene, and BTEX compounds. The mean ratio of i-pentane to n-pentane found at the elementary school, residential area, Fossil Creek NA, Soapstone NA, and the gas station was 1.07, 1.17, 1.16, 1.05, and 2.35, respectively, indicating that the air mass is heavily influenced by O&NG emissions at all sampling locations, except the gas station. Using a multivariate regression technique that accounts for the correlations of VOCs to propane and acetylene, the elementary school, residential area, and Fossil Creek NA were found to have a large percentage of VOCs attributable to O&NG emissions. In addition, meteorological data coupled with real-time GC VOC measurements provide strong evidence that local O&NG sources can have a large impact on air quality at a residential area in northeast Fort Collins.

Fossil Creek NA showed the largest total OH reactivity in the fall while Soapstone NA displayed the lowest. At Soapstone NA, 66.7% of the total OH reactivity resulted from aromatics, which is the highest, and 11.4% resulted from alkenes, which is the lowest compared to each group's contribution at other sites, likely due to its location far from emission sources

allowing time for the chemical processing of more reactive hydrocarbons. At the elementary school the largest OH reactivity was seen in the winter. The lowest OH reactivity was seen in the summer; however, 3.2% of the OH reactivity in the summer was attributed to isoprene, whereas in the fall, winter, and spring only 2.0%, 0.41%, and 0.76% of the OH reactivity resulted from isoprene, respectively. OH reactivity did not vary much diurnally in total or speciation at the residential area, but displayed a similar pattern and magnitude to previous studies in the CNFR.

Development of new unconventional O&NG wells is ongoing in the CNFR and there are plans to develop wells in close proximity to the elementary school sampling location in Timnath. In order to estimate potential impacts of this project, the AMS/EPA steady-state air dispersion model AERMOD was utilized to project the potential increased concentration of benzene at the elementary school as a results of this development. The site was modeled using the 5^{th}, 25^{th}, median, 75^{th}, and 95^{th} percentile production well site emission rates of benzene found by Collett et al., [2016] in the CNFR and annual average concentration increases above current background at the school (0.18 ± 0.08ppbv) were found to be 0.0067, 0.11, 0.33, 0.89, and 6.7ppbv, respectively. None of these annual average concentration increases exceeded established OSHA or NIOSH benzene exposure limits. The annual average concentration increase for the 95^{th} percentile emission rate exceeds the intermediate and chronic MRLs listed by the ATSDR. However, this simulation assumes a constant emission rate, and it is unlikely that a well would be emitting benzene at the 95^{th} percentile rate for an entire year. Under the median emission rate scenario, the strongest benzene enhancement at the school occurred 00:00 (midnight) - 08:00 and 17:00 - 23:00 (0.46ppbv). The elementary school attendance hours are 08:35 - 15:13 and during that time, the annual average benzene concentration increase is only 0.024ppbv, much less when compared to the overall annual average increase of 0.33ppbv. Factoring in all times of day, the 75^{th} percentile emission rate exceeded the acute ATSDR MRL for one 24 hour period during the year while the 95^{th} percentile emission rate exceeded the acute ATSDR MRL for several 24 hour periods.

If O&NG development continues to increase by approximately 4% over the next several years, as projected, wells will likely continue to be drilled in relatively close proximity to residential areas, schools, and businesses. Therefore, continued monitoring of ambient VOC levels in areas such as the CNFR where there is dense O&NG development is needed. Future sampling at the same or similar locations throughout Fort Collins and Timanth should be conducted in order to utilize this data set as a baseline to assess potential increases in ambient VOC concentrations as O&NG development and population grow. Also, with additional data, including further VOC speciation, the OH reactivity and photochemical age calculations discussed in this work could be expanded in order to further address the ongoing issue of O_3 production in the CNFR.

Sampling should be resumed at the elementary school once the proposed drilling project has been initiated. Sampling using the same methods detailed in this thesis would provide not only continued monitoring of the potential increased VOC exposure of the students and staff, but also could serve as a direct comparison data set for the concentration increases projected by the presented AERMOD simulations. Also, collecting real-time BTEX concentration measurements using proton-transfer-reaction mass spectrometry (PTR-MS) coupled with an AIO weather station would provide detailed concentration ranges and meteorological data on a s^{-1} time interval, thus providing a better understanding of the effect of local meteorology on the concentration increases seen at the school. There is a residential neighborhood that surrounds the elementary school. Therefore, to better understand specific benzene exposure for students and other sensitive populations, it may be necessary to evaluate days and hours in which school is in session combined with benzene enhancement at other receptor points located within the residential neighborhood. This more in-depth analysis could provide a better look at student exposure during and outside of school attendance hours.

To further investigate HAP exposure through sampling techniques, the use of personal VOC monitors that can be worn by students or staff could be implemented to provide a more accurate assessment of the personal exposure individuals experience on a daily basis.

These monitors could be worn during and outside of school hours, and combined with a more in-depth AERMOD analysis, could allow for a targeted assessment as to the percentage of students and staff exposed to elevated VOC levels. In addition, it may be useful to implement indoor time-integrated whole air VOC sampling at the school to compare with the outdoor measurements collected on the campus. These data sets could be compared to establish exposure limits and MRLs to give additional context to health risks.

References

Abeleira, A., Pollack, I. B., Sive, B., Zhou, Y., Fischer, E. V., & Farmer, D. K. (2017). Source characterization of volatile organic compounds in the Colorado Northern Front Range Metropolitan Area during spring and summer 2015. Journal of Geophysical Research: Atmospheres, 122(6), 3595-3613. doi: 10.1002/2016JD026227

Agency for Toxic Substances and Disease Registry (ATSDR). (2017). Minimal Risk Levels (MRLs). https://www.atsdr.cdc.gov/mrls/index.asp

American Petroleum Institute (API). (2017). Facts About Shale Gas. http://www.api.org/oil-and-natural-gas/wells-to-consumer/exploration-and-production/hydraulic-fracturing/facts-about-shale-gas

Air Resource Specialists (ARS). (2014). City of Fort Collins Data Summary Report: H_2S and VOC Air Monitoring Project. City of Fort Collins Environmental Services Department. https://www.fcgov.com/oilandgas/pdf/fc-airquality-project-data-report.pdf

Baird, C., & Michael, C. C. (2012). Environmental Chemistry. W.H. Freeman.

Baker, A. K., Beyersdorf ,A. J., Doezema, L. A., Katzenstein, A., Meinardi, S., Simpson, I. J., Blake, D. R., & Sherwood, R. F. (2008). Measurements of nonmethane hydrocarbons in 28 United States cities, Atmos. Environ., 42(1), 170-182, doi: 10.1016/j.atmosenv.2007.09.007

Berezin, I. V., Denisov, E. T., & Emanuel, N. M. (1966). The Oxidation of Cyclohexane. Oxford: Pergamon Press Ltd.

Bertman, S. B., Roberts, J. M., Parrish, D. D., Buhr, M. P., Goldan, P. D., Kuster, W. C., Fehsenfeld, F. C., Montzka, S. A. and Westberg, H. (1995). Evolution of alkyl nitrates with air mass age. Journal of Geophysical Research: Atmospheres, 100(D11), 22805-22813. doi: 10.1029/95JD02030

Blake, D. R. (2014). [FRAPPÉ ground level canister grab sampling data set (UCI)]. Unpublished raw data.

Blake, N. J., & Blake, D. R. (2002). Tropospheric chemistry and composition. doi: 10.1006/rwas.2002.0422

Bolden, A. L., Kwiatkowski, C. F., & Colborn, T. (2015). New look at BTEX: are ambient levels a problem?. Environmental science & technology, 49(9), 5261-5276. doi:10.1021/es505316f

Borbon, A., Fontaine, H., Veillerot, M., Locoge, N., Galloo, J. C., & Guillermo, R. (2001). An investigation into the traffic-related fraction of isoprene at an urban location. Atmospheric Environment, 35, 3749-3760. doi: 10.1016/S1352-2310(01)00170-4

Broderick, B. M., & Marnane, I. S. (2002) A comparison of the C_2 C_9 hydrocarbon compositions of vehicle fuels and urban air in Dublin, Ireland, Atmos. Environ., 36(6), 975986. doi: 10.1016/S1352-2310(01)00472-1

Canadian Centre for Energy Information (CCEI). (2013). Components of Raw Natural Gas. http://history.alberta.ca/energyheritage/gas/premodern-global-history/physical-character-of-natural-gas.aspx

Cimorelli, A. J., Perry, S. G., Venkatram, A., Weil, J. C., Paine, R. J., Wilson, R. B., Lee, R. F., Peters, W. D., Brode, R. W., & Paumier, J. O. (2004). AERMOD: Description of Model Formulation. United States Environmental Protection Agency (USEPA). https://www3.epa.gov/scram001/7thconf/aermod/aermod_mfd.pdf

City of Fort Collins, Larimer County. (2003) Resource Management & Implementation Plan for Fossil Creek Reservoir Regional Open Space. http://www.fcgov.com/naturalareas/pdf/fossil_creek_plan.pdf?1262729110

Cloke, M. (1995) Encyclopedia of chemical technology (4th edition), vol. 62. John Wiley &Sons, Inc.

CoAgMet Network. (n.d.) CoAgMet. Colorado State University. http://www.coagmet.colostate.edu/

Collett, J.L., Hecobian, A., Ham, J., Pierce, J., Clements, A., Shonkwiler, K., Zhou, Y., Desyaterik, Y., MacDonald, L., Wells, B., & Hilliard, N. (2016). North Front Range Oil and Gas Air Pollution Emission and Dispersion Study. https://www.colorado.gov/airquality/tech_doc_repository.aspx?action=open&file=CSU_NFR_Report_Final_20160908.pdf

Colorado Department of Public Health and Environment (CDPHE). (2011). Colorado Modeling Guideline for Air Quality Permits. https://www.colorado.gov/airquality/permits/guide.pdf

Colorado Department of Public Health and Environment (CDPHE). (2016). [Ozone Precursor Study]. Unpublished Raw Data.

Colorado Department of Public Health and Environment (CDPHE) Air Quality Control Commission (AQCC). (2016). Moderate Area Ozone SIP for the Denver Metro and North Front Range Non-attainment area. https://raqc.egnyte.com/dl/q5zyuX9QC1/

Colorado Department of Transportation (CDOT). (2015). Transportation Planning Reports. http://dtdapps.coloradodot.info/otis/Statistics

Colorado Oil and Gas Conservation Commission (COGCC). (2007). Greater Wattenberg Area Baseline Study. http://cogcc.state.co.us/documents/library/AreaReports/DenverBasin/GWA/Greater_Wattenberg_Baseline_Study_Report_062007.pdf

Colorado Oil and Gas Conservation Commission (COGCC). (2016a). Colorado Oil and Gas Information System. http://cogcc.state.co.us/data.html

Colorado Oil and Gas Conservation Commission (COGCC). (2016b). Series Safety Regulations. https://cogcc.state.co.us/documents/reg/Rules/LATEST/600Series.pdf

Colorado Oil and Gas Conservation Commission (COGCC). (2017). COGCC Interactive Map. http://cogcc.state.co.us/maps.html#/gisonline

Daguat, P., Ristori, A., Bakali, E., & Cathonnet, M. (2002). Experimental and kinetic modeling study of the oxidation of n-propylbenzene. Fuel, 81, 173-184. doi: 10.1016/S0016-2361(01)00139-9

Di Carlo, P., Brune, W. H., Martinez, M., Harder, H., Lesher, R., Ren, X., Thornberry, T., Carroll, M. A., Young, V., Shepson, P. B., & Riemer, D. (2004). Missing OH reactivity in a forest: Evidence for unknown reactive biogenic VOCs. Science, 304(5671), 722-725. doi: 10.1126/science.1094392

Doskey, P. V., Porter, J. A., & Scheff, P. A., (1992). Source fingerprints for volatile non-methane hydrocarbons. Journal of the Air & Waste Management Association, 42(11), 1437-1445. doi: 10.1080/10473289.1992.10467090

U.S. Energy Information Administration (EIA). (2014). U.S. Energy Information Admin-

stration - Independent Statistics & Analysis. http://www.eia.gov/state/analysis.cfm?sid=CO

U.S. Energy Information Administration (EIA). (2016). Colorado Profile State Profile and Energy Estimates, Energy Information Agency, U.S. Department of Energy. http://www.eia.gov/state/?sid=CO

U.S. Energy Information Administration (EIA). (2017). Annual Energy Outlook. Energy Information Agency, U.S. Department of Energy. https://www.eia.gov/outlooks/aeo/pdf/0383(2017).pdf

Entech. (2015). CS1200E Flow Controller Operation and Care Guide. http://www.entechinst.com/download/cs1200e-passive-canister-sampler/

U.S. Environmental Protection Agency (EPA). (1994). Locating and Estimating Air Emissions from Sources of Xylene. (Office of Air Quality Standards, Ed.) http://www3.epa.gov/ttnchie1/le/xylene.pdf

U.S. Environmental Protection Agency (EPA). (2004). User's Guide for the AMS/EPA Regulatory Model - AERMOD. USEPA Office of Air Quality Planning and Standards Emissions Monitoring and Analysis Division. https://www3.epa.gov/ttn/scram/models/aermod/aermod_userguid addendum_v11059_draft.pdf

U.S. Environmental Protection Agency (EPA). (2015). What are Hazardous Air Pollutants? https://www.epa.gov/haps/what-are-hazardous-air-pollutants.

U.S. Environmental Protection Agency (EPA). (2016). Cumene. https://www.epa.gov/sites/production/files/2016-09/documents/cumene.pdf

Ebben, C. J., Sparks, T. L., Wooldridge, P. J., Campos, T. L., Cantrell, C. A., Mauldin, R. L., Weinheimer, A. J., & Cohen, R. C. (2017) Evolution of NOx in the Denver Urban Plume during the Front Range Air Pollution and Photochemistry Experiment. Atmos. Chem. Phys. Discuss., doi: 10.5194/acp-2017-671

Evanoski-Cole, A. R., Gebhart, K. A., Sive, B. C., Zhou, Y., Capps, S. L., Day, D. E., Prenni, A. J., Schurman, M. I., Sullivan, A. P., Li, Y., & Hand, J. L. (2017). Composition and sources of winter haze in the Bakken oil and gas extraction region. Atmospheric Environment, 156, 77-87. doi: 10.1016/j.atmosenv.2017.02.019

Fraser, M. P., Cass, G. R., & Simoneit, B. R. T. (1998). Gas-phase and particle-phase organic compounds emitted from motor vehicle traffic in a Los Angeles roadway tunnel. Environ. Sci. Technol., 32 (14), 20512060. doi: 10.1021/es970916e

Friesema, H. P. (2012). Kerr-McGee oil and gas onshore LP (KMG), Greater Natural Buttes: environmental impact statement. United States. Bureau of Land Management. https://catalog.hathitrust.org/Record/100981013

U.S. Geological Survey (USGS). (2017). Multi-Resolution Land Characteristics Consortium (MRLC). https://www.mrlc.gov/ finddata.php

Gilman, J. B., Lerner B. M. , Kuster W. C., & de Gouw J. A. (2013). Source signature of volatile organic compounds from oil and natural gas operations in northeastern Colorado, Environ. Sci. Technol.. 47 (3), 1297-1305. doi: 10.1021/es304119a

GuoYi, H., Jian, L., ZhiSheng, L., Xia, L., QingWu, S., & ChengHua, M. (2008). Preliminary study on the orgin identification of natural gas by the parameters of light hydrocarbon. Science in China Series D: Earth Sciences, 51, 131-139. doi: 10.1007/s11430-008-5017-x

Graedel, T. E. (1978). Chemical Compounds in the Atmosphere. New York, New York: Academic Press Inc.

Graedel, T. E., Hawkins, D. T., & Claxton, L. D. (1986). Atmospheric Chemical Compounds: Sources, Occurence, and Bioassay. Orlando, Florida: Academic Press Inc.

Halliday, H. S., Thompson, A. M., Wisthaler, A., Blake, D. R., Hornbrook, R. S., Mikoviny, T., Mller, M., Eichler, P., Apel, E. C. and Hills, A. J., (2016) Atmospheric benzene observations from oil and gas production in the DenverJulesburg Basin in July and August 2014. Journal of Geophysical Research: Atmospheres, 121(18). doi: 10.1002/2016JD025327

Haley, M., Mccawley M., Epstein A. C., Arrington B., & Bjerke, E. F. (2016). Adequacy of Current State Setbacks for Directional High-Volume Hydraulic Fracturing in the Marcellus, Barnett, and Niobrara Shale Plays. Environmental Health Perspectives, 124(9), 1323. doi: 10.1289/ehp.1510547

Harper, H. W. (2014). Hydraulic Fracturing:A Comprehensive and Balanced Review. PDH Online. https://pdhonline.com/courses/c746/Hydraulic%20Fracturing%20-%20A%20Comprehensive%20&%20Balanced%20Review%20_%20Rev-2.pdf

Hilliard, N. G., (2016). Volatile Organic Compound And Methane Emissions From Well Development Operations In the Piceance Basin, MS Thesis. Colorado State University.

Ho, K. F., Lee, S. C., Guo, H., & Tsai, W. Y. (2004). Seasonal and diurnal variations of volatile organic compounds (VOCs) in the atmosphere of Hong Kong. Science of the Total Environment, 322, 155-166. doi: 10.1016/j.scitotenv.2003.10.004

Hoffman, J. (2015). Potential Health and Environmental Effects of Hydrofracking in the Williston Basin, Montana. Geology and Human Health. https://serc.carleton.edu/NAGTWorkshops/health/case_studies/hydrofracking_w.html

Howard, P. H. (1989). Large Production and Priority Pollutants: Handbook of Environmental Fate and Exposure Data for Organic Chemicals (Vol. I). Boca Raton, Florida: CRC Press LLC.

Howard, P. H. (1993). Solvents 2: Handbook of Environmental Fate and Exposure Data for Organic Chemicals (Vol. IV). Chelsea, Michigan: Lewis Publishers.

Howard, P. H. (1997). Solvents 3: Handbook of Environmental Fate and Exposure Data for Organic Chemicals (Vol. V). Boca Raton, Florida: CRC Press Inc.

Jacob, D. J. (1999). Introduction to Atmospheric Chemistry. Princeton University Press.

Kenny, D. A. (1994) "Chapter 16: Testing Measures of Association." Statistics for the Social and Behavioral Sciences, HarperCollins College Publishing, Inc.

Khoder, M. I. (2007). Ambient levels of volatile organic compounds in the atmosphere of Greater Cairo. Atmospheric Environment, 41, 554-566. doi: 10.1016/j.atmosenv.2006.08.051

Kim, S., VandenBoer, T. C., Young, C. J., Riedel, T. P., Thornton, J. A., Swarthout, B., Sive, B., Lerner, B., Gilman, J. B., Warneke, C., & Roberts, J. M. (2014). The primary and recycling sources of OH during the NACHTT2011 campaign: HONO as an important OH primary source in the wintertime. Journal of Geophysical Research: Atmospheres, 119(11),

6886-6896. doi: 10.1002/2013JD019784

King, H., Cole, B., & King, A. (2017). What is Shale Gas? Geology.com. http://geology.com/energy/shale-gas/

Koppmann, R., Johnen, F. J., Khedim, A., Rudolph, J., Wedel, A., & Wiards, B. (1995). The influence of ozone on light nonmethane hydrocarbons during cryogenic preconcentration. Journal of Geophysical Research: Atmospheres, 100(D6), 11383-11391. doi: 10.1029/95JD00561

Kyle, S. J. (2015). Timnath residents worry about drilling's health effects. The Coloraodan. http://www.coloradoan.com/story/news/2015/01/15/timnath-residents-worry-drillings-health-effects/21833875/

LeBouf, R. F., Stefaniak, A. B., & Virji, M. A. (2012). Validation of evacuated canisters for sampling volatile organic compounds in healthcare settings. Journal of Environmental Monitoring, 14(3), 977-983. doi: 10.1039/C2EM10896H

Lee, B. H., Munger, J. W., Wofsy, S. C., & Goldstein, A. H. (2006). Anthropogenic emissions of nonmethane hydrocarbons in the northeastern United States: Measured seasonal variations from 1992-1996 and 1999-2001. Journal of Geophysical Research: Atmospheres, 111(D20). doi: 10.1029/2005JD006172

Malone, E. (2009). [CDPHE Rawhide Meteorological Measuring Station]. Unpublished raw data.

Miller, L., Xiaohong, X., Grgicak-Mannon, A., Brook, J., & Wheeler, A. (2012). Multi-season, multi-year concentrations and correlations amongst the BTEX group of VOCs in an urbanized industrial city. Atmospheric Environment, 61, 305-315. doi: 10.1016/j.atmosenv.2012.07.041

National Institute for Occupational Safety and Health (NIOSH). (2014). Benzene. Center for Disease Control and Prevention (CDC). https://www.cdc.gov/niosh/idlh/71432.html

Netto, K. (2016). Fracking In Europe. Anglicity. http://anglicity.com/fracking-in-europe/

Nolscher, A. C., Williams, J., Sinha, V., Custer, T., Song, W., Johnson, A. M., Axinte, R., Bozem, H., Fischer, H., Pouvesle, N., & Phillips, G. (2012). Summertime total OH reactivity

measurements from boreal forest during HUMPPA-COPEC 2010. Atmospheric chemistry and Physics, 12(17), 8257-8270. doi: 10.5194/acp-12-8257-2012

Occupational Safety and Health Administration (OSHA). (2017). Occupational Safety and Health Standards, Toxic and Hazardous Substances: Benzene. https://www.osha.gov/pls/oshaweb/owadisp.show_document?p_id=10042&p_table=standards

Perry, S. G., Cimorelli, A. J., Paine, R. J., Brode, R. W., Weil, J. C., Venkatram, A., Wilson, R. B., Lee, R. F., & Peters, W. D. (2005). AERMOD: A dispersion model for industrial source applications. Part II: Model performance against 17 field study databases. Journal of applied meteorology, 44(5), 694-708. doi: 10.1175/JAM2228.1

Pétron, G., Frost, G., Miller, B. R., Hirsch, A. I., Montzka, S. A., Karion, A., Trainer, M., Sweeney, C., Andrews, A. E., Miller, L., Kofler, J., Bar-Ilan, A., Dlugokencky, E. J., Patrick, L., Moore, C. T., Jr., Ryerson, T. B., Siso, C., Kolodzey, W., Lang, P. M., Conway, T., Novelli, P., Masarie, K., Hall, B., Guenther, D., Kitzis, D., Miller, J., Welsh, D., Wolfe, D., Neff, W., & Tans, P. (2012). Hydrocarbon emissions characterization in the Colorado Front Range: A pilot study. J. Geophys. Res. Atmos 117(D4) doi: 10.1029/2011jd016360

Poudre School District (PSD). (2017). Calendar. https://bet.psdschools.org/calendar

Ridlington, E. & Rumpler, J. (2013). Fracking by the Numbers: Key Impacts of Dirty Drilling at the State and National Level. Frontier Group and Environment America Research & Policy Center. http://www.environmentamerica.org/sites/environment/files/reports/EA_FrackingNumbers_scrn.pdf

Russo, R. S., Zhou, Y., White, M. L., Mao, H., Talbot, R., & Sive, B. C. (2010). Multi-year (2004-2008) record of nonmethane hydrocarbons and halocarbons in New England: seasonal variations and regional sources. Atmospheric Chemistry and Physics, 10(10), 4909-4929. doi: 10.5194/acp-10-4909-2010

Sanchez, M., Karnae, S., & John, K. (2008). Source characterization of volatile organic compounds affecting the air quality in a urban area of South Texas. International Journal of Environmental Research and Public Health, 5(3), 130-138. doi: 10.3390/ijerph5030130

Schauer, J. J., Kleeman, M. J., Cass, G. R., & Simoneit, B. R. (2002). Measurement of emissions from air pollution sources. 5. C_1 - $C_3$2 organic compounds from gasoline-powered motor vehicles. Environmental Science & Technology, 36(6), 1169-1180. doi: 10.1021/es0108077

Seinfeld, J. H., & Pandis, S. N. (2016) Atmospheric Chemistry and Physics: From Air Pollution to Climate Change. Hoboken, NJ: John Wiley & Sons.

Sillman, S. (2003). Tropospheric ozone and photochemical smog. Treatise on Geochemistry, 9, 612. doi: 10.1016/B0-08-043751-6/09053-8

Sive, B. C. (1999). Atmospheric nonmethane hydrocarbons: Analytical methods and estimated hydroxyl radical concentrations, PhD Dissertation. University of California, Irvine.

Sive, B. C., Zhou, Y., Troop, D., Wang, Y., Little, W. C., Wingenter, O. W., Russo, R. S., Varner, R. K., & Talbot, R. (2005). Development of a cryogen-free concentration system for measurements of volatile organic compounds. Analytical chemistry, 77(21), 6989-6998. doi: 10.1021/ac0506231

Spivakovsky, C. M., Logan, J. A., Montzka, S. A., Balkanski, Y. J., ForemanFowler, M., Jones, D. B. A., Horowitz, L. W., Fusco, A. C., Brenninkmeijer, C. A. M., Prather, M. J., & Wofsy, S. C. (2000). Three-dimensional climatological distribution of tropospheric OH: Update and evaluation. Journal of Geophysical Research: Atmospheres, 105(D7), 8931-8980. doi: 10.1029/1999JD901006

Swarthout, R. F. (2014). Volatile Organic Compound Emissions from Unconventional Natural Gas Production: Source Signatures and Air Quality Impacts, Ph.D. Dissertation, Univ. of New Hampshire, New Hampshire.

Swarthout, R. F., Russo R. S., Zhou Y., Hart A. H., & Sive B. C. (2013). Volatile organic compound distributions during the NACHTT campaign at the Boulder Atmospheric Observatory: Influence of urban and natural gas sources, J. Geophys. Res. Atmos., 118(18). doi: 10.1002/jgrd.50722.

Swarthout, R. F., Russo, R. S., Zhou, Y., Miller, B. M., Mitchell, B., Horsman, E., Lipsky,

E., McCabe, D. C., Baum, E., & Sive, B. C. (2015). Impact of Marcellus Shale natural gas development in southwest Pennsylvania on volatile organic compound emissions and regional air quality. Environmental science & technology, 49(5), 3175-3184. doi: 10.1021/es504315f.

Texas Commission on Environmental Quality (TCEQ). (2015). Benzene. https://www.tceq.texas.gov/assets/public/implementation/tox/dsd/final/benzene.pdf

Timnath Ranch (KCOTIMNA3). (n.d.). Weather Underground. The Weather Company, LLC. https://www.wunderground.com/personal-weather-station/dashboard?ID=KCOTIMNA3#history/tgraphs/s20160115/e20160122/mweek

Thompson, C. R., Hueber, J., & Helmig, D. (2014). Influence of oil and gas emissions on ambient atmospheric non-methane hydrocarbons in residential areas of Northeastern Colorado. Elem Sci Anth, 3. doi: 10.12952/journal.elementa.000035

Warneke, C., Gouw, J. A., Edwards, P. M., Holloway, J. S., Gilman, J. B., Kuster, W. C., Graus, M., Atlas, E., Blake, D., Gentner, D. R., & Goldstein, A.H. (2013). Photochemical aging of volatile organic compounds in the Los Angeles basin: Weekdayweekend effect. Journal of Geophysical Research: Atmospheres, 118(10), 5018-5028. doi: 10.1002/jgrd.50423

Washenfelder, R. A., Trainer, M., Frost, G. J., Ryerson, T. B., Atlas, E. L., De Gouw, J. A., Flocke, F. M., Fried, A., Holloway, J. S., Parrish, D.D. & Peischl, J. (2010). Characterization of NOx, SO2, ethene, and propene from industrial emission sources in Houston, Texas. Journal of Geophysical Research: Atmospheres, 115(D16). doi: 10.1029/2009JD013645

Weiner, C. (2014). Oil and Gas Development in Colorado - 10.639. Colorado State University Extension - Oil and Gas Development in Colorado. http://extension.colostate.edu/docs/pubs/consumer/10639.pdf

Weissermel, K. & Hans-Jurgen, A. (2003). Industrial Organic Chemistry (Vol. IV). Weinheim: Wiley-VCH Verlag GmbH & Co. doi: 10.1002/9783527619191

Zhang, Y., Mu, Y., Liu, J., & Mellouki, A. (2012). Levels, sources and health risks of carbonyls and BTEX in the ambient air of Beijing, China. Journal of Environmental Sciences, 24(1), 124-130. doi: 10.1016/S1001-0742(11)60735-3.

Zhou, Y. (2014). [FRAPPÉ ground level canister grab sampling data set (CSU)]. Unpublished raw data.

Zhou, Y., Shively, D., Mao, H., Russo, R. S., Pape, B., Mower, R. N., Talbot, R., & Sive, B. C. (2010). Air toxic emissions from snowmobiles in Yellowstone National Park. Environmental Science and Technology, 44(1), 222-228. doi: 10.1021/es9018578

Zhou, Y., Sive, B. C., Benedict K. B., Evanoski-Cole, A. Sullivan, A. P., Prenni, A. J., Fischer, E., Schichtel, B., & Collett, J.L. (2017). Impacts of oil and gas and urban source regions and long range transport on air quality in Rocky Mountain National Park: Measurements from FRAPPÉ. In Preparation.

Appendix A

GC Analytical Systems Information

Table A.1: 5 channel GC instrumental parameters for analysis of VOCs from canister samples.

	GC 1		GC 2		GC 3
Primary Analytes	C_2-C_7 NMHCs	C_6-C_{10} NMHCs	C_4-C_{10} NMHCs	C_1-C_2 halocarbons C_1-C_5 alkyl nitrates	C_6-C_{10} NMHCs C_1-C_2 halocarbons
Column Type	Al_2O_3/$NaSO_4$ PLOT	(1) CP-PoraBond Q (2) Restek XTI-5	VF-1ms	OV-1701	OV-624
Column Length (m)	50	(1) 25 (2) 30	60	60	60
Column I.D. (mm)	0.53	0.25	0.32	0.25	0.25
Film Thickness (µm)	10	(1) 3 (2) 0.25	1	1	1.4
Detector Type	FID	FID	FID	ECD	MS
Detector Temp (°C)	250	250	250	250	250
Detector Gas	UHP N_2, UHP H_2, zero air	UHP N_2, UHP H_2, zero air	UHP N_2, UHP H_2, zero air	UHP N_2	

Table A.2: 5 channel GC method parameters for analysis of VOCs from canister samples.

	GC 1	GC 2	GC 3
Initial Temp. (°C)	40	40	40
Initial Time (min)	2	4	4
Ramp 1 (°C/min)	15	5	9
Temp. 2 (°C)	135	60	-
Ramp 2 (°C/min)	6	8.5	-
Final Temp. (°C)	200	190	220
Final Hold Time (min)	4	-	-
Carrier Gas	UHP He	UHP He	UHP He

Table A.3: In-situ real-time GC instrumental parameters for analysis of VOCs.

	GC 1		GC 2	
Primary Analytes	C_2-C_7 NMHCs	C_6-C_{10} NMHCs	OVOCs	C_1-C_2 halocarbons C_1-C_5 alkyl nitrates
Column Type	Al_2O_3/$NaSO_4$ PLOT	VF-1ms	CP-PoraBond Q	VF-1701
Column Length (m)	50	60	25	60
Column I.D. (mm)	0.53	0.32	0.25	0.25
Film Thickness (µm)	10	1	3	1
Detector Type	FID	FID	FID	ECD
Detector Temp (°C)	250	250	250	250
Detector Gas	UHP N_2, UHP H_2, zero air	UHP N_2, UHP H_2, zero air	UHP N_2, UHP H_2, zero air	UHP N_2

Table A.4: In-situ real-time GC method parameters for analysis of VOCs.

	GC 1	GC 2
Initial Temp. (°C)	35	35
Initial Time (min)	3	3
Ramp (°C/min)	10	10
Final Temp. (°C)	200	190
Final Hold Time (min)	5	5
Carrier Gas	UHP He	UHP He

Appendix B

GC Analytical System Calibration Statistics

Table B.1: Calibration statistics for the VOCs measured on the 5 channel GC system

VOC	Calibration Curve Correalation (r^2)	LOD (ppbv)	Slope of Calibration Curve	Standard Range (ppbv)
ethane	0.999	0.105	137	0.4-3362
propane	0.999	0.02	1294	0.4-3203
i-butane	0.999	0.008	1682	0.4-3171
n-butane	0.999	0.01	1691	0.4-3140
i-pentane	0.999	0.009	2110	0.4-3171
n-pentane	0.998	0.007	2039	0.4-3108
2,4-dimethylpentane	0.992	0.004	4049	0.4-3330
2,3-dimethylpentane	0.998	0.013	1049	0.4-3362
2,2,4-trimethylpentane	0.998	0.018	1196	0.4-3298
2,3,4-trimethylpentane	0.999	0.009	1174	0.4-3299
n-hexane	0.999	0.012	2467	0.4-3267
2-methylhexane	0.999	0.01	1079	0.4-3299
3-methylhexane	0.999	0.014	1064	0.4-3299
n-heptane	0.995	0.009	3164	0.4-3299
2-methylheptane	0.999	0.022	1165	0.4-3299
3-methylheptane	0.999	0.016	1177	0.4-3267
n-octane	0.999	0.016	1115	0.4-3299
n-nonane	0.999	0.01	1165	0.4-3235
n-decane	0.999	0.011	1131	0.4-3299
cyclopentane	0.999	0.009	2097	0.4-3171
cyclohexane	0.999	0.015	895	0.4-3330
methylcyclohexane	0.999	0.019	1058	0.4-3299
ethene	0.999	0.053	945	0.4-3362
propene	0.999	0.009	1179	0.4-3203
t-2-butene	0.999	0.018	1662	0.4-3108
1-butene	0.998	0.013	1651	0.4-3104
c-2-butene	0.999	0.022	1756	0.4-3362
isoprene	0.998	0.012	2202	0.4-3171
t-2-pentene	0.996	0.014	1809	0.4-3203
1-pentene	0.998	0.023	1909	0.4-3076
cis-2-pentene	0.998	0.012	1917	0.4-3330
acetylene	0.999	0.013	1186	0.4-3362
benzene	0.999	0.01	903	0.4-3266
1,3,5-trimethylbenzene	0.999	0.012	1091	0.4-3235
1,2,3-trimethylbenzene	0.996	0.012	1074	0.4-3140
1,2,4-trimethylbenzene	0.997	0.0124	1077	0.4-3171
ethylbenzene	0.999	0.019	1066	0.4-3266
1,3-diethylbenzene	0.998	0.027	1136	0.4-3140
1,4-diethylbenzene	0.998	0.013	1133	0.4-3108
isopropylbenzene	0.999	0.011	1171	0.4-3140
n-propylbenzene	0.998	0.012	1157	0.4-3108
toluene	0.998	0.017	1028	0.4-3266
2-ethyltoluene	0.999	0.025	1128	0.4-3140
3-ethyltoluene	0.995	0.014	1084	0.4-3235
4-ethyltoluene	0.998	0.015	1102	0.4-3171
styrene	0.996	0.014	1008	0.4-3298
m+p-xylenes	0.995	0.014	1754	0.8-6596
o-xylene	0.999	0.006	1087	0.4-3203

Appendix C

VOC Information

Table C.1: Chemical formulae and relevant sources for the VOCs measured on the GC analytical systems.

VOC	Chemical Formula	Sources
ethane	C_2H_6	Main constituent of natural gas [Thompson et al., 2014].
propane	C_3H_8	Oil and natural gas production. Natural gas processing and crude oil refinement [Thompson et al., 2014].
i-butane	C_4H_{10}	Blending component with petroleum and natural gas [EIA, 2014]. Evaporation and combustion of fossil fuels [Lee et al., 2006].
n-butane		Blending component with petroleum and natural gas [EIA, 2014]. Natural gas and automobiles [Thompson et al., 2014]. Evaporation and combustion of fossil fuels [Lee et al., 2006].
i-pentane	C_5H_{12}	Vehicle exhaust. Oil and natural gas emissions [Gilman et al., 2013]
n-pentane		Combustion of gasoline and diesel fueled engines [Howard, 1993]. Oil and natural gas emissions [Gilman et al., 2013]
n-hexane	C_6H_{14}	Refining of crude oil. Diesel, gasoline vapor, natural gas, petroleum manufacturing [Graedel, 1978]
n-heptane	C_7H_{16}	Vehicle exhaust, gasoline vapor, natural gas, solvent, petroleum manufacturing [Graedel, 1978]
n-octane	C_8H_{18}	Major component of gasoline and vehicle emissions [Schauer et al., 2002]
n-nonane	C_9H_{20}	Vehicle emissions, biomass/coal combustion, diesel, gasoline vapor, petroleum manufacturing [Graedel et al., 1986].
n-decane	$C_{10}H_{22}$	Paraffin fraction of crude oil and natural gas [Howard, 1993]. Flare emissions [Sanchez et al., 2008]
2,4-dimethylpentane	C_7H_{16}	Vehicle emissions and gasoline vapor [Graedel, 1978]
2,3-dimethylpentane	C_7H_{16}	Vehicle emissions, gasoline vapor, and natural gas [Graedel, 1978]
2,2,4-trimethylpentane	C_8H_{18}	Vehicle emissions, gasoline vapor, and natural gas [Graedel, 1978]
2,3,4-trimethylpentane		Vehicle emissions and gasoline vapor [Graedel, 1978]
2-methylhexane	C_7H_{16}	Vehicle emissions [Graedel, 1978]
3-methylhexane		Vehicle emissions, gasoline vapor, natural gas [Graedel, 1978]
2-methylheptane	C_8H_{18}	Vehicle emissions, gasoline vapor, natural gas, petroleum manufacturing [Graedel et al., 1986]
3-methylheptane		Vehicle emissions, gasoline vapor [Graedel et al., 1986]
cyclohexane	C_6H_{12}	Component of crude oil [Berezin et al., 1966]. Natural gas emissions [Sanchez et al., 2008]
methylcyclohexane	C_7H_{14}	Component of natural gas [GuoYi et al., 2008]
cyclopentane	C_5H_{10}	Natural gas, petroleum manufacturing, gasoline vapor, and vehicle emissions [Graedel, 1978]

VOC	Chemical Formula	Sources
ethene	C_2H_4	Natural gas emissions [Sanchez et al., 2008]. Petroleum combustion [Borbon et al., 2001].
acetylene	C_2H_2	Vehicular exhaust [Gilman et al., 2013].
propene	C_3H_6	Oil refining and natural gas processing [Washenfelder et al., 2010]
t-2-butene	C_4H_8	By products of refining motor fuel and cracking processes of butane or gas oil for gasoline production [Weissermel, 2003]
1-butene		Byproducts of refining motor fuel and cracking processes of butane or gas oil for gasoline production [Weissermel, 2003]
i-butene		Byproducts of refining motor fuel and cracking processes of butane or gas oil for gasoline production [Weissermel, 2003]
c-2-butene		Byproducts of refining motor fuel and cracking processes of butane or gas oil for gasoline production [Weissermel, 2003]
isoprene	C_5H_8	Biogenic emissions [Di Carlo et al., 2004].
t-2-pentene	C_5H_{10}	Flare emissions [Sanchez et al., 2008]. Crude oil and gasoline [Cloke, 1995]
1-pentene		Flare emissions [Sanchez et al., 2008]. Combustion of gasoline an diesel [Graedel, 1978]
cis-2-pentene		Flare emissions [Sanchez et al., 2008]. Crude oil and gasoline [Cloke, 1995]
benzene	C_6H_6	Gasoline and automobile exhaust [Haliday et al., 2016]. Oil and natural gas emissions [Bolden et al., 2015].
toluene	C_7H_8	Crude oil from gasoline production [EPA, 1994]. Gasoline evaporation [Ho et al., 2004]. Oil and natural gas emissions [Bolden et al., 2015].
ethylbenzene	C_8H_{10}	Vehicle exhaust [Miller et al., 2012]. Diesel gasoline vapor [Graedel et al., 1986]. Oil and natural gas emissions [Bolden et al., 2015].
m+p-xylene	C_8H_{10}	Vehicle exhaust [Khoder et al., 2006]. Gasoline vapors [Graedel et al., 1986]. Oil and natural gas emissions [Bolden et al., 2015].
o-xylene		Petroleum and constituent of smoke from many combustion sources [EPA ,1994]. Oil and natural gas emissions [Bolden et al., 2015].
styrene	C_8H_8	Automobile exhaust, stack emissions from waste incineration [Howard, 1989]
n-propylbenzene	C_9H_{12}	Engine combustion fuel evaporation, diesel fuel, and kerosene [Daguat et al., 2002]
isopropylbenzene		Constituent of crude oil, petroleum refining, evaporation of petroleum products [EPA, 2016]
1,3,5-trimethylbenzene		Traffic emissions and fuel evaporation [Khoder et al., 2007]. Flare emissions [Sanchez et al., 2008]
1,2,3-trimethylbenzene		Traffic emissions and fuel evaporation [Khoder et al., 2007]
1,2,4-trimethylbenzene		Traffic emissions and fuel evaporation [Ho et al., 2004]
1,3-diethylbenzene	$C_{10}H_{14}$	Component of gasoline, combustion engines, wastewater from oil refineries [Howard, 1997]
1,4-diethylbenzene		Component of gasoline, combustion engines, wastewater from oil refineries [Howard, 1997]
2-ethyltoluene	C_9H_{12}	Automobile emissions and gasoline vapor [Graedel et al.,1986]
3-ethyltoluene		Automobile emissions and gasoline vapor [Graedel et al., 1986]
4-ethyltoluene		Automobile emissions and gasoline vapor [Graedel et al., 1986]

Appendix D

Whole Air Sampling Results Summary

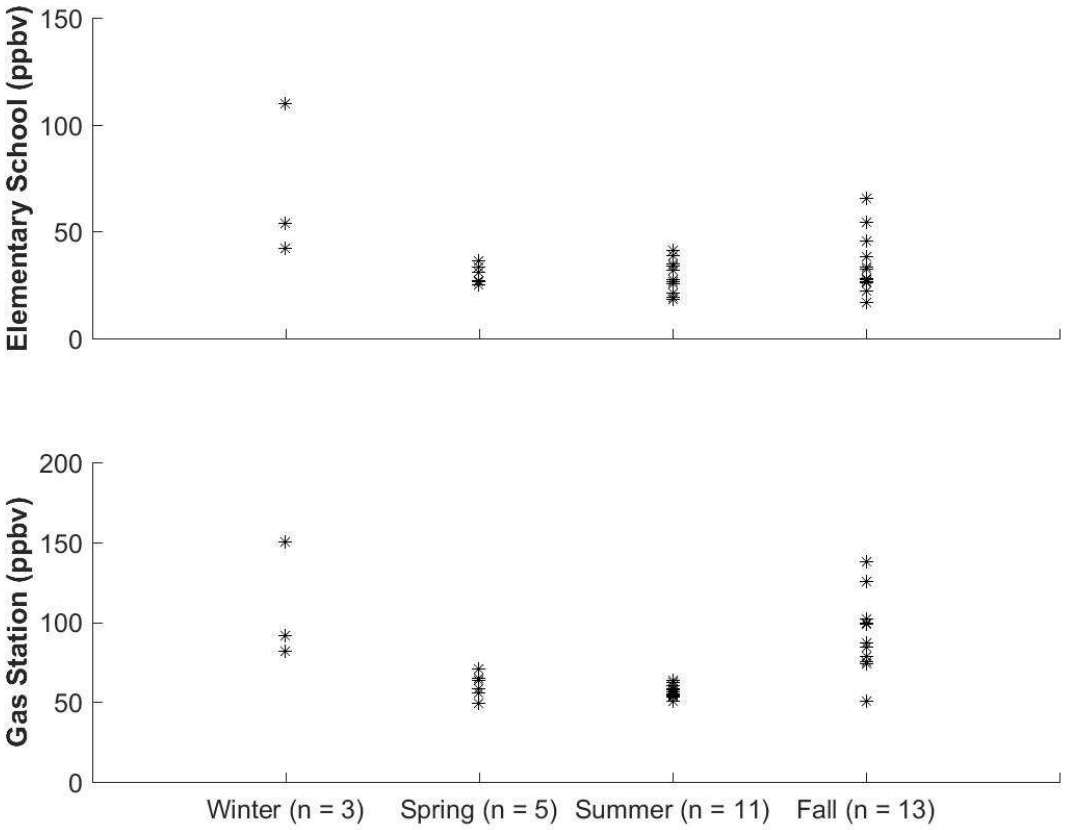

Figure D.1: Comparison of seasonal total VOC concentrations at the elementary school and the gas station.

Table D.2: Mean, median, standard deviation, minimum, and maximum of VOC measurements from canisters at the elementary school.

VOC	Mean (ppbv)	Median (ppbv)	Std. Deviation (ppbv)	Min. (ppbv)	Max (ppbv)
ethane	12.78	10.83	6.68	6.74	42.96
propane	11.11	9.67	5.52	5.30	33.50
i-butane	1.83	1.60	0.93	0.80	5.58
n-butane	5.41	4.77	2.79	2.34	16.64
i-pentane	1.46	1.31	0.69	0.71	4.35
n-pentane	1.44	1.22	0.83	0.54	4.82
2,4-dimethylpentane	0.07	0.05	0.05	0.01	0.23
2,3-dimethylpentane	0.08	0.07	0.06	0.01	0.32
2,2,4-trimethylpentane	0.05	0.05	0.02	0.01	0.12
2,3,4-trimethylpentane	0.01	0.01	0.01	0.00	0.04
n-hexane	0.35	0.31	0.18	0.17	1.10
2-methylhexane	0.03	0.03	0.02	0.00	0.13
3-methylhexane	0.07	0.06	0.06	0.00	0.24
n-heptane	0.09	0.08	0.04	0.01	0.25
2-methylheptane	0.03	0.03	0.02	0.01	0.08
3-methylheptane	0.05	0.02	0.10	0.01	0.54
n-octane	0.08	0.07	0.03	0.04	0.19
n-nonane	0.03	0.03	0.02	0.01	0.11
n-decane	0.03	0.03	0.02	0.01	0.12
cyclopentane	0.11	0.10	0.05	0.06	0.32
cyclohexane	0.14	0.13	0.09	0.00	0.39
methylcyclohexane	0.15	0.13	0.06	0.08	0.40
ethene	0.47	0.41	0.21	0.26	1.22
propene	0.11	0.10	0.03	0.07	0.21
t-2-butene	0.01	0.01	0.00	0.00	0.02
1-butene	0.03	0.02	0.01	0.01	0.07
c-2-butene	0.02	0.02	0.02	0.00	0.07
isoprene	0.02	0.02	0.02	0.01	0.07
t-2-pentene	0.03	0.01	0.04	0.00	0.18
1-pentene	0.01	0.01	0.00	0.00	0.01
cis-2-pentene	0.16	0.14	0.11	0.00	0.55
acetylene	0.37	0.32	0.19	0.19	1.06
benzene	0.20	0.18	0.08	0.09	0.38
1,3,5-trimethylbenzene	0.03	0.02	0.03	0.00	0.13
1,2,3-trimethylbenzene	0.05	0.04	0.05	0.00	0.24
1,2,4-trimethylbenzene	0.36	0.26	0.47	0.02	2.72
ethylbenzene	0.03	0.02	0.02	0.01	0.11
1,3-diethylbenzene	0.03	0.01	0.04	0.00	0.18
1,4-diethylbenzene	0.12	0.08	0.15	0.00	0.78
isopropylbenzene	0.03	0.01	0.04	0.00	0.17
n-propylbenzene	0.03	0.02	0.03	0.00	0.16
toluene	0.23	0.22	0.08	0.13	0.44
2-ethyltoluene	0.06	0.02	0.09	0.01	0.41
3-ethyltoluene	0.02	0.02	0.02	0.00	0.12
4-ethyltoluene	0.02	0.01	0.06	0.00	0.31
styrene	0.13	0.11	0.09	0.00	0.41
m+p-xylenes	0.07	0.07	0.03	0.04	0.20
o-xylene	0.06	0.05	0.04	0.02	0.20

Table D.3: Mean, median, standard deviation, minimum, and maximum of VOC measurements from canisters at the residential area.

VOC	Mean (ppbv)	Median (ppbv)	Std. Deviation (ppbv)	Min. (ppbv)	Max (ppbv)
ethane	9.64	9.36	1.49	8.14	11.71
propane	8.09	7.94	1.14	6.94	9.55
i-butane	1.49	1.45	0.23	1.27	1.78
n-butane	3.84	3.76	0.52	3.35	4.51
i-pentane	1.09	1.07	0.14	0.95	1.26
n-pentane	0.94	0.93	0.16	0.77	1.11
2,4-dimethylpentane	0.06	0.06	0.02	0.05	0.09
2,3-dimethylpentane	0.06	0.06	0.01	0.05	0.07
2,2,4-trimethylpentane	0.05	0.05	0.01	0.04	0.06
2,3,4-trimethylpentane	0.01	0.01	0.00	0.00	0.01
n-hexane	0.24	0.23	0.03	0.22	0.28
2-methylhexane	0.02	0.02	0.00	0.02	0.03
3-methylhexane	0.08	0.09	0.02	0.06	0.10
n-heptane	0.08	0.07	0.01	0.07	0.09
2-methylheptane	0.02	0.02	0.01	0.01	0.03
3-methylheptane	0.02	0.03	0.00	0.02	0.03
n-octane	0.07	0.07	0.02	0.05	0.10
n-nonane	0.02	0.02	0.00	0.02	0.02
n-decane	0.02	0.02	0.00	0.02	0.03
cyclopentane	0.07	0.07	0.01	0.06	0.08
cyclohexane	0.11	0.11	0.01	0.09	0.12
methylcyclohexane	0.11	0.11	0.01	0.10	0.12
ethene	0.54	0.52	0.09	0.45	0.65
propene	0.13	0.12	0.01	0.12	0.15
t-2-butene	0.02	0.02	0.01	0.01	0.02
1-butene	0.02	0.02	0.00	0.02	0.03
c-2-butene	0.01	0.01	0.00	0.01	0.01
isoprene	0.01	0.01	0.00	0.01	0.01
t-2-pentene	0.01	0.01	0.00	0.01	0.01
1-pentene	0.01	0.01	0.00	0.01	0.01
cis-2-pentene	0.16	0.15	0.02	0.14	0.18
acetylene	0.45	0.44	0.14	0.32	0.60
benzene	0.14	0.14	0.02	0.12	0.18
1,3,5-trimethylbenzene	0.02	0.02	0.01	0.01	0.03
1,2,3-trimethylbenzene	0.07	0.07	0.05	0.02	0.13
1,2,4-trimethylbenzene	0.19	0.21	0.09	0.07	0.28
ethylbenzene	0.04	0.04	0.01	0.03	0.04
1,3-diethylbenzene	0.01	0.01	0.00	0.01	0.01
1,4-diethylbenzene	0.04	0.02	0.05	0.01	0.12
isopropylbenzene	0.01	0.01	0.00	0.00	0.01
n-propylbenzene	0.01	0.01	0.00	0.00	0.01
toluene	0.20	0.20	0.02	0.18	0.23
2-ethyltoluene	0.02	0.02	0.01	0.01	0.03
3-ethyltoluene	0.02	0.03	0.01	0.02	0.03
4-ethyltoluene	0.01	0.01	0.00	0.00	0.01
styrene	0.08	0.08	0.05	0.02	0.15
m+p-xylenes	0.07	0.07	0.01	0.06	0.08
o-xylene	0.09	0.06	0.07	0.05	0.19

Table D.4: Mean, median, standard deviation, minimum, and maximum of VOC measurements from canisters at Fossil Creek NA.

VOC	Mean (ppbv)	Median (ppbv)	Std. Deviation (ppbv)	Min. (ppbv)	Max (ppbv)
ethane	13.07	14.01	3.22	8.75	17.34
propane	10.69	11.60	2.62	6.73	13.78
i-butane	2.06	2.22	0.52	1.37	2.64
n-butane	5.50	6.11	1.59	3.28	7.51
i-pentane	2.01	1.91	0.69	1.23	3.01
n-pentane	1.73	1.85	0.52	1.10	2.62
2,4-dimethylpentane	0.10	0.08	0.05	0.05	0.19
2,3-dimethylpentane	0.11	0.10	0.03	0.08	0.16
2,2,4-trimethylpentane	0.12	0.12	0.03	0.08	0.17
2,3,4-trimethylpentane	0.02	0.02	0.02	0.00	0.06
n-hexane	0.44	0.47	0.11	0.28	0.57
2-methylhexane	0.05	0.05	0.02	0.03	0.07
3-methylhexane	0.14	0.13	0.04	0.10	0.19
n-heptane	0.17	0.15	0.11	0.10	0.47
2-methylheptane	0.06	0.06	0.02	0.03	0.09
3-methylheptane	0.04	0.04	0.01	0.03	0.07
n-octane	0.19	0.14	0.17	0.07	0.60
n-nonane	0.03	0.03	0.01	0.02	0.05
n-decane	0.03	0.03	0.02	0.01	0.06
cyclopentane	0.12	0.13	0.04	0.08	0.18
cyclohexane	0.18	0.19	0.03	0.13	0.22
methylcyclohexane	0.18	0.20	0.04	0.13	0.25
ethene	0.98	0.86	0.46	0.52	2.04
propene	0.22	0.21	0.07	0.12	0.38
t-2-butene	0.04	0.04	0.02	0.01	0.08
1-butene	0.04	0.04	0.01	0.03	0.07
c-2-butene	0.03	0.03	0.02	0.01	0.08
isoprene	0.04	0.01	0.05	0.01	0.16
t-2-pentene	0.02	0.02	0.01	0.01	0.04
1-pentene	0.01	0.01	0.00	0.01	0.02
cis-2-pentene	0.06	0.02	0.10	0.01	0.25
acetylene	0.66	0.53	0.37	0.33	1.54
benzene	0.32	0.32	0.07	0.22	0.45
1,3,5-trimethylbenzene	0.04	0.03	0.02	0.02	0.08
1,2,3-trimethylbenzene	0.15	0.04	0.23	0.02	0.66
1,2,4-trimethylbenzene	0.56	0.32	0.72	0.08	2.42
ethylbenzene	0.08	0.08	0.03	0.05	0.14
1,3-diethylbenzene	0.04	0.03	0.05	0.01	0.16
1,4-diethylbenzene	0.10	0.04	0.13	0.01	0.39
isopropylbenzene	0.02	0.01	0.03	0.01	0.11
n-propylbenzene	0.02	0.02	0.01	0.01	0.05
toluene	0.53	0.52	0.10	0.41	0.70
2-ethyltoluene	0.03	0.03	0.02	0.01	0.09
3-ethyltoluene	0.06	0.06	0.02	0.03	0.08
4-ethyltoluene	0.02	0.02	0.01	0.01	0.04
styrene	0.16	0.09	0.16	0.01	0.53
m+p-xylenes	0.19	0.19	0.06	0.11	0.32
o-xylene	0.13	0.12	0.05	0.07	0.23

Table D.5: Mean, median, standard deviation, minimum, and maximum of VOC measurements from canisters at Soapstone NA.

VOC	Mean (ppbv)	Median (ppbv)	Std. Deviation (ppbv)	Min. (ppbv)	Max (ppbv)
ethane	3.19	3.37	0.92	1.54	4.71
propane	2.05	2.18	0.69	0.87	3.24
i-butane	0.34	0.36	0.10	0.16	0.46
n-butane	0.94	1.00	0.27	0.46	1.32
i-pentane	0.34	0.34	0.06	0.26	0.45
n-pentane	0.33	0.33	0.06	0.24	0.43
2,4-dimethylpentane	0.01	0.01	0.01	0.00	0.04
2,3-dimethylpentane	0.01	0.01	0.00	0.01	0.02
2,2,4-trimethylpentane	0.02	0.01	0.05	0.00	0.16
2,3,4-trimethylpentane	0.01	0.00	0.01	0.00	0.02
n-hexane	0.07	0.06	0.02	0.05	0.10
2-methylhexane	0.01	0.01	0.00	0.00	0.01
3-methylhexane	0.03	0.01	0.04	0.01	0.12
n-heptane	0.04	0.04	0.02	0.02	0.09
2-methylheptane	0.01	0.01	0.00	0.00	0.01
3-methylheptane	0.12	0.05	0.16	0.01	0.57
n-octane	0.02	0.02	0.01	0.00	0.03
n-nonane	0.01	0.01	0.01	0.01	0.02
n-decane	0.06	0.02	0.14	0.01	0.47
cyclopentane	0.02	0.02	0.01	0.01	0.03
cyclohexane	0.04	0.04	0.02	0.01	0.08
methylcyclohexane	0.03	0.03	0.01	0.02	0.06
ethene	0.12	0.13	0.03	0.08	0.17
propene	0.05	0.05	0.02	0.03	0.08
t-2-butene	0.01	0.01	0.00	0.00	0.02
1-butene	0.03	0.02	0.03	0.00	0.11
c-2-butene	0.02	0.01	0.01	0.01	0.04
isoprene	0.02	0.01	0.02	0.01	0.07
t-2-pentene	0.01	0.01	0.00	0.01	0.01
1-pentene	0.01	0.01	0.00	0.01	0.02
cis-2-pentene	0.02	0.03	0.02	0.01	0.05
acetylene	0.18	0.16	0.05	0.10	0.26
benzene	0.11	0.09	0.07	0.05	0.25
1,3,5-trimethylbenzene	0.02	0.01	0.01	0.00	0.05
1,2,3-trimethylbenzene	0.24	0.07	0.38	0.01	1.31
1,2,4-trimethylbenzene	0.76	0.42	0.80	0.14	2.89
ethylbenzene	0.02	0.02	0.02	0.00	0.06
1,3-diethylbenzene	0.10	0.02	0.19	0.01	0.64
1,4-diethylbenzene	0.09	0.08	0.09	0.01	0.29
isopropylbenzene	0.07	0.04	0.09	0.00	0.32
n-propylbenzene	0.15	0.10	0.13	0.01	0.38
toluene	0.10	0.08	0.05	0.05	0.21
2-ethyltoluene	0.08	0.02	0.11	0.01	0.33
3-ethyltoluene	0.01	0.01	0.01	0.01	0.03
4-ethyltoluene	0.01	0.01	0.00	0.01	0.01
styrene	0.11	0.11	0.09	0.00	0.32
m+p-xylenes	0.05	0.04	0.04	0.01	0.14
o-xylene	0.03	0.02	0.02	0.01	0.07

Table D.6: Mean, median, standard deviation, minimum, and maximum of VOC measurements from canisters at the gas station.

VOC	Mean (ppbv)	Median (ppbv)	Std. Deviation (ppbv)	Min. (ppbv)	Max (ppbv)
ethane	10.30	9.70	5.77	0.89	35.61
propane	11.63	10.65	5.08	0.97	31.49
i-butane	5.29	4.35	2.95	2.21	13.78
n-butane	26.35	18.18	21.46	7.85	89.65
i-pentane	16.89	16.13	7.48	6.41	50.09
n-pentane	7.13	6.80	2.83	2.51	18.28
2,4-dimethylpentane	0.32	0.12	0.72	0.07	4.27
2,3-dimethylpentane	0.58	0.33	1.53	0.01	9.18
2,2,4-trimethylpentane	1.12	0.52	3.66	0.04	21.82
2,3,4-trimethylpentane	0.25	0.09	0.94	0.00	5.57
n-hexane	1.46	1.23	1.22	0.57	8.09
2-methylhexane	0.23	0.23	0.11	0.01	0.48
3-methylhexane	0.60	0.39	1.23	0.17	7.51
n-heptane	0.43	0.22	1.07	0.12	6.49
2-methylheptane	0.27	0.11	0.95	0.04	5.64
3-methylheptane	0.22	0.09	0.69	0.04	4.13
n-octane	0.25	0.14	0.64	0.05	3.85
n-nonane	0.08	0.06	0.15	0.01	0.90
n-decane	0.05	0.05	0.03	0.00	0.16
cyclopentane	0.51	0.49	0.33	0.17	2.21
cyclohexane	0.71	0.57	0.96	0.00	5.97
methylcyclohexane	0.62	0.35	1.64	0.01	9.89
ethene	0.85	0.79	0.33	0.07	1.66
propene	0.26	0.24	0.11	0.04	0.57
t-2-butene	0.31	0.29	0.19	0.02	0.73
1-butene	0.15	0.14	0.07	0.04	0.30
c-2-butene	0.27	0.24	0.14	0.03	0.59
isoprene	0.05	0.03	0.05	0.00	0.17
t-2-pentene	0.32	0.33	0.23	0.01	0.90
1-pentene	0.13	0.12	0.12	0.01	0.55
cis-2-pentene	0.90	0.29	2.29	0.07	13.66
acetylene	0.52	0.50	0.23	0.01	1.12
benzene	0.54	0.55	0.17	0.30	1.26
1,3,5-trimethylbenzene	0.10	0.07	0.16	0.01	0.96
1,2,3-trimethylbenzene	0.09	0.06	0.07	0.01	0.26
1,2,4-trimethylbenzene	0.83	0.62	0.84	0.03	4.61
ethylbenzene	0.35	0.16	1.01	0.05	6.03
1,3-diethylbenzene	0.02	0.01	0.02	0.00	0.08
1,4-diethylbenzene	0.14	0.15	0.10	0.00	0.40
isopropylbenzene	0.03	0.01	0.06	0.00	0.26
n-propylbenzene	0.06	0.05	0.08	0.01	0.52
toluene	2.33	1.20	6.03	0.62	36.35
2-ethyltoluene	0.06	0.04	0.06	0.01	0.36
3-ethyltoluene	0.15	0.11	0.26	0.01	1.57
4-ethyltoluene	0.07	0.04	0.12	0.00	0.70
styrene	0.20	0.16	0.18	0.00	0.81
m+p-xylenes	0.61	0.34	1.52	0.11	9.16
o-xylene	0.32	0.20	0.70	0.05	4.26

Table D.7: Mean, median, standard deviation, minimum, and maximum of VOC measurements from the in-situ real-time GC at the residential area.

VOC	Mean (ppbv)	Median (ppbv)	Std. Deviation (ppbv)	Min. (ppbv)	Max (ppbv)
ethane	10.41	7.51	1.71	32.68	9.78
propane	8.58	5.57	0.63	27.46	9.26
i-butane	1.56	1.10	0.13	4.99	1.63
n-butane	4.05	2.51	0.22	13.09	4.64
i-pentane	1.10	0.81	0.09	3.43	1.10
n-pentane	1.18	0.76	0.07	3.80	1.31
n-hexane	0.33	0.24	0.02	1.05	0.34
n-heptane	0.09	0.06	0.01	0.30	0.10
n-octane	0.02	0.02	0.03	0.07	0.03
n-nonane	0.02	0.01	0.04	0.05	0.03
cyclopentane	0.10	0.08	0.02	0.28	0.09
ethene	0.70	0.52	0.11	1.90	0.63
propene	0.14	0.10	0.03	0.39	0.13
t-2-butene	0.02	0.01	0.02	0.05	0.02
1-butene	0.03	0.02	0.01	0.07	0.02
c-2-butene	0.02	0.01	0.01	0.04	0.01
isoprene	0.01	0.00	0.00	0.00	0.03
acetylene	0.61	0.50	0.21	1.41	0.41
benzene	0.14	0.12	0.04	0.34	0.10
ethylbenzene	0.03	0.02	0.03	0.08	0.03
toluene	0.25	0.18	0.01	0.67	0.24
m+p-xylenes	0.09	0.06	0.01	0.26	0.09
o-xylene	0.03	0.02	0.04	0.09	0.03
2-butyl nitrate	0.02	0.01	0.01	0.00	0.06
2-pentyl nitrate	0.00	0.00	0.00	0.00	0.02

Appendix E

Propane and Acetylene Correlation Coefficient Statistics

Statistical method detailed in Kenny [1994].

Correlation coefficients were transformed into a "z-score" using the Fisher Z-Transformation (Table E.1):

$z = \frac{1}{2}[ln(1+r) - ln(1-r)]$

where r is the correlation coefficient between a VOC and propane or acetylene.

The $z_{observed}$ between the propane and acetylene "z-scores" was calculated by (Table E.2):

$z_{observed} = \frac{z_{propane} - z_{acetylene}}{\sqrt{\frac{2}{N-3}}}$

where $z_{propane}$ and $z_{acetylene}$ are the "z-scores" and N is the number of week-long canister samples collected at the site.

The $z_{observed}$ values were then compared to the 95% confidence interval critical value of $\pm$ 1.96 to determine if the values were significantly different (Table 3.2).

Table E.1: "z scores" calculated from the propane and acetylene correlation coefficients.

	Propane					Acetylene				
	Elementary School	Residential Area	Fossil Creek NA	Soapstone NA	Gas Station	Elementary School	Residential Area	Fossil Creek NA	Soapstone NA	Gas Station
ethane	1.94	1.77	1.44	2.08	1.68	0.58	1.15	0.50	0.72	0.75
i-butane	2.99	2.99	1.23	2.00	0.56	1.25	1.00	0.47	0.00	0.64
n-butane	2.99	2.99	1.34	1.77	0.44	0.52	1.64	0.31	0.65	0.95
i-pentane	2.44	2.99	0.64	0.56	0.00	0.55	1.68	0.62	0.64	0.00
n-pentane	2.18	2.29	1.05	0.50	0.17	0.48	1.42	0.20	0.67	0.10

Table E.2: $z_{observed}$ values between the propane and acetylene "z-scores".

	Elementary School	Residential Area	Fossil Creek NA	Soapstone NA	Gas Station
ethane	5.18	0.44	1.64	2.73	3.55
i-butane	6.63	1.41	1.32	4.01	-0.30
n-butane	9.41	0.96	1.79	2.23	-1.96
i-pentane	7.20	0.93	0.05	-0.16	0.00
n-pentane	6.46	0.62	1.46	-0.34	0.28

Appendix F

OH reactivity (k_{OH}) Rate Constants

Table F.1: k_{OH} values for all measured VOCs.

VOC	k_{OH}	Sources
ethane	2.50E-13	Abeleira et al., 2017
propane	1.09E-12	Abeleira et al., 2017
i-butane	2.10E-12	Abeleira et al., 2017
n-butane	2.40E-12	Abeleira et al., 2017
i-pentane	3.80E-12	Abeleira et al., 2017
n-pentane	3.60E-12	Abeleira et al., 2017
2,4-dimethylpentane	4.77E-12	Atkinson et al., 2003
2,3-dimethylpentane	7.00E-12	Abeleira et al., 2017
2,2,4-trimethylpentane	3.59E-11	Abeleira et al., 2017
2,3,4-trimethylpentane	6.60E-12	Abeleira et al., 2017
n-hexane	5.20E-12	Abeleira et al., 2017
2-methylhexane	6.72E-12	Abeleira et al., 2017
3-methylhexane	6.54E-12	Abeleira et al., 2017
n-heptane	6.76E-12	Abeleira et al., 2017
2-methylheptane	9.00E-12	Abeleira et al., 2017
3-methylheptane	9.00E-12	Abeleira et al., 2017
n-octane	8.11E-12	Abeleira et al., 2017
n-nonane	1.02E-11	Rosen et al., 2004
n-decane	1.16E-11	Rosen et al., 2004
cyclopentane	5.10E-12	Abeleira et al., 2017
cyclohexane	7.49E-12	Abeleira et al., 2017
methylcyclohexane	1.04E-11	Abeleira et al., 2017
ethene	8.50E-12	Abeleira et al., 2017
propene	2.63E-11	Abeleira et al., 2017
t-2-butene	6.40E-11	Rosen et al., 2004
1-butene	3.14E-11	Rosen et al., 2004
c-2-butene	5.64E-11	Abeleira et al., 2017
isoprene	1.00E-10	Abeleira et al., 2017
t-2-pentene	6.70E-11	Rosen et al., 2004
1-pentene	3.14E-11	Rosen et al., 2004
cis-2-pentene	6.50E-11	Rosen et al., 2004
acetylene	8.70E-13	Abeleira et al., 2017
benzene	2.22E-12	Abeleira et al., 2017
1,3,5-trimethylbenzene	5.75E-11	Rosen et al., 2004
1,2,3-trimethylbenzene	3.27E-11	Rosen et al., 2004
1,2,4-trimethylbenzene	3.27E-11	Rosen et al., 2004
ethylbenzene	7.00E-12	Abeleira et al., 2017
isopropylbenzene	6.30E-12	Atkinson et al., 2003
n-propylbenzene	5.80E-12	Atkinson et al., 2003
toluene	5.63E-12	Abeleira et al., 2017
styrene	5.80E-11	Rosen et al., 2004
m+p-xylenes	1.43E-11	Rosen et al., 2004
o-xylene	1.36E-11	Abeleira et al., 2017

Appendix G

VOC Categories

Table G.1: VOC categories used in the OH reactivity calculations for whole air canister samples.

Alkanes	Alkenes	Aromatics	Other
ethane	ethene	benzene	Acetylene
propane	propene	toluene	Cyclopentane
i-butane	t-2-butene	ethylbenzene	Cyclohexane
n-butane	1-butene	m+p-xylene	Methylcyclohexane
i-pentane	c-2-butene	styrene	2,4-Dimethylpentane
n-pentane	t-2-pentene	o-xylene	2,3-Dimethylpentane
n-hexane	1-pentene	isopropylbenzene	2-Methylhexane
n-heptane	cis-2-pentene	n-propylbenzne	3-Methylhexane
n-octane		1,3,5-trimethylbenzene	2,2,4-trimethylpentane
n-nonane		1,2,4-trimethylbenzene	2,3,4-trimethylpentane
n-decane		1,2,3-trimethylbenzene	2-Methylheptane
			3-Methylheptane

Table G.2: VOC categories used in the OH reactivity calculations for the in-situ real-time GC at the residential area.

Alkanes	Alkenes	Aromatics	Other
ethane	ethene	Benzene	Acetylene
propane	propene	Toluene	Cyclopentane
i-butane	t-2-butene	Ethylbenzene	
n-butane	1-butene	m+p-Xylene	
i-pentane	c-2-butene	Styrene	
n-pentane		o-Xylene	
n-hexane			
n-heptane			
n-octane			
n-nonane			

Appendix H

AERMOD Contour Plots

In Figures H.1 - H.4 the center of the well pad is denoted by a red dot, the elementary school campus can be seen in the lower left corner, and the contours around the school are labeled with the concentration increase in ppbv.

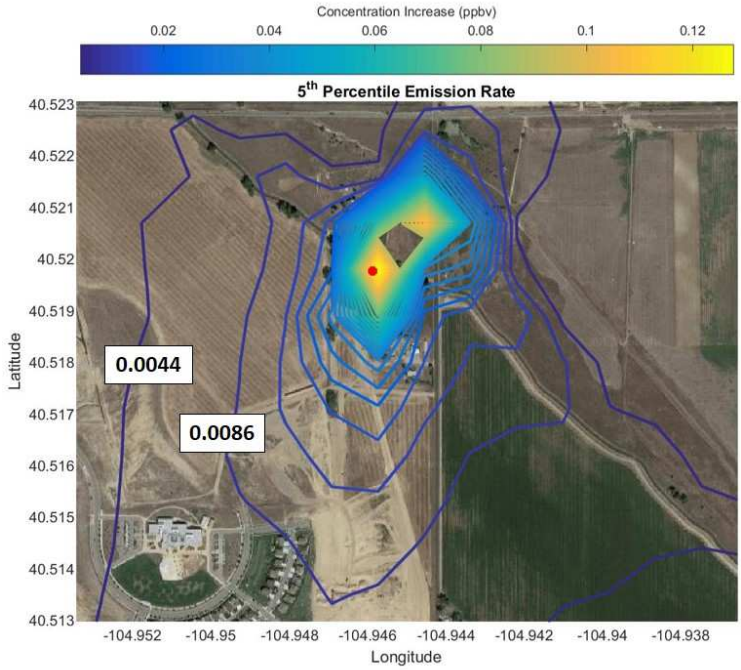

Figure H.1: Contour plot of benzene concentration increase around the well pad under the 5^{th} percentile emission rate scenario ($5.0 \times 10^{-5} \frac{g}{s}$).

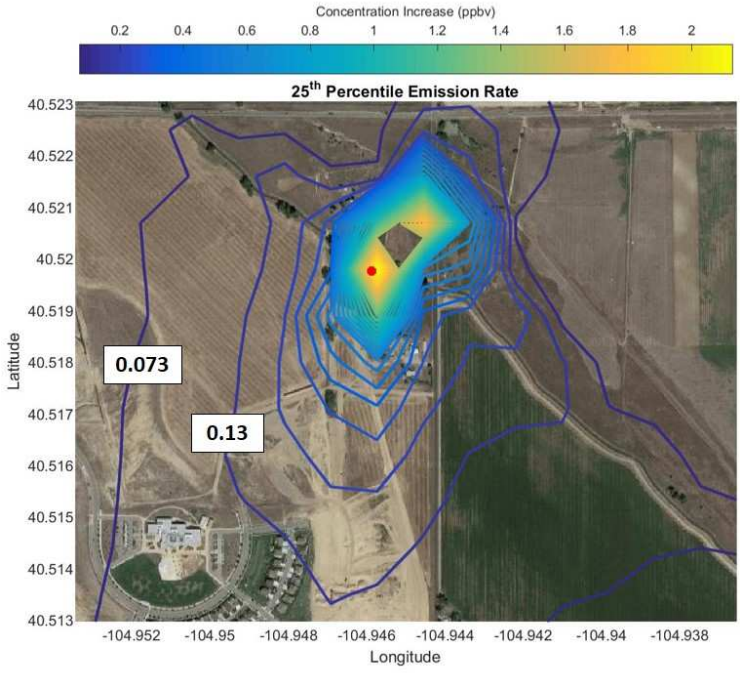

Figure H.2: Contour plot of benzene concentration increase around the well pad under the 25^{th} percentile emission rate scenario ($5.0 \times 10^{-4} \frac{g}{s}$).

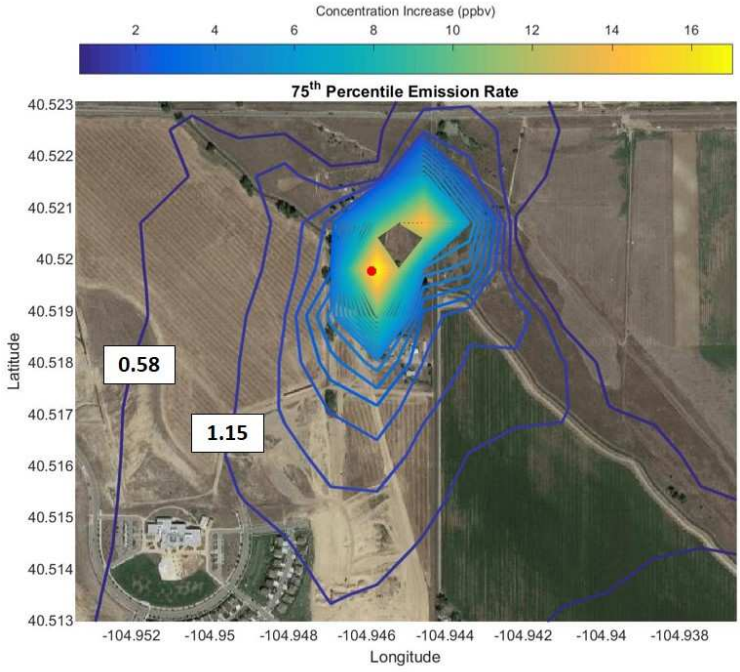

Figure H.3: Contour plot of benzene concentration increase around the well pad under the 75^{th} percentile emission rate scenario ($4.0 \times 10^{-3} \frac{g}{s}$).

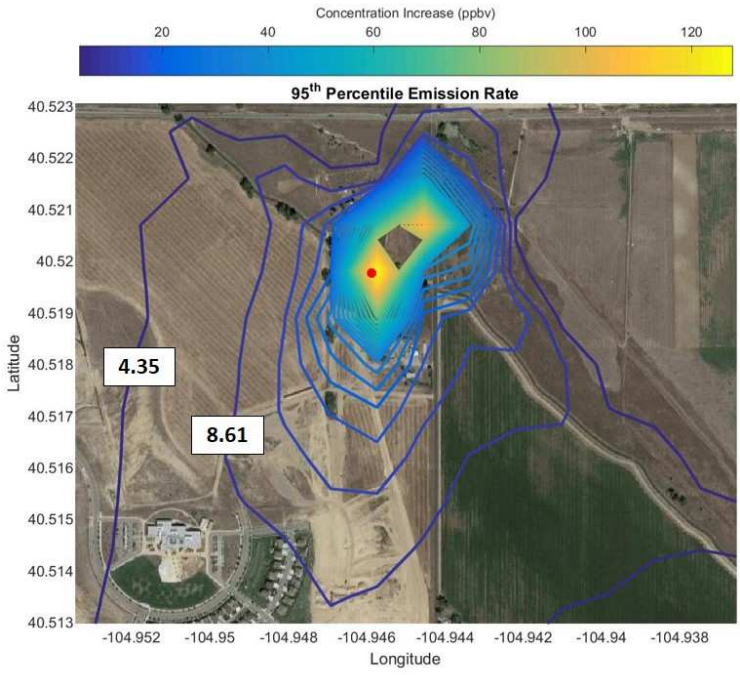

Figure H.4: Contour plot of benzene concentration increase around the well pad under the 95^{th} percentile emission rate scenario ($3.0 \times 10^{-2} \frac{g}{s}$).